Brain-Derived Neurotrophic Factor influences cholesterol trafficking between astrocytes and neurons - Effects of Aging or a Fructose-rich diet on neurotrophin levels and markers of brain functioning

UNIVERSITY OF NAPLES FEDERICO II
Department of Biology

PhD in Biology

XXXI cycle

PhD Student

Lucia Iannotta

Tutor

Luisa Cigliano

ACADEMIC YEAR 2018/2019

Naples

Table of contents

Abstract

Cholesterol is critical to maintain membrane plasticity, cellular function and synaptic integrity. The neurotrophin Brain-derived neurotrophic factor (BDNF) exerts a critical role in brain synaptic plasticity, learning and memory. It was previously reported that BDNF elicits cholesterol biosynthesis and promote the accumulation of presynaptic proteins in cholesterol-rich lipid rafts, but no further data are available on its ability to modulate physiological mechanisms involved in brain cholesterol homeostasis. One aim of this PhD research project was to investigate whether BDNF influences cholesterol homeostasis, focusing on the effect of the neurotrophin on Apolipoprotein E (ApoE) synthesis, cholesterol efflux from astrocytes and cholesterol incorporation into neurons. Our results show that BDNF significantly stimulates cholesterol efflux by astrocytes, as well as ATP binding cassette A1 (ABCA1) transporter and the expression of ApoE in cellular models of human astrocytes. On the other hand, BDNF reduce cholesterol incorporation in neurons by enhancing LXR-beta expression, protecting these cells from cholesterol excess-induced apoptosis. These results evidence a novel role of BDNF in the modulation of ApoE and cholesterol homeostasis in glial and neuronal cells.

A further objective of this research project was to investigate the effects of a short-term (two-weeks) fructose-rich diet on brain redox homeostasis, autophagy, as well as on BDNF, its receptor TrkB and synaptic function markers, in the cortex of young and adults rats, in order to highlight the early risks to which brain is exposed. The results showed that a short-term fructose feeding was associated with an imbalance of redox homeostasis, as lower amount of Nuclear factor (erythroid derived 2)-like 2, lower activity of Glucose 6-phosphate dehydrogenase and Glutathione reductase, together with lower GSH/GSSG ratio, were found in fructose-fed young and adult rats. Fructose-rich diet was also associated with the activation of autophagy, as higher levels of Beclin, LC3 II and P62 were detected in cortex of fructose-fed rats. A diet-associated decrease of synaptophysin, synapsin I, and synaptotagmin I, suggests an impairment of synaptic transmission in fructose-fed young and adult rats. Interestingly, BDNF amount was significantly lower only in fructose-fed adult rats, while the level of its receptor TrkB decreased in both group of treated rats. A further marker of brain functioning, Acetylcholinesterase activity was found increased only in fructose-fed young animals. Overall, our findings suggest that young rats may severely suffer from the deleterious influence of fructose on brain health as the adults and provide experimental data suggesting the need of targeted nutritional strategies to reduce its amount in foods.

Riassunto

Il colesterolo svolge un ruolo fondamentale nella regolazione della fluidità e della permeabilità della membrana plasmatica e la sua presenza regola la funzione di proteine e recettori ancorati alla membrana. Il Fattore Neurotrofico di Derivazione cerebrale (Brain-Derived Neurotrophic factor- BDNF) è la neurotrofina maggiormente espressa nel sistema nervoso centrale dove svolge un ruolo chiave nel differenziamento neuronale, nella sinaptogenesi, nell'apprendimento e nella memoria. È stato dimostrato che il BDNF è in grado di promuovere la sintesi di colesterolo e l'accumulo di proteine presinaptiche a livello delle zattere lipidiche, ma non ci sono ulteriori dati circa il suo ruolo nella modulazione dei meccanismi fisiologici coinvolti nell'omeostasi del colesterolo cerebrale. Uno degli obiettivi di questo progetto di dottorato è stato, quindi, valutare il ruolo del BDNF nella regolazione di meccanismi critici dell'omeostasi del colesterolo nel cervello, vale a dire: a) l'efflusso di colesterolo da parte degli astrociti; b) la produzione di Apolipoproteina E; c) l'incorporazione di colesterolo nei neuroni. I risultati evidenziano che il BDNF stimola l'efflusso di colesterolo dagli astrociti, induce l'espressione del trasportatore ABCA1 e la sintesi di ApoE in modelli di astrociti umani, riduce l'incorporazione del colesterolo da parte dei neuroni mediante l'induzione dell'espressione di LXR-beta e protegge queste cellule dall'apoptosi indotta da un eccesso di colesterolo. Questi risultati mostrano una nuova funzione del BDNF nella modulazione di ApoE e dell'omeostasi del colesterolo in neuroni e cellule gliali.

Un ulteriore obiettivo di questo progetto di dottorato è stato valutare l'effetto di una dieta di breve durata (solo due settimane), ricca in fruttosio, sull'omeostasi redox, l'autofagia, i livelli di BDNF, del suo recettore TrkB e di alcuni marcatori di funzionalità sinaptica. Lo studio è stato condotto sulla corteccia prefrontale di ratti giovani ed adulti, allo scopo di chiarire quali sono gli effetti precoci di questa dieta a livello cerebrale. I dati ottenuti hanno dimostrato che una dieta contenente elevate concentrazioni di questo zucchero, induce l'alterazione dell'omeostasi redox in seguito alla riduzione dei livelli del fattore trascrizionale Nrf-2, dell'attività degli enzimi GSR e G6PD e del rapporto GSH/GSSG. Ulteriori effetti di questa dieta sono l'attivazione di autofagia come dimostrato dall'aumento dei livelli di beclina, p62 ed LC3 II nei ratti trattati rispetto ai controlli e dalla riduzione dei livelli di marker di funzionalità sinaptica come sinaptofisina, sinapsina I e sinaptotagmina I. I livelli di BDNF sono risultati significativamente ridotti solo nei ratti adulti trattati con dieta ricca in fruttosio mentre i livelli di TrkB sono risultati ridotti sia nei ratti giovani che nei ratti adulti nutriti con fruttosio. L'attività dell'Acetilcolinesterasi, un ulteriore marcatore di funzionalità cerebrale, è stata

trovata significativamente aumentata nei ratti giovani nutriti con questo tipo di dieta. Questi risultati dimostrano che un'alimentazione ricca in fruttosio è deleteria per la salute cerebrale di giovani e adulti e inducono a riflettere sulla necessità di trovare strategie nutrizionali mirate a ridurre la quantità di questo zucchero negli alimenti.

Abbreviations

24-OHC	24S-hydroxycholesterol
ABC	ATP-binding cassette
ACAT1/SOAT1	Acylcoenzyme A: cholesterol acyltransferase 1
AChE	Acetylcholinesterase
AD	Alzheimer's disease
ApoE	Apolipoprotein E
ApoER2	ApoE receptor 2
ATCI	Acetylthiocholine iodide
BBB	Blood brain barrier
BDNF	Brain Derived Neurotrophic Factor
BSA	Bovine serum albumin fraction V
CNS	Central nervous system
CREB	cAMP response element-binding protein
CY46A1	Cytochrome P450 oxidase
DAG	Diacylglycerol
DTNB	5,5-dithiobis-2-nitrobenzoate
ERK	Extracellular signal-regulated kinases
FA	Fatty acid
FAD	Familial AD
FBS	Fetal bovine serum
G6PD	Glucose 6-phosphate dehydrogenase
GAM-HRP	Goat anti-mouse Horseradish Peroxidase-conjugated IgG
GAR-HRP	Goat anti-rabbit Horseradish Peroxidase-conjugated IgG
GSH	Reduced glutathione
GSR	Glutathione reductase
GSSG	Oxidized Glutathione
HDL	High-density lipoprotein
HMGCR	3-hydroxy-3-methylglutaryl-CoA reductase
HPRT1	Hypoxanthine phosphoribosyltransferase 1
IP3	Inositol 1,4,5-trisphosphate
LC3	Microtubule associated protein light chain
LDLR	Low-density lipoprotein receptor

LRP1	Low-density lipoprotein receptor-related protein 1
LTP	Long-term potentiation
MAPK	Mitogen-activated protein kinases
mTOR	Mammalian Target of Rapamycin
MTT	3-(4,5-dimethylthiazol-2-yl)-2,5- diphenyltetrazolium bromide
NFkB	Nuclear factor kappa B
NHA	Normal human astrocyte
Nrf2	Nuclear factor (erythroid derived 2)-like 2
P62	P62-sequestosome-1
PI3K	Phosphoinositide 3-kinase
PKC	Protein kinase C
PLC-γ	Phospholipase C-γ
PVDF	Polyvinylidene difluoride
RA	Retinoic acid
SCA17	Spinocerebellar ataxia 17
SCAP	Sterol-sensitive SREBP cleavage activating protein
SREBP2	Sterol regulatory element protein 2
TrkB	Tropomyosin Kinase B
TrkB-FL	Full length Tropomyosin Kinase B
TrkB-T	Truncated Tropomyosin Kinase B
VLDLR	Lipoprotein receptor

Chapter 1

Introduction and research plans

Introduction

A major aim of the PhD research plan was to study the role of Brain Derived Neurotrophic Factor (BDNF), a member of neurotrophin family, in the modulation of brain cholesterol homeostasis. In addition, the deleterious effects of sugars-rich diet on BDNF and its receptor levels and other markers of brain functioning were in parallel investigated. BDNF regulates protein synthesis and neurotransmitter release, modulates neuronal cell survival, neurite growth, synaptic transmission, postsynaptic density, structural plasticity at dendritic spines and adult neurogenesis (Yoshii and Constantine-Paton, 2010; Lu, 2003; Leal et al., 2016).

BDNF is translated as pro-BDNF and is cleaved into mature BDNF by endoproteases in the cytoplasm or in the extracellular matrix by plasmin or matrix metalloproteinases (Lima Giacobbo et al., 2018). Physiological responses to BDNF are mediated by the activation of two classes of membrane-bound receptors: the low affinity neurotrophin receptor p75 that mainly mediates cell death responses and the high affinity Tropomyosin Kinase B (TrkB) receptor, which mediates cell survival responses (Vidaurre at al., 2012; Gomes et al., 2012; Leal et al., 2016). The binding of BDNF to TrkB induces receptor dimerization, autophosphorylation, and the activation of three main intracellular signalling cascades, depending of the phosphorylation site:

1) The mitogen-activated protein kinases (MAPK)/extracellular signal-regulated kinases (ERK) pathway is activated after the phosphorylation of Tyr515 residue by Shc. The result is the activation of cAMP response element-binding protein (CREB) transcription factor, which enhances the transcription of pro-survival genes (Reichardt, 2006).
2) The recruitment of Shc to TrkB also allows the activation of the phosphoinositide 3-kinase (PI3K)/Akt pathway, that lead to the transcription of BDNF and other proteins mRNA, by activating the Mammalian Target of Rapamycin (mTOR) (Takei et al., 2004; Sarbassov et al., 2005). Additionally, through Akt pathway, BDNF can modulate gene expression by activating Nuclear Factor-Kappa B (NF-κB) transcription factor (Yoshii and Constantine-Paton, 2010).
3) The phospholipase C (PLC)-γ pathway (short-term response) is activated after the phosphorylation of Tyr785 residue. PLCγ hydrolyses phosphatidylinositol 4,5-bisphosphate to obtain diacylglycerol (DAG) and inositol 1,4,5-trisphosphate (IP3) (Huang and Reichardt, 2003; Reichardt, 2006). DAG activates protein kinase C (PKC) while IP3 releases Ca2+ from intracellular stores (Yoshii and Constantine-Paton, 2010).

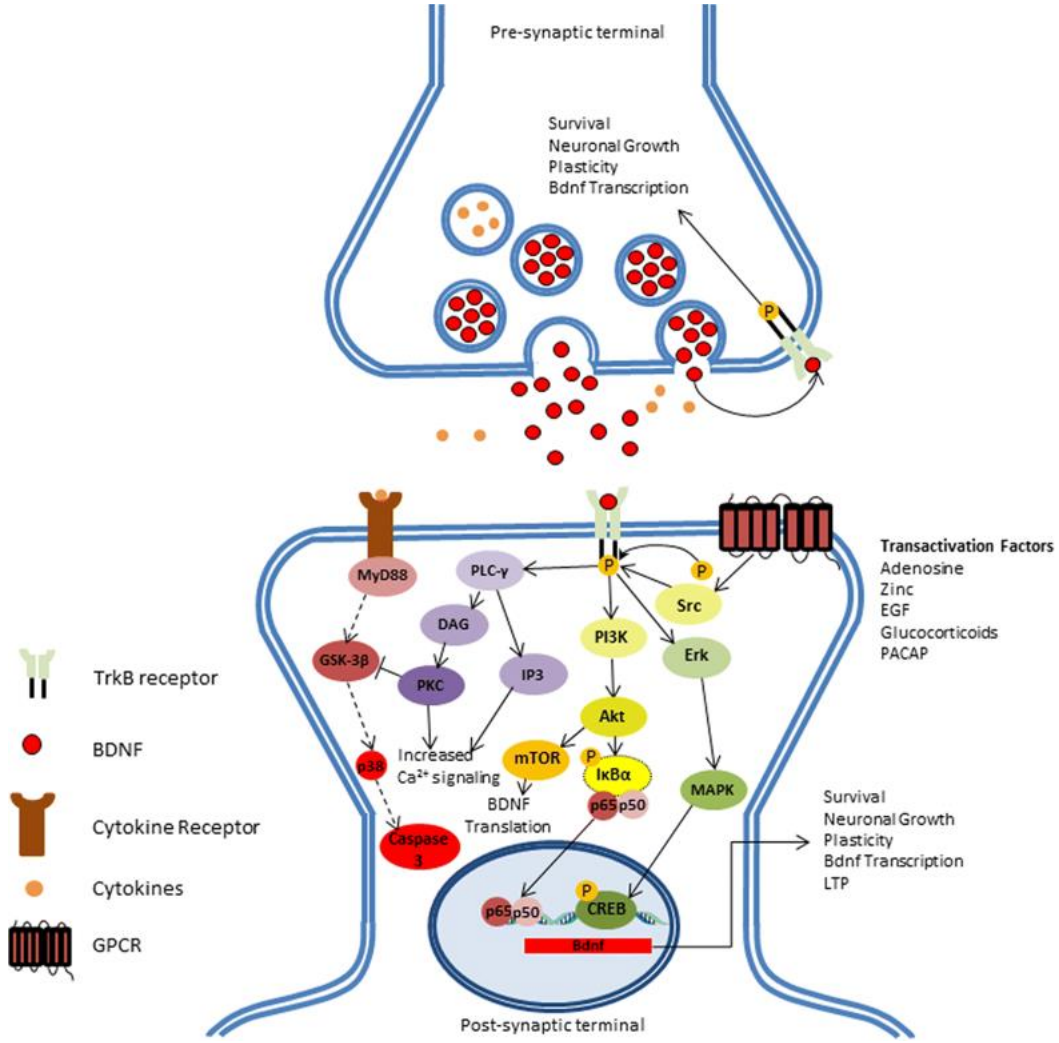

Figure 1. Downstream pathways of BDNF-TrkB signalling. *After the binding of BDNF to TrkB, three different pathways can be activated: MAPK/ERK pathway, PI3K/Akt pathway and PLC-γ pathway. (Lima Giacobbo et al., 2018).*

BDNF and regulation of cholesterol homeostasis in brain

Few data were available in the literature on the role played by BDNF in the regulation of cerebral cholesterol. One interesting investigation was from Suzuki and co-workers, which demonstrated that the translocation of TrkB in cholesterol-rich lipid rafts is important for BDNF-induced synaptic modulation and that pharmacological depletion of cholesterol reduced BDNF-dependent synaptic transmission (Suzuki et al, 2004). Also, BDNF induces cholesterol biosynthesis in cortical and hippocampal neurons by stimulating the transcription of enzymes involved in cholesterol biosynthesis such as 3-hydroxy-3-methylglutaryl-CoA reductase (HMGCR), the rate-limiting enzyme of cholesterol synthesis (Suzuki et al., 2007). Furthermore, BDNF increase cholesterol and presynaptic proteins accumulation in lipid rafts (Suzuki et al., 2007). Cholesterol is important for neuronal membrane integrity and neuronal physiology (i.e.

synaptic signalling and plasticity) during development and throughout adulthood (Egawa et al., 2016). Almost all the cholesterol contained in brain derives from de novo synthesis (Zhang and Liu, 2015) since the blood brain barrier (BBB) is impermeable not only to cholesterol but also to the circulating plasma lipoproteins. De novo synthesis rate of cholesterol in brain is not homogeneous among the different cell type and during the cell development. As mature, in fact, neurons are no more able to synthetize cholesterol de novo (Vitali et al., 2014) so they become dependent to other cell type, mainly astrocytes (Ikonen, 2008). Mature neurons uptake cholesterol secreted by astrocytes via Apolipoprotein E (ApoE)-containing lipoproteins, through the low-density lipoprotein receptor (LDLR) and the low-density lipoprotein receptor-related protein 1 (LRP1) (Posse de Chaves et al., 2000; Herz, 2009).

In the adult brain, the amount of cholesterol is finely regulated with minimal loss (Moutinho et al., 2016). Cholesterol homeostasis in brain is maintained by different mechanisms. On one hand, cholesterol biosynthesis con be modulated by a) ubiquitination of HMGCR and its consequent degradation in the proteasome; b) modulation of HMGR gene expression by ER-bound membrane transcription factor sterol regulatory element protein 2 (SREBP2), whose activation depends on the sterol-sensitive SREBP cleavage activating protein (SCAP). On the other hand, to avoid cholesterol overload, brain cells can: a) directly excrete cholesterol through ATP-binding cassette (ABC) transporters and ApoE-containing lipoproteins; b) esterify and store cholesterol in lipid droplets through acylcoenzyme A: cholesterol acyltransferase 1 (ACAT1/SOAT1) activity; c) convert cholesterol to 24S-hydroxycholesterol (24-OHC) through cytochrome P450 oxidase (CYP46A1) (Arenas at al., 2017).

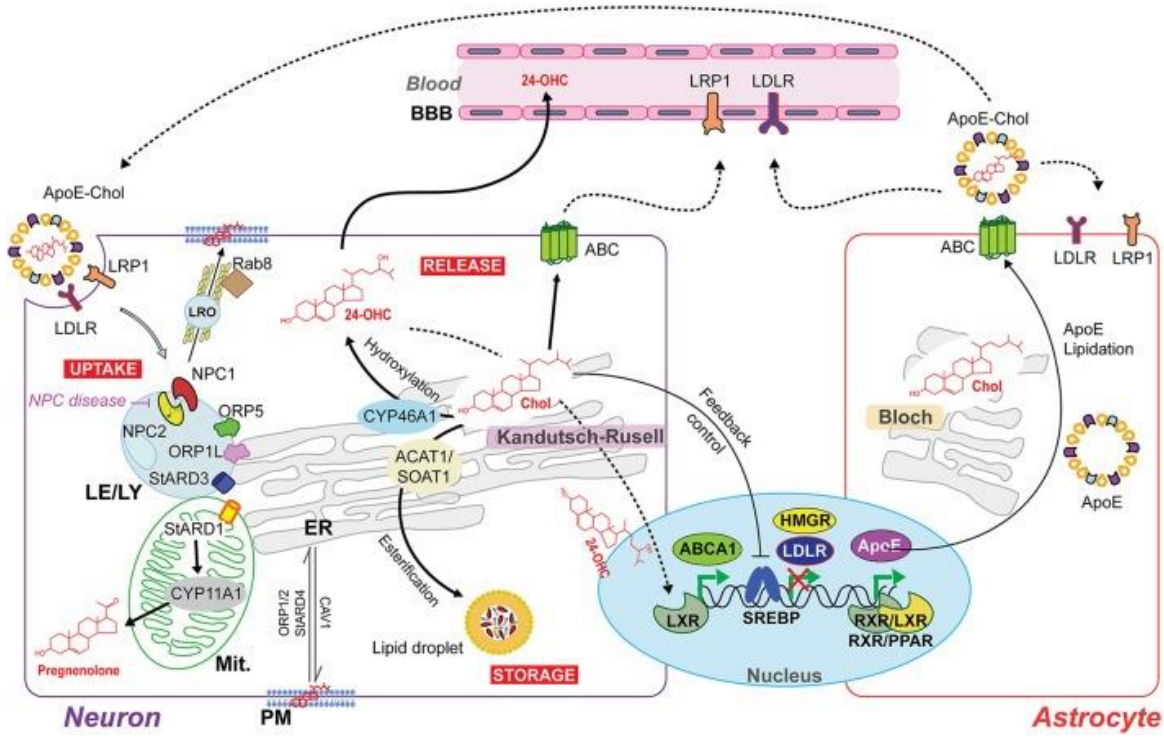

Figure 2. ***Cholesterol homeostasis in brain.*** *Cholesterol produced by astrocytes is delivered to neurons by the secretion of cholesterol-rich apolipoprotein E (ApoE-Chol). Cholesterol is taken by the cells through a receptor-mediated endocytosis of ApoE-Chol. Cholesterol overload is handle through its esterification by (ACAT1/SOAT1) and through release via ABC transporters or after CYP46A1-dependent conversion to 24-OHC which can freely cross the BBB and upregulate ABCA1 expression via activation of nuclear liver X receptor (LXR). (Arenas et al., 2017).*

Since cholesterol alteration as well as BDNF signalling impairment are both associated with the development of neurodegenerative diseases, we considered interesting to investigate whether BDNF can modulate cholesterol homeostasis, by focusing on its potential role in cholesterol trafficking between astrocytes and neurons. In particular, we analyzed the effect of BDNF on critical steps of cholesterol homeostasis, namely a) ApoE synthesis, b) cholesterol efflux from astrocytes and c) cholesterol incorporation into neurons (see *Chapter 2* of this thesis for details).

Apolipoprotein E

In the central nervous system (CNS), ApoE is the most abundantly produced apolipoprotein and is primarily synthesized by astrocytes and to a lesser extent by microglia (Shi and

Holtzman, 2018). In the CNS, cholesterol and phospholipids produced by glia are critical for formation and maintenance of healthy synapses (Pfrieger, 2010). As an apolipoprotein, ApoE forms in brain lipoprotein particles with lipids and cholesterol, namely high-density lipoprotein (HDL)-like particles, in order to mediate their transport between cells (Mahley, 2016). ApoE is crucial for cellular cholesterol efflux in which this sterol is transferred to the lipoprotein via ATP-binding cassette subfamily A member 1 (ABCA1) while the uptake of these particles by the cells is mediated through the binding of ApoE to LDL receptor family members (Mahley, 2016). *In vitro* studies with neuronal cell models and primary cells showed that ApoE plays a critical role in differentiation and neurite outgrowth through the activation of the Erk pathway (Huang and Mahley, 2014). In addition, *in vivo* studies showed that ApoE plays a role in the development, remodelling and regeneration of the nervous system (Han, 2004). Also, it was demonstrated that a genetic deficiency of ApoE results in a reduction of synapse number partially due to the loss of HDL-like particles (Lane-Donovan C, et al., 2016). Besides cholesterol trafficking, ApoE is involved in critical step of the onset and progression of Alzheimer's disease (AD), namely amyloid precursor protein processing and β-amyloid production, deposition and clearance (Bales et al., 1999; Yu et al., 2014).

In humans, ApoE is a polymorphic protein with three common isoforms, ApoE2, ApoE3, and ApoE4, which differ for a single amino acid substitution at the residues 112 and 158. In particular, ApoE3 has cysteine (Cys)-112 and arginine (Arg)-158, whereas ApoE4 has arginines and ApoE2 has cysteine on both sites (Kim et al., 2014; Mahley, 2016). These aminoacid differences among the isoforms significantly alter ApoE's folding structure affecting its ability to bind lipids, lipoprotein receptors and β-amyloid (Lin et al., 2018).

The ε4 isoform of ApoE (ApoE4) was identified as a major genetic risk factor for AD (Rebeck GW, 2017). In particular, compared with ApoE3/3 homozygosity, ApoE4 increases the risk of developing AD by 4-fold (heterozygotes) to 14-fold (homozygotes) and the age of onset of the pathology by 8 years for each ApoE4 allele (Mahley, 2016). In AD patients, the ε4 allele detrimentally triggers β-amyloid aggregation, induces heavier β-amyloid plaque formation, marked brain atrophy, faster disease progression and an exacerbated tau-mediated neurodegeneration compared with the other ApoE alleles (Uddin et al., 2018).

In addition to their effects on β-amyloid clearance, ApoE isoforms affect synaptic plasticity in an isoform-dependent manner. For instance, ApoE4 is associated with deficits in spatial learning and memory (Grootendorst et al., 2005; Knoferle et al., 2014), and with reduced dendritic arborization (Dumanis et al., 2009; Wang et al., 2005), neuronal activity (Gillespie et al., 2016), neurotransmitter release (Klein et al., 2010; Klein et al., 2014; Dolejší et al., 2016),

and dendritic spine density (Rodriguez et al., 2013; Dumanis et al., 2009; Ji et al., 2003). Interestingly, it was recently shown that ApoE4 can translocate to the nucleus, bind DNA, and act as a transcription factor in human glioblastoma cells In particular, the data indicated that the ApoE4 DNA binding sites include about 1700 gene promoter regions, including genes associated with synaptic function, neuroinflammation, and insulin resistance (Theendakara et al., 2016). ApoE4 was also shown to directly impair mitochondrial function, thus having deleterious effects on cerebral energy metabolism (Wolf et al., 2013). Furthermore, ApoE4 can induce endoplasmic reticulum stress in astrocytes (Zhong et al., 2009), but not in neurons (Brodbeck et al., 2011) thus suggesting that ApoE4 may alter neuronal metabolic functioning also affecting astrocytes, which provide neurons with essential metabolic support (Zhong et al., 2009). As regard to BDNF, it was demonstrated that the three ApoE isoforms differentially regulate BDNF expression and secretion from human astrocytes (Sen et al., 2017). In particular, the results indicate that the treatment with ApoE2 and ApoE3 mediate a positive regulation of BDNF release while ApoE4-treated cells secrete negligible amounts of the neurotrophin. These interactions of the ApoE isoforms with BDNF may help explain the increased risk of AD associated with the ApoE4 isoform.

Interplay between BDNF and diet

A further focus of this research project was to study the effect of unbalanced diet, particularly rich in sugars, on BDNF as well as others brain markers of brain functioning. A continued rise in children, adolescents and adults obesity has been described in the last forty years (McCrory et al., 2016; Lee and Yoon, 2018). Interestingly, hypothalamic reduction of BDNF or mutations in its receptor TrkB, are associated with hyperfagia, weight gain, and obesity (Sandrini et al., 2018). On the other hand, Smiljanic and co-workers recently demonstrated that a long-term dietary restriction upregulates BDNF expression and TrkB levels in cortex of middle-aged rats (Smiljanic et al. 2014). In addition, according to recent experimental studies, some dietary factors can influence both plasma and brain levels of BDNF. Among these, n-3 fatty acid (FA), vitamin E and flavonoids were found to positively influence BDNF expression (Cysneiros et al., 2010; Hou et al., 2010) while diets rich in saturated FA decrease brain levels of BDNF, neuronal plasticity and induce cognitive decline (Molteni et al., 2002; Wu et al., 2004; Pistell et al., 2010). Moreover, a seven days high fat/ high fructose diet, was associated with both BDNF and synaptic reduction in rat hippocampus (Calvo-Ochoa et al., 2014).

In the last decade, an increase in fructose consumption was registered (Campos et al., 2016) mainly because of a strong rise in using corn syrup for sweeten industrial foods and beverages. Fructose has been suggested to induce overweight and body weight gain as well as dyslipidaemia, insulin resistance and related metabolic diseases (Malik et al., 2010; Stanhope, 2016; Aragno and Mastrocola, 2017).

In the last decade, some studies demonstrated that fructose intake may also affects brain health inducing cognitive decline (Hsu et al., 2015; Mastrocola et al., 2016), a reduction of hippocampal neurogenesis (Van der Borght et al., 2011), widespread reactive gliosis, and altered mitochondrial activity in the hippocampus (Mastrocola et al., 2016). Most of these studies reported the effect of sugar-rich diets on brain by using long-term treatments (at least 4-8 weeks) particularly on adults animal models. Therefore, our aim was to investigate the early effect of fructose-rich diets not only in adults but also in young rats (see *Chapter 3* of this thesis for details).

References

Aragno M, Mastrocola R. (2017). Dietary Sugars and Endogenous Formation of Advanced Glycation Endproducts: Emerging Mechanisms of Disease. Nutrients. 9(4). pii: E385. doi: 10.3390/nu9040385.

Arenas F, Garcia-Ruiz C, Fernandez-Checa JC. (2017). Intracellular Cholesterol Trafficking and Impact in Neurodegeneration. Front Mol Neurosci. 10:382. doi:10.3389/fnmol.2017.00382.

Bales KR, Verina T, Cummins DJ, Du Y, Dodel RC, Saura J, Fishman CE, DeLong CA, Piccardo P, Petegnief V, Ghetti B, Paul SM. (1999). Apolipoprotein E is essential for amyloid deposition in the APP(V717F) transgenic mouse model of Alzheimer's disease. Proc Natl Acad Sci U S A.;96(26):15233-8.

Brodbeck J, McGuire J, Liu Z, Meyer-Franke A, Balestra ME, Jeong DE, Pleiss M, McComas C, Hess F, Witter D, Peterson S, Childers M, Goulet M, Liverton N, Hargreaves R, Freedman S, Weisgraber KH, Mahley RW, Huang Y. (2011). Structure-dependent impairment of intracellular apolipoprotein E4 trafficking and its detrimental effects are rescued by small-molecule structure correctors. J Biol Chem.; 286(19):17217-26. doi: 10.1074/jbc.M110.217380.

Calvo-Ochoa E, Hernandez-Ortega K, Ferrera P, Morimoto S, Arias C. (2014). Short-term high-fat-and-fructose feeding produces insulin signaling alterations accompanied by neurite and synaptic reduction and astroglial activation in the rat hippocampus. J Cereb Blood Flow Metab.34:1001-8. doi: 10.1038/jcbfm.2014.48.

Campos VC, Tappy L. (2016). Physiological handling of dietary fructose-containing sugars: implications for health. Int J Obes (Lond) Suppl 1:S6-11. doi: 10.1038/ijo.2016.8.

Cysneiros RM, Ferrari D, Arida RM, Terra VC, de Almeida AC, Cavalheiro EA, Scorza FA. (2010). Qualitative analysis of hippocampal plastic changes in rats with epilepsy supplemented with oral omega-3 fatty acids. Epilepsy Behav. 17(1):33-8. doi: 10.1016/j.yebeh.2009.11.006.

Dolejší E, Liraz O, Rudajev V, Zimčík P, Doležal V, Michaelson DM. (2016). Apolipoprotein E4 reduces evoked hippocampal acetylcholine release in adult mice. J Neurochem.; 136(3):503-9. doi: 10.1111/jnc.13417.

Dumanis SB, Tesoriero JA, Babus LW, Nguyen MT, Trotter JH, Ladu MJ, Weeber EJ, Turner RS, Xu B, Rebeck GW, Hoe HS. (2009). ApoE4 decreases spine density and dendritic complexity in cortical neurons in vivo. J Neurosci.; 29(48):15317-22. doi: 10.1523/JNEUROSCI.4026-09.2009.

Egawa J, Pearn ML, Lemkuil BP, Patel PM, Head BP. (2016). Membrane lipid rafts and neurobiology: age-related changes in membrane lipids and loss of neuronal function. J Physiol; 594(16):4565-79. doi: 10.1113/JP270590.

Gillespie AK, Jones EA, Lin YH, Karlsson MP, Kay K, Yoon SY, Tong LM, Nova P, Carr JS, Frank LM, Huang Y. (2016). Apolipoprotein E4 Causes Age-Dependent Disruption of Slow Gamma Oscillations during Hippocampal Sharp-Wave Ripples. Neuron.;90(4):740-51. doi: 10.1016/j.neuron.2016.04.009.

Gomes JR, Costa JT, Melo CV, Felizzi F, Monteiro P, Pinto MJ, Inácio AR, Wieloch T, Almeida RD, Grãos M, Duarte CB. (2012). Excitotoxicity downregulates TrkB.FL signaling and upregulates the neuroprotective truncated TrkB receptors in cultured hippocampal and striatal neurons. J Neurosci 32: 4610-4622. doi: 10.1523/JNEUROSCI. 0374-12.2012.

Grootendorst JA, Bour E, Vogel C, Kelche P, Sullivan M, Dodart JC, Bales K, Mathis C. (2005). Human apoE targeted replacement mouse lines: h-apoE4 and h-apoE3 mice differ on spatial memory performance and avoidance behavior. Behav Brain Res.; 159(1):1-14. doi: 10.1016/j.bbr.2004.09.019

Han X. (2004). The role of apolipoprotein E in lipid metabolism in the central nervous system. Cell Mol Life Sci. ;61(15):1896-906.

Herz J. (2009). Apolipoprotein E Receptors in the Nervous System. Curr Opin Lipidol 20(3):190-6. doi: 10.1097/MOL.0b013e32832d3a10.

Hou Y, Aboukhatwa MA, Lei DL, Manaye K, Khan I, Luo Y. (2010). Anti-depressant natural flavonols modulate BDNF and beta amyloid in neurons and hippocampus of double TgAD mice. Neuropharmacology; 58(6):911–20. doi: 10.1016/j.neuropharm.2009.11.002.

Hsu TM, Konanur VR, Taing L, Usui R, Kayser BD, Goran MI, Kanoski SE. (2015). Effects of sucrose and high fructose corn syrup consumption on spatial memory function and hippocampal neuroinflammation in adolescent rats. Hippocampus. 25(2):227-39. doi: 10.1002/hipo.22368.

Huang EJ, Reichardt LF. (2003). Trk receptors: roles in neuronal signal transduction. Annu Rev Biochem. 72:609–642. doi: 10.1146/annurev.biochem.72.121801.161629.

Huang Y, Mahley RW. (2014). Apolipoprotein E: Structure and Function in Lipid Metabolism, Neurobiology, and Alzheimer's Diseases. Neurobiol Dis; 72PA: 3–12. doi:10.1016/j.nbd.2014.08.025.

Ikonen E. (2008). Cellular cholesterol trafficking and compartmentalization. Nat Rev Mol Cell Biol; 9(2):125-38. doi: 10.1038/nrm2336.

Ji Y, Gong Y, Gan W, Beach T, Holtzman DM, Wisniewski T. (2003). Apolipoprotein E isoform-specific regulation of dendritic spine morphology in apolipoprotein E transgenic mice and Alzheimer's disease patients. Neuroscience.; 122(2):305-15.

Kim J, Yoon H, Basak J, Kim J. (2014). Apolipoprotein E in synaptic plasticity and Alzheimer's disease: potential cellular and molecular mechanisms. Mol Cells.; 37(11):767-76. doi: 10.14348/molcells.2014.0248.

Klein RC, Acheson SK, Mace BE, Sullivan PM, Moore SD. (2014). Altered neurotransmission in the lateral amygdala in aged human apoE4 targeted replacement mice. Neurobiol Aging.; 35(9):2046-52. doi: 10.1016/j.neurobiolaging.2014.02.019.

Klein RC, Mace BE, Moore SD, Sullivan PM. (2010). Progressive loss of synaptic integrity in human apolipoprotein E4 targeted replacement mice and attenuation by apolipoprotein E2. Neuroscience.; 171(4):1265-72. doi: 10.1016/j.neuroscience.2010.10.027.

Knoferle J, Yoon SY, Walker D, Leung L, Gillespie AK, Tong LM, Bien-Ly N, Huang Y. (2014). Apolipoprotein E4 produced in GABAergic interneurons causes learning and memory deficits in mice. J Neurosci.;34(42):14069-78. doi: 10.1523/JNEUROSCI.2281-14.2014.

Lane-Donovan C, Wong WM, Durakoglugil MS, Wasser CR, Jiang S, Xian X, Herz J. (2016). Genetic Restoration of Plasma ApoE Improves Cognition and Partially Restores Synaptic Defects in ApoE-Deficient Mice. J Neurosci.;36(39):10141-50. doi: 10.1523/JNEUROSCI.1054-16.2016.

Leal G, Bramham CR, Duarte CB. (2016). BDNF and Hippocampal Synaptic Plasticity. Vitam Horm. 104:153-195. doi: 10.1016/bs.vh.2016.10.004.

Lee EY, Yoon KH. (2018). Epidemic obesity in children and adolescents: risk factors and prevention. Front Med. doi: 10.1007/s11684-018-0640-1. [Epub ahead of print]

Lima Giacobbo B, Doorduin J, Klein HC, Dierckx RAJO, Bromberg E, de Vries EFJ. (2018). Brain-Derived Neurotrophic Factor in Brain Disorders: Focus on Neuroinflammation. Mol Neurobiol. doi: 10.1007/s12035-018-1283-6.

Lin YT, Seo J, Gao F, Feldman HM, Wen HL, Penney J, Cam HP, Gjoneska E, Raja WK, Cheng J, Rueda R, Kritskiy O, Abdurrob F, Peng Z, Milo B, Yu CJ, Elmsaouri S, Dey D, Ko T, Yankner BA, Tsai LH. (2018). APOE4 Causes Widespread Molecular and Cellular Alterations Associated with Alzheimer's Disease Phenotypes in Human iPSC-Derived Brain Cell Types. Neuron.; 98(6):1141-1154.e7. doi: 10.1016/j.neuron.2018.05.008.

Lu, B. (2003). BDNF and activity-dependent synaptic modulation. Learn. Mem.10:86–98 doi: 10.1101/lm.54603.

Mahley RW. (2016). Central Nervous System Lipoproteins: ApoE and Regulation of Cholesterol Metabolism. Arterioscler Thromb Vasc Biol; 36(7): 1305–1315. doi:10.1161/ATVBAHA.116.307023.

Malik VS, Popkin BM, Bray GA, Després JP, Hu FB. (2010). Sugar-sweetened beverages, obesity, type 2 diabetes mellitus, and cardiovascular disease risk. Circulation. 121 (11):1356-64. doi: 10.1161/CIRCULATIONAHA.109.876185.

Mastrocola R, Nigro D, Cento AS, Chiazza F, Collino M, Aragno M. (2016). High-fructose intake as risk factor for neurodegeneration: Key role for carboxymethyllysine accumulation in mice hippocampal neurons. Neurobiol Dis 89:65-75. doi: 10.1016/j.nbd.2016.02.005.

McCrory MA, Shaw AC, Lee JA. (2016). Energy and Nutrient Timing for Weight Control: Does Timing of Ingestion Matter? Endocrinol Metab Clin North Am. 45(3):689-718. doi: 10.1016/j.ecl.2016.04.017.

Molteni R, Barnard RJ, Ying Z, Roberts CK, Gómez-Pinilla F. (2002) A high-fat, refined sugar diet reduces hippocampal brain-derived neurotrophic factor, neuronal plasticity, and learning. Neuroscience. 112:803-14.

Moutinho M, Nunes MJ, Rodrigues E. (2016). Cholesterol 24-hydroxylase: brain cholesterol metabolism and beyond. Biochim. Biophys. Acta 1861 (12 Pt A), 1911–1920. doi: 10.1016/j.bbalip.2016.09.011

Pfrieger FW. (2010). Role of glial cells in the formation and maintenance of synapses. Brain Res Rev.; 63(1-2):39-46. doi: 10.1016/j.brainresrev.2009.11.002.

Pistell PJ, Morrison CD, Gupta S, Knight AG, Keller JN, Ingram DK, Bruce-Keller AJ. (2010). Cognitive impairment following high fat diet consumption is associated with brain inflammation. J Neuroimmunol; 219(1–2):25–32. doi: 10.1016/j.jneuroim.2009.11.010.

Posse De Chaves EI, Vance DE, Campenot RB, Kiss RS, Vance JE. (2000). Uptake of lipoproteins for axonal growth of sympathetic neurons. J Biol Chem 275(26):19883-90.

Rebeck GW. (2017). The role of APOE on lipid homeostasis and inflammation in normal brains. J Lipid Res.; 58(8):1493-1499. doi: 10.1194/jlr.R075408.

Reichardt LF. (2006). Neurotrophin-regulated signalling pathways. Philos Trans R Soc Lond B Biol Sci. 2006 Sep 29;361(1473):1545-64. doi: 10.1098/rstb.2006.1894.

Rodriguez GA, Burns MP, Weeber EJ, Rebeck GW. (2013). Young APOE4 targeted replacement mice exhibit poor spatial learning and memory, with reduced dendritic spine density in the medial entorhinal cortex. Learn Mem.; 20(5):256-66. doi: 10.1101/lm.030031.112.

Sandrini L, Di Minno A, Amadio P, Ieraci A, Tremoli E, Barbieri SS. (2018). Association between Obesity and Circulating Brain-Derived Neurotrophic Factor (BDNF) Levels: Systematic Review of Literature and Meta-Analysis. Int J Mol Sci.;19(8). pii: E2281. doi: 10.3390/ijms19082281.

Sarbassov DD, Ali SM, Sabatini DM. (2005). Growing roles for the mTOR pathway. Curr Opin Cell Biol. 17(6):596-603. Epub 2005 Oct 13. doi: 10.1016/j.ceb.2005.09.009.

Sen A, Nelson TJ, Alkon DL. (2017). ApoE isoforms differentially regulates cleavage and secretion of BDNF. Mol Brain.; 10(1):19. doi: 10.1186/s13041-017-0301-3.

Shi Y, Holtzman DM. (2018). Interplay between innate immunity and Alzheimer disease: APOE and TREM2 in the spotlight. Nat Rev Immunol. doi: 10.1038/s41577-018-0051-1. [Epub ahead of print]

Smiljanic K, Pesic V, Mladenovic Djordjevic A, Pavkovic Z, Brkic M, Ruzdijic S, Kanazir S. (2015). Long-term dietary restriction differentially affects the expression of BDNF and its receptors in the cortex and hippocampus of middle-aged and aged male rats. Biogerontology. 16(1):71-83. doi: 10.1007/s10522-014-9537-9.

Stanhope KL. (2016). Sugar consumption, metabolic disease and obesity: The state of the controversy Crit Rev Clin Lab Sci 53:52-67. doi: 10.3109/10408363.2015.1084990.

Suzuki S, Kiyosue K, Hazama S, Ogura A, Kashihara M, Hara T, Koshimizu H, Kojima M. (2007). Brain-derived neurotrophic factor regulates cholesterol metabolism for synapse development. J Neurosci. 27(24):6417-27. doi:10.1523/JNEUROSCI.0690-07.2007.

Suzuki S, Numakawa T, Shimazu K, Koshimizu H, Hara T, Hatanaka H, Mei L, Lu B, Kojima M.(2004). BDNF-induced recruitment of TrkB receptor into neuronal lipid rafts: roles in synaptic modulation. J Cell Biol. 167(6):1205-15. Epub 2004 Dec 13. doi: 10.1083/jcb.200404106.

Takei N, Inamura N, Kawamura M, Namba H, Hara K, Yonezawa K, Nawa H. (2004). Brain-derived neurotrophic factor induces mammalian target of rapamycin-dependent local activation of translation machinery and protein synthesis in neuronal dendrites. J Neurosci. 24(44):9760-9. doi:10.1523/JNEUROSCI.1427-04.2004.

Theendakara V, Peters-Libeu CA, Spilman P, Poksay KS, Bredesen DE, Rao RV. (2016). Direct Transcriptional Effects of Apolipoprotein E. J Neurosci.;36(3):685-700. doi:10.1523/JNEUROSCI.3562-15.2016.

Uddin MS, Kabir MT, Al Mamun A, Abdel-Daim MM, Barreto GE, Ashraf GM. (2018). APOE and Alzheimer's Disease: Evidence Mounts that Targeting APOE4 may Combat Alzheimer's Pathogenesis. Mol Neurobiol. doi: 10.1007/s12035-018-1237-z.

Van der Borght K, Köhnke R, Göransson N, Deierborg T, Brundin P, Erlanson-Albertsson C, Lindqvist A. (2011). Reduced neurogenesis in the rat hippocampus following high fructose consumption. Regul Pept 167:26-30. doi: 10.1016/j.regpep.2010.11.002.

Vidaurre OG, Gascón S, Deogracias R, Sobrado M, Cuadrado E, Montaner J, Rodríguez-Peña A, Díaz-Guerra M. (2012). Imbalance of neurotrophin receptor isoforms TrkB-FL/TrkB-T1 induces neuronal death in excitotoxicity. Cell Death Dis 3: e256. doi: 10.1038/cddis.2011.143.

Vitali C, Wellington CL, Calabresi L. (2014). HDL and cholesterol handling in the brain. Cardiovasc Res; 103(3):405-13. doi: 10.1093/cvr/cvu148.

Wang C, Wilson WA, Moore SD, Mace BE, Maeda N, Schmechel DE, Sullivan PM. (2005). Human apoE4-targeted replacement mice display synaptic deficits in the absence of neuropathology. Neurobiol Dis. ;18(2):390-8.

Wolf AB, Valla J, Bu G, Kim J, LaDu MJ, Reiman EM, Caselli RJ. (2013). Apolipoprotein E as a β-amyloid-independent factor in Alzheimer's disease. Alzheimers Res Ther.; 5(5):38. doi: 10.1186/alzrt204. eCollection 2013.

Wu A, Ying Z, Gomez-Pinilla F. (2004). The interplay between oxidative stress and brain-derived neurotrophic factor modulates the outcome of a saturated fat diet on synaptic plasticity and cognition. Eur J Neurosci.; 19:1699-707. doi: 10.1111/j.1460-9568.2004.03246.x.

Yoshii A, Constantine-Paton M. (2010). Postsynaptic BDNF-TrkB signaling in synapse maturation, plasticity, and disease. Dev Neurobiol. 70(5):304-22. doi: 10.1002/dneu.20765.

Yu JT, Tan L, Hardy J. (2014). Apolipoprotein E in Alzheimer's disease: an update. Annu Rev Neurosci.; 37:79-100. doi: 10.1146/annurev-neuro-071013-014300.

Zhang J, Liu Q. (2015). Cholesterol metabolism and homeostasis in the brain. Protein Cell. 6(4):254-64. doi: 10.1007/s13238-014-0131-3.

Zhong N, Ramaswamy G, Weisgraber KH. (2009). Apolipoprotein E4 domain interaction induces endoplasmic reticulum stress and impairs astrocyte function. J Biol Chem.;284(40):27273-80. doi: 10.1074/jbc.M109.014464.

Chapter 2

Brain-derived neurotrophic factor modulates cholesterol homeostasis and apolipoprotein E synthesis in human cell models of astrocytes and neurons.

*Maria Stefania Spagnuolo, Aldo Donizetti, **Lucia Iannotta**, Vincenza Aliperti, Chiara Cupidi, Amalia Cecilia Bruni & Cigliano Luisa.*

Journal of Cellular Physiology, 2018. doi: 10.1007/s12035-017-0518-2.

Introduction

Brain-derived neurotrophic factor (BDNF) is a member of the neurotrophin family of growth factors, and regulates neuronal survival, differentiation and plasticity by activating the receptor tyrosine kinase TrkB and p75 low-affinity neurotrophin receptor (Huang and Reichardt, 2001; Poo, 2001). Binding of BDNF rapidly activates TrkB, which in turn triggers multiple intracellular signaling pathways (Reichardt, 2006). Cholesterol-rich microdomains, called lipid rafts, provide a signaling platform for neurotrophic factor signaling (Simons and Toomre, 2000; Paratcha and Ibáñez, 2002), and are required for BDNF-induced synaptic modulation (Suzuki et al., 2004) and chemotrophic guidance of nerve growth cones (Guirland et al., 2004). Pharmacological depletion of cholesterol reduced BDNF-dependent synaptic transmission (Suzuki et al., 2004), suggesting a fundamental role of cholesterol in the neurotrophin biology. It has been previously demonstrated that both BDNF and cholesterol increase dramatically during cortical development (Suzuki et al., 2004), evidencing that this neurotrophic factor regulates cholesterol biosynthesis in the brain. Indeed, BDNF was demonstrated to elicit cholesterol biosynthesis and promote the accumulation of presynaptic proteins in cholesterol-rich lipid rafts for the development of presynaptic functions in the central nervous system (CNS) (Suzuki et al., 2007). The maintenance of the correct balance of cholesterol is critical for neuronal function, and any alteration in its level may severely affect brain performance (Cartocci et al., 2017). For instance, suppression of the mevalonate pathway was shown to cause defects in learning and memory (Kotti et al., 2006), highlighting the importance of cholesterol for the CNS. Further, impaired brain cholesterol distribution and metabolism has been pointed to as likely involved in the pathogenesis of Alzheimer's disease (AD), and other neurodegenerative diseases (Solomon et al., 2007; Foley, 2010; Vance, 2012). In the brain, cholesterol is transported by high-density lipoprotein (HDL)-like particles, whose major protein component is the Apolipoprotein E (ApoE), which mainly mediates the transport of lipids between astrocytes and neurons. Cholesterol is locally synthesized in the CNS and brain cholesterol metabolism is largely separated from peripheral cholesterol metabolism by the blood-brain barrier. Cholesterol synthesis and clearance are highly regulated, thus keeping overall levels constant (Vitali et al., 2014). During development and myelinogenesis, both astrocytes and neurons produce cholesterol in a cell-autonomous manner, while, as the brain matures, neurons downregulate the expression of many genes involved in the cholesterol synthesis (Vitali et al., 2014). Therefore adult neurons rely on the import of cholesterol released from astrocytes (Ikonen, 2008). In particular, astrocytes secrete cholesterol via ApoE-containing lipoproteins, which are lipidated by ATP binding cassette (ABC) transporters. The

low-density lipoprotein receptor (LDLR) and the low-density lipoprotein receptor related protein 1 (LRP1) mediate uptake of cholesterol by neurons (Posse de Chaves et al., 2000; Herz, 2009), and neuronal uptake of cholesterol helps to maintain membrane plasticity, cellular function, and synaptic integrity. In this way, cholesterol is shuttled from astrocytes to neurons (Mauch et al., 2001; Vance and Hayashi, 2010). Despite the importance of cholesterol trafficking between astrocytes and neurons, the effect of BDNF on physiological players involved in this pathway remains to be identified. Hence, we investigated the ability of BDNF to influence cholesterol metabolism by focusing on the influence of this neurotrophin on ApoE synthesis, cholesterol efflux from astrocytes and cholesterol incorporation into neurons.

Materials and methods

Materials

Bovine serum albumin fraction V (BSA), lecithin, cholesterol, retinoic acid (RA) mouse anti-β actin IgG, goat anti-rabbit Horseradish Peroxidase-conjugated IgG (GAR-HRP), goat anti-mouse Horseradish Peroxidase-conjugated IgG (GAM-HRP), rabbit anti-goat Horseradish Peroxidase-conjugated IgG (RAG-HRP), o-Phenylenediamine, and MTT [3-(4,5-dimethylthiazol-2-yl)-2,5- diphenyltetrazolium bromide], were purchased from Sigma-Aldrich (St. Louis, MO, USA). Recombinant human ApoE3 and recombinant human BDNF were from PeproTech (London, UK). Goat anti-human ApoE IgG (Chemicon), Protein G Plus-Agarose Suspension (Calbiochem), and the chemiluminescent HRP substrate (Immobilon Western) were purchased from Merk Millipore (Milano, Italy). Mouse anti-human ApoE IgG, and rabbit anti-human TrkB IgG were purchased from Santa Cruz Biotechnology (Santa Cruz, CA, USA). The dye reagent for protein titration, and the polyvinylidene difluoride (PVDF) membrane were from Bio-Rad (Bio-Rad, Hercules, CA). Polystyrene 96-wells ELISA MaxiSorp plates, 96-, 24-, and 6-well cell culture plates were purchased from Nunc (Roskilde, Denmark). Fuji Super RX 100 film was from Laboratorio Elettronico Di Precisione (Napoli, Italy). DMEM, F12, fetal bovine serum (FBS), L-glutamine, Neuroblastoma growth supplement N2, penicillin and streptomycin were from Gibco (Life Technologies Italy, Monza, Italy). Cell culture flasks, and sterile pipettes of Sarstedt (Verona, Italy) were used. [1α,2α-3H]-Cholesterol (52.5 Ci/mmol) and the liquid scintillation counting cocktail Ultima Gold were obtained from Perkin-Elmer (Boston, MA, USA).

Cell culture

The human neuroblastoma cell line SH-SY5Y and the human glioblastoma-astrocytoma cell line U-87 MG were from ATCC (distributed by LGC Standards, Milano, Italy). Normal human astrocyte (NHA) were from Lonza (distributed by Euroclone, Milano, Italy). SH-SY5Y cells (500,000) were seeded in 50 ml tissue culture flasks (25 cm2 surface), and grown in a mixture of DMEM and F12 medium (1:1, v:v) supplemented with 10% FBS, 2 mM L-glutamine, 100 U/mL penicillin, and 100 µg/mL streptomycin (complete medium) at 37°C and under humidified atmosphere of 5% CO2 in air. The medium was changed twice a week, and cells were sub-cultivated when confluent. Cells were differentiated to mature neuronal phenotype by incubation in low-serum medium containing RA, essentially according to published procedures (Påhlman et al., 1984; Nordin- Andersson et al., 2003). In detail, the complete medium was changed to DMEM/F12 containing 1 % FBS, 2 mM L-glutamine, 100 IU/mL penicillin, 100 µg/mL streptomycin, 0.5% neuroblastoma growth supplement N2. The cells were seeded into 96-, 12-, 24-, or 6-well plates (at the cell density reported below), and allowed to attach for 4 h before adding RA (10 µM final concentration). Cells were differentiated for six days, and RA was added every 48 hours. The differentiated cells were finally used for the assays reported below. NHA were seeded in 50 ml tissue culture flasks (5,000 cells/cm2), and grown in recommended medium AGM™ BulletKit™ (Lonza), according with manufacturer's instructions. Culture medium was replenished every 48 h, and cells were subcultivated after reaching 85% confluence. In detail, NHA were seeded in 96-, 24- or 6-well plates at 10,000 cells/cm2 in AGM medium, and incubated (37°C, 5% CO2) for 20 hours. After removal of the medium, and washing with serum-free medium, the cells were used in the assays described below. U-87 MG cells (900,000 cells) were seeded in 250 mL tissue culture flasks (75 cm2 surface), and grown in DMEM supplemented with 10% FBS, 2 mM L-glutamine, 100 U/mL penicillin, and 100 µg/mL streptomycin (complete medium) at 37°C under humidified atmosphere of 5% CO2 in air. The medium was changed twice a week, and cells were sub-cultivated when confluent. U-87 MG cells were seeded into 96- or 6-well plates (at 15,000 cells/well or 400,000 cells/well density, respectively) in complete medium, and incubated (37°C, 5% CO2) for 20 hours. After removal of the medium, and washing with DMEM, the cells were used in the assays described below.

Brain tissues

The study was conducted with brain samples from 4 patients affected by familial AD (FAD) and bearing the Met146Leu mutation of the Presenilin1 gene. The mean age of death of the

patients was 48 ± 8.2 years, and they were at the terminal stage of dementia (stage 5, according to the Clinical Dementia Rating scale). For all patients, the Braak staging for AD pathology (AD-related neurofibrillary pathology) was VI. Brain tissues from a patient affected by spinocerebellar ataxia 17 (SCA17) and from a healthy age-matched control subject were also analysed in this study. The healthy subject died for accidental intracerebral bleeding in left brain hemisphere, and the sample was taken from the contralateral brain hemisphere. Histopathological lesions suggestive of AD (neurofibrillary pathology, deposition of Aβ protein) were excluded in the control subject. The ApoE genotype, determined on DNA from peripheral blood lymphocytes, was E3/E3 for all patients. Tissues were sampled from prefrontal cortical areas. The brain samples were collected at 4-36 hours post-mortem and stored at -80°C until use. Brain tissue samples from human subjects were provided by the Regional Neurogenetic Center (CRN, ASP CZ, Lamezia Terme). All brain donors or their legal tutors gave written informed consent during their lifetime. The protocol for the collection of the brains and their use in the study conformed to The Code of Ethics of the World Medical Association (Declaration of Helsinki), printed in the British Medical Journal (18 July 1964), and was supported by the Italian Health Ministry with appropriate local Ethics committee approval (Prot n° 21334-30/12/2003).

TrkB expression and cell viability assay

SH-SY5Y cells (500,000 cells/well into 6-well plates) were differentiated for six days as above described. U-87 MG or NHA cells were cultured into 6 well-plate (400,000 or 100,000 cells/well respectively) for 20 hours in their specific complete medium. Medium was then removed, cells were rinsed with serum-free medium, and then incubated (20 h, 37°C) in serum free medium. U-87 MG and SH-SY5Y were detached by treatment (5 min, 37°C) with 500 µl of trypsin (TrypLE Express, Gibco), while NHA were detached by treatment with ReagentPack™ (Lonza), according with the manufacturer's instructions. Cells were then lysed with 0.1 mL of RIPA buffer (150 mM NaCl, 50 mM Tris-HCl, 0.5% NP-40, 0.5% sodium deoxycholate, 0.1% SDS, pH 8) containing Tissue Protease Inhibitor Cocktail (Sigma-Aldrich, 1:500, v/v) and Tissue Phosphatase inhibitor cocktail (Sigma-Aldrich, 1:100, v/v). The lysates were centrifuged (12,000 g, 30 min, 4°C), and analyzed for their protein concentration (Bradford, 1976). Aliquots (60 µg) of lysates were fractionated by 10% SDS-PAGE and blotted onto PVDF membrane for revealing TrkB. In detail, after protein transfer onto PVDF membrane, the membrane was rinsed in T-TBS (130 mM NaCl, 20 mM Tris-HCl, 0.05% Tween 20, pH 7.4), blocked with T-TBS containing 5% non-fat milk (1 h, 37°C), and finally incubated

(overnight, 4°C) with rabbit anti-human TrkB IgG (1: 1,000 dilution in T-TBS containing 3% non-fat milk), followed by GAR-HRP IgG (1: 5,000 dilution; 1h, 37°C). After TrkB detection, the membrane was extensively washed with T-TBS, and submerged in stripping buffer (100 mM β-mercaptoethanol, 2% SDS, 62.5 mM Tris-HCl, pH 6.7; 45 min, 50°C). Membrane was then incubated (overnight, 4°C) with mouse anti-β-actin IgG (1:1,000 dilution in T-TBS containing 0.25% non-fat milk) followed by GAM-HRP IgG (1:10,000 dilution). The immunocomplexes were detected by the ECL detection system. In order to assess whether BDNF affects astrocytes survival, U-87 MG or NHA were cultured (96 wellplates; 15,000 or 4000 cells/well respectively) in complete medium for 20 hours. After medium removal, cells were rinsed and then incubated (20 h, 37°C) in serum-free medium containing different amounts of BDNF (0, 5, 10, 20, or 30 ng/mL). The medium was then removed and cell survival was evaluated by MTT assay, as previously described (Spagnuolo et al., 2015, Valiante et al., 2015). The data were expressed as viability percentage, assuming the absorbance value from untreated cells as 100%.

BDNF effect on cholesterol efflux

Basal cellular cholesterol efflux from astrocytes was measured essentially according to Spagnuolo et al. (2014 a). In detail, NHA (24 well-plates; 18,000 cells/well) or U-87 MG (96 well-plates; 15,000 cells/well) were cultured in their specific complete medium for 20 hours. After medium removal, cells were rinsed with serum free medium, and labeled by incubation (20 h, 37°C) with [1α,2α-3H]- Cholesterol (52.5 Ci/mmol; 0.026 μCi/well) in DMEM (U-87 MG) containing 0.5% FBS, 100 IU penicillin/mL, 100 μg streptomycin/mL or in AGM medium (NHA), in presence of different amounts of BDNF (0, 5, 10 or 20 ng/mL). The medium was removed, cells were rinsed twice, and then incubated in serum-free medium containing 0.2% BSA. Media samples were collected after 5 hours, and cleared of any cellular debris by centrifugation at 400 g for 5 min. The cells were extensively washed, lysed with 0.1 M NaOH, and finally centrifuged at 12,000 g for 30 min. Aliquots (70 μL) of supernatants and lysates were then analysed by scintillation counting, and the amount of cholesterol effluxed to the medium was calculated as a percentage of total radioactivity in the cell lysates and medium. Experiments were routinely performed in triplicate and repeated three times.

RNA isolation, retrotranscription and quantitative PCR (qPCR) analysis

NHA (100,000 cells/well) or U-87 MG (400,000 cells/well) were seeded into 6 well-plate in their specific complete medium, and cultured for 20 hours. After medium removal, cells were

rinsed, and incubated (0, 1 or 24 h, 37°C) in serum free medium containing 10 ng/mL of BDNF. SH-SY5Y were seeded in low-serum medium into a 6-well plate (500,000 cells/well), as above described, and cultured for six days in RA-supplemented medium. After removal of the culture medium, the cells were incubated (20 h, 37°C) in serum-free DMEM/F12 containing 0.2% BSA, 100 IU/mL penicillin, 100 µg/mL streptomycin, 2 mM L-glutamine, and different amounts of cholesterol (0, 1.5, or 4.5 µM). At the end of each treatment, total cellular RNA was isolated using Trizol Reagent (Invitrogen) according to the manufacturer's instructions. The concentration and the purity of the RNA sample were assessed using NanoDrop® 1000 (Thermo Scientific). For the ApoE and ABCA1 gene expression analysis in U-87 MG and NHA cells, 1 µg of RNA was reverse transcribed into cDNA using SuperScript III reverse transcriptase (Invitrogen). For BDNF expression analysis in SH-SY5Y, we used a couple of primers both designed in the CDS containing exon 9. For this reason, a DNase treatment was performed accordingly with the manufacturer's instructions, before cDNA synthesis to efficiently remove contaminating genomic DNA from the total RNA. For BDNF gene expression analysis, l.5 µg of RNA was reverse transcribed into cDNA using SuperScript III reverse transcriptase (Invitrogen). qPCR was performed in technical duplicate using the SYBR green method and an Applied Biosystems 7500 System. The reaction mixture contained 20 ng of cDNA template for ApoE and ABCA1 genes or 75 ng of cDNA template for BDNF gene. The reaction mixture contained 400 nM of each forward and reverse primer in a final volume of 15 µL for the analysis of ApoE and ABCA1 in U-87 MG and for analysis of BDNF and HMGCR in SH-SY5Y. For the gene expression analysis in NHA cells, the qPCR reaction was optimized using a different couple of primers for ApoE (indicated by the subscript in the Supplementary Table 1) and by a reaction mixture containing 400 nM of each forward and reverse primer for ABCA1 and ApoE, and 600 nM of each forward and reverse primer for the reference gene hypoxanthine phosphoribosyltransferase 1 (HPRT1) in a final volume of 15 µL. The PCR cycle parameters included a denaturation step (95°C for 10 minutes) followed by 40 cycles of amplification and quantification (95°C for 35 seconds, 60°C for 1 minute). Relative gene expression levels were normalized to HPRT1 and calculated by the $2^{-\Delta\Delta Ct}$ method. The sequences of the primers used are reported in Supplementary Table 1. The results from independent biological replicates in triplicate are expressed as mean ± SEM. Statistical analysis of the qPCR data was carried out using a two-tailed t test (Prism 6 software) with a p-value cut-off of 0.05.

ApoE secretion by astrocyte

NHA or U-87 MG were seeded into 6 well-plate (100,000 or 400,000 cells/well respectively) in complete AGM medium or DMEM, respectively, and cultured for 20 hours. After medium removal, cells were rinsed, and incubated (24 h, 37°C) in serum free medium containing different amounts of BDNF (0, 5, 10, or 20 ng/mL). At the end of incubation, the cells were extensively washed with serum free medium, detached and lysed with RIPA buffer as above described, and analyzed for their protein concentration (Bradford, 1976). Media samples were collected, supplemented with Tissue Protease Inhibitor Cocktail (Sigma-Aldrich, 1:500, v/v), cleared of any cellular debris by centrifugation (400 g, 10 min), and finally immunoprecipitated (overnight, 4°C) with 1 µg of goat anti-human ApoE (NHA) or with 1 µg of mouse anti-human ApoE (U-87 MG). Twenty µl of protein G Plus Agarose Suspension were added to each sample, and a further incubation (3 h, 4°C) was carried out. Immunoprecipitates were collected by centrifugation (10 min, 300 g), washed with TBS (130 mM NaCl, 20 mM Tris-HCl, pH 7.4) containing 0.05% SDS, fractionated by 12.5% SDS-PAGE and finally blotted onto PVDF membrane for revealing ApoE. After blocking with T-TBS containing 5% non-fat milk (1 h, 37°C), the membrane was incubated (overnight, 4°C) with goat anti-human ApoE IgG (U-87 MG; 1: 500 dilution in T-TBS containing 0.25% non-fat milk) or with mouse anti-ApoE IgG (NHA; 1: 300 dilution in TTBS containing 3% BSA), followed by RAG-HRP IgG (1: 20,000 dilution; 1h, 37°C) or GAM-HRP IgG (1: 40,000 dilution; 1 h, 37°C) respectively. The immunocomplexes were detected by the ECL detection system. Quantitative densitometry of the bands was carried out by analyzing digital images of X-ray films exposed to immunostained membranes. Quantification of the signal was performed by Un- Scan-It gel software (Silk Scientific, UT, USA). The intensities of the band was calculated as total pixels, and band intensities per mg of cell protein were then calculated.

Analysis of human brain homogenates by Western Blotting

Postmortem brain tissues from one healthy subject, four AD patients, and one subject affected by SCA17 were homogenized in ice cold RIPA buffer (1:7, w/v) containing Tissue Protease Inhibitor Cocktail (1:500, v/v) and Tissue Phosphatase inhibitor cocktail (1:100, v/v). Homogenates were centrifuged (14,000 g, 45 min, 4°C) and protein concentration of supernatants was measured (Bradford, 1976). Aliquots (30 µg) of homogenates from each sample were processed by 15% SDS-PAGE and western blotting for titrating BDNF and ApoE. In particular, after blocking with T-TBS containing 5% non-fat milk (1 h, 37°C), the membrane was incubated with rabbit anti-BDNF IgG (Santa Cruz Biotechnology; 1: 750 dilution in T-

TBS containing 0.25% non-fat milk; overnight, 4°C) followed by GAR-HRP IgG (1: 95,000 dilution; 1 h, 37°C), or with goat anti-ApoE IgG (1:1,000 dilution in T-TBS containing 0.25% non-fat milk; overnight, 4°C) followed by RAG-HRP IgG (1: 18,000 dilution; 1 h, 37°C). The immunocomplexes were detected by the ECL detection system, and densitometric analysis of the signal was carried out. After BDNF or ApoE detection, the membrane was extensively washed with T-TBS, and submerged in stripping buffer (45 min, 50°C) for reprobing with anti-β-actin. After washing with T-TBS, the membrane was incubated (1 h, 37°C) with mouse anti-β-actin IgG (1:1000 dilution), followed by GAM-HRP IgG (1:10,000 dilution; 1 h, 37°C).

Extracellular signal-regulated kinase (Erk) 1 and 2 pathway analysis

NHA (100,000 cells/well) or U-87 MG (400,000 cells/well) were seeded into 6 well-plate in their specific complete medium, and cultured for 20 hours. After medium removal, cells were rinsed with serum-free medium, and incubated (30, 60, or 120 min, 37°C) in the presence or absence of 10 ng/mL BDNF. At the end of incubation, cells were treated as above described, and aliquots (40 μg) of lysates were fractionated by electrophoresis on 10% SDS-PAGE. After electrophoresis, proteins were blotted onto PVDF membrane, and blocking was performed with T-TBS containing 5% non-fat milk (1 h, 7°C). p-Erk 1 and 2 were revealed by incubation (overnight, 4°C) with anti-p-Erk IgG (Cell Signaling, MA, USA, 1:1,000 dilution in T-TBS containing 3% BSA), followed by GAR-HRP IgG (1:30,000 dilution in T-TBS containing 3% non-fat milk; 1 h, 37°C). After p-Erk detection, the membrane was extensively washed with T-TBS, and submerged in stripping buffer (45 min, 50°C). Erk1/2 was revealed by incubation (overnight, 4°C) with rabbit anti-Erk1/2 (Cell Signaling, MA, USA, 1:2,000 in T-TBS containing 3% BSA) followed by RAG-HRP IgG (1: 120,000 dilution in T-TBS containing 3% non-fat milk; 1h, 37°C). After further stripping, loading control was carried out by incubating the membranes (overnight, 4°C) with mouse anti- β-actin IgG (1:1,000 dilution in T-TBS containing 0.25% non-fat milk) followed by GAM-HRP IgG (1:10,000 dilution). All the above immunocomplexes were detected by the ECL detection system. Quantification of signals was carried out by Un-Scan-It gel software (Silk Scientific, UT, USA).

Microarray Experiment Analysis

BDNF stimulation of differentiated SH-SY5Y cells, RNA extraction and labeling, and microarray analysis were essentially performed as reported in Aliperti and Donizetti (2016). Briefly, SH-SY5Y cells were differentiated by decreasing FBS concentration from 15 to 1.5% and adding 10 μM of RA for 6 days (the medium was refreshed every 2 days). After 6 days of

differentiation, the medium containing 1.5% FBS and RA was removed and substituted with a medium without FBS for two groups of cells. One of these groups was used as a control for the gene expression analysis, whereas the second group was treated with 10 ng/mL of BDNF for 24 h. RNA extracted from biological duplicate samples was used for microarray experiments. The labeled cRNA was hybridized for 17 h at 65°C on an Agilent SurePrint G3 8 × 60K custom lncRNA expression array (Agilent Technologies) that contains probes for 17,535 randomly chosen protein-coding transcripts. After hybridization, the slide was washed according to Agilent protocols and scanned using a High-Resolution Microarray C Scanner (Agilent Technologies). The image file was processed using Agilent Feature Extraction software (v10.7.3). The microarray grid was correctly placed, and outlier pixels (which were rejected) and inlier pixels were identified. Normalization was performed according to the Quantile method. qPCR validation for HMGCR gene was performed using biological replicates in triplicate as reported in the previous section.

BDNF effect on cholesterol incorporation

The ApoE-dependent internalization of cholesterol into differentiated SH-SY5Y was carried out essentially according to Spagnuolo et al. (2014 a). In detail, cells were seeded in low-serum medium (50,000 cells per well) into 24-well plate, as above described, and cultured for six days in presence of RA. After medium removal, cells were rinsed with DMEM, and incubated (3 or 24 h, 37°C) in serumfree DMEM/F12 containing 0.2% BSA, 100 IU/mL penicillin, 100 µg/mL streptomycin, 2 mM Lglutamine, and different amounts of BDNF (0, 5, or 10 ng/ml). Cells were then washed with DMEM/F12, and further incubated (3 h, 37°C) in DMEM/F12 containing 0.2% BSA, 100 IU/mL penicillin, 100 µg/mL streptomycin, 2 mM L-glutamine, labeled proteoliposome (ApoE final concentration 30 nM; cholesterol final concentration 60 nM), and unlabeled liposome (cholesterol final concentration 300 nM). At the end of incubation, media samples were collected, and cleared of any cellular debris by centrifugation at 400 g for 5 min. The cells were extensively washed with DMEM, lysed with 0.1 M NaOH, and finally centrifuged at 12,000 g for 30 min. Aliquots (170 µl) of supernatants and lysates were then analysed by scintillation counting, for evaluating the amount of labeled cholesterol incorporated by cells. Protein concentration in cell lysates was measured by Bradford assay. The amount of cholesterol internalized was calculated as d.p.m in lysates per mg cell protein. Experiments were routinely performed in triplicate and repeated three times. Liposomes containing ApoE/lecithin/cholesterol molar ratio of 1 : 100 : 2 were prepared by the cholate dialysis procedure (Spagnuolo et al., 2014 a). [1α,2α-3H]-Cholesterol (specific activity 102.4

x106 dpm x nmol-1) in proteoliposome containing 10 μM ApoE was used. An unlabeled liposome, prepared without apolipoprotein, was used to evaluate non-apolipoprotein-mediated uptake of cholesterol. In detail, nonspecific internalization was determined in the presence of a 5-fold excess of the unlabelled cholesterol.

BDNF effect on ApoE binding to neurons

The effect of BDNF on the interaction between ApoE and neurons was evaluated on differentiated SH-SY5Y, essentially according to Maresca et al. (2015). As described above, SH-SY5Y were seeded into a 96-well plate (10,000 cells/well), and differentiated for six days in RA-supplemented medium. After removal of the culture medium, the cells were incubated (3 or 24 h, 37°C) in serum-free DMEM/F12 containing 0.2% BSA, 100 IU/mL penicillin, 100 μg/mL streptomycin, 2 mM L-glutamine, and different amounts of BDNF (0, 5, 10, 20, or 50 ng/ml). Cells were then washed with PBS, and fixed by incubation (30 min, 4°C) with 0.3% glutaraldheyde in PBS. After removing glutaraldheyde, the wells were gentle washed with PBS, and finally blocked with PBS containing 1% BSA (overnight, 4°C). After extensive washing, the wells were incubated (90 min, 37°C) with 0.7 μM ApoE3. The amount of ApoE bound to cells was measured by treatment with goat anti-ApoE IgG (1: 1,000 dilution in PBS; 1 h, 37°C), followed by RAG-HRP IgG (1: 70,000 dilution in PBS; 1 h, 37°C), and color development at 492 nm. Absorbance values were converted to the percent of the value obtained from untreated cells (assumed as 100% of ApoE binding).

BDNF effect on LXR-beta expression in neurons

The effect of BDNF on LXR-beta expression was evaluated on differentiated SH-SY5Y exposed to cholesterol. As described above, SH-SY5Y were seeded into a 12-well plate (150,000 cells/well), and cultured for six days in RA-supplemented medium. After removal of the culture medium, the cells were incubated (3 or 24 h, 37°C) in serum-free DMEM/F12 containing 0.2% BSA, 100 IU/mL penicillin, 100 μg/mL streptomycin, 2 mM L-glutamine, and different amounts of BDNF (0, 5, or 10 ng/ml). Cells were then washed with DMEM/F12, and further incubated (3 h, 37°C) as for the cholesterol internalization assay. At the end of incubation, media samples were discarded, while cells were extensively washed with DMEM, and lysed with 0.07 mL of RIPA buffer containing the protease (1:500, v/v) and the phosphatase (1:100, v/v) inhibitor cocktails. The lysates were centrifuged (12,000 g, 30 min, 4°C), and analyzed for their protein concentration. Aliquots (30 μg) of lysates were fractionated by 10% SDS-PAGE and blotted onto PVDF membrane. The membrane was blocked as above reported

(1 h, 37°C), and then incubated (overnight, 4°C) with rabbit anti-human LXR-beta IgG (GeneTex, 1: 1,000 dilution in 0.25% non-fat milk), followed by GAR-HRP IgG (1: 15,000 dilution; 1h, 37°C). The immunocomplexes were detected by the ECL detection system. The membrane was then stripped for reprobing with mouse anti-β-actin IgG (1:1000 dilution), followed by GAM-HRP IgG (1:10,000 dilution; 1 h, 37°C). The immunocomplexes were detected by the ECL detection system, and densitometric analysis of the signal was carried out.

Apoptosis analysis

SH-SY5Y were seeded in low-serum medium into a 12-well plate (150,000 cells/well), as above described, and cultured for six days in RA-supplemented medium. After removal of the culture medium, the cells were incubated (20 h, 37°C) in serum-free DMEM/F12 containing 0.2% BSA, 100 IU/mL penicillin, 100 μg/mL streptomycin, 2 mM L-glutamine, and different amounts of cholesterol (0, 5, 10, or 15 μM) in the absence or presence of 10 ng/mL BDNF. At the end of incubation, media samples were discarded, while cells were extensively washed with DMEM, and lysed with 0.07 mL of RIPA buffer containing the protease (1:500, v/v) and the phosphatase (1:100, v/v) inhibitor cocktails. After centrifugation (12,000 g, 30 min, 4°C), aliquots of lysate (45 or 20 μg) were fractionated by 12.5% SDS-PAGE and blotted onto PVDF membrane for detecting native or cleaved caspase 3 or PARP. The membrane was blocked (1 h, 37°C), and then incubated (overnight, 4°C) with rabbit anti- Cleaved Caspase-3 (Asp175) (5A1E) IgG (Cell Signalling, 1: 1,000 dilution in 3% BSA), followed by GAR-HRP IgG (1: 6,000 dilution in 3% non-fat milk; 1h, 37°C), or with rabbit anti-Caspase 3 (Immunological Science, AB-83625, 1: 500 dilution in 3% BSA) followed by GAR-HRP IgG (1: 50,000 dilution in 3% non-fat milk; 1h, 37°C), or with rabbit anti-human PARP IgG (Santa Cruz, 1: 750 dilution in 3% BSA), followed by GAR-HRP IgG (1: 4,000 dilution in 5% non-fat milk; 1h, 37°C). The immunocomplexes were detected by the ECL detection system. The membrane was then stripped for reprobing with mouse anti-β-actin IgG (1:1,000 dilution), followed by GAM-HRP IgG (1:10,000 dilution; 1 h, 37°C). The immunocomplexes were detected by the ECL detection system, and densitometric analysis of the signal was carried out.

Cholesterol effect on BDNF synthesis

SH-SY5Y were seeded in low-serum medium into a 6-well plate (500,000 cells/well), as above described, and cultured for six days in RA-supplemented medium. After removal of the culture medium, the cells were incubated (20 h, 37°C) in serum-free DMEM/F12 containing 0.2% BSA, 100 IU/mL penicillin, 100 μg/mL streptomycin, 2 mM L-glutamine, and different

amounts of cholesterol (0, 1.5, or 4.5μM). At the end of treatment, media samples were collected, and cleared of any cellular debris by centrifugation (400 g, 10 min). Cells were extensively washed with DMEM, detached by treatment with trypsin, washed with ice-cold PBS, and finally lysed with 0.1mL of RIPA buffer supplemented with the protease (1: 500, v/v) and the phosphatase (1: 100, v/v) inhibitor cocktails. The lysates were centrifuged (12,000 g, 30 min, 4°C) and then analyzed for their protein concentration (Bradford, 1976). BDNF concentration in cell lysates was assessed by both immunoblotting and sandwich ELISA. For western blotting analysis, aliquots (50 μg) of cell lysates were fractionated by electrophoresis on 15% polyacrylamide gel, under denaturing and reducing conditions, and blotted onto PVDF membrane for revealing BDNF. After blocking, BDNF was revealed by incubation (overnight, 4°C) with rabbit anti-human BDNF IgG (Immunological Sciences, distributed by Società Italiana Chimici; 1: 500 dilution in T-TBS containing 0.25% non-fat milk), followed by GAR-HRP IgG (1: 80,000 dilution; 1h, 37°C). After BDNF detection, the membrane was extensively washed with T-TBS, stripped and reprobed with anti-β-actin (mouse anti-β-actin IgG 1:500 dilution, followed by GAM-HRP IgG 1:6,000 dilution; 1 h, 37°C). The immunocomplexes were detected by the ECL detection system, and densitometric analysis of the signal was carried out. The quantification by ELISA was carried out using the BDNF ELISA kit (Immunological Sciences, distributed by Società Italiana Chimici, Rome, Italy), essentially according to the manufacturer instructions. Each sample was diluted 1:100, 1:300, 1:1000 in the assay, and data were reported as pg of BDNF per mg of cell proteins.

Statistical analysis

Samples were processed in triplicate in all experiments, and data were expressed as mean value ± SEM. The program "GraphPad Prism 5.01" (GraphPad Software, San Diego, CA) was used to perform linear regression analysis, Student's t-test, for comparing two groups of data, and one-way ANOVA, followed by Tukey's test, for multiple group comparisons. $P < 0.05$ was set as indicating significance.

Results

BDNF effect on cholesterol efflux from astrocytes

BDNF was previously reported to act on astrocytes essentially through the truncated isoform of TrkBreceptor, thus regulating calcium entry (Rose et al., 2003), morphology and cytoskeletal changes (Ohira, 2005; Ohira et al., 2007), activity and trafficking of GABA transporter-1 (Vaz et al., 2011), or glycine uptake (Aroeira et al., 2015). In order to verify the expression of the

full length (TrkB-FL) and truncated (TrkB-T) isoform of TrkB-receptor in normal human astrocytes (NHA) and astrocyte cell line U-87 MG, we performed a preliminary Western Blotting of cell lysates. As shown in Supplementary Figure 1 A, U-87 MG and NHA predominantly expressed the truncated form (95 kDa) of TrkB compared to the full length (145 kDa), while in differentiated neurons SH-SY5Y a predominance of TrkB-FL on TrkB-T was found. Further, a MTT assay was performed in order to assess BDNF effect on astrocyte survival and/or proliferation. The treatment of NHA or U-87 MG with different concentrations of BDNF (5-30 ng/ml) for 24 hours did not affect cell viability (Supplementary Figure 1 B). In order to evaluate the effect of BDNF on cholesterol efflux from astrocytes, NHA or U-87 MG were labeled (20 hours) with [3H] cholesterol in the presence of different amounts of BDNF (0, 5, 10 or 20 ng/ml). After extensive washing, the cells were incubated (5 hours) in serum-free medium. At the end of incubation, the amount of cholesterol effluxed to the medium was evaluated by scintillation counting as reported in methods. As shown in Figure 1, BDNF stimulated cholesterol efflux from astrocytes in a dose dependent manner. Indeed, after treatment with 5, 10, or 20 ng/ml BDNF, the percent of cholesterol effluxed from NHA increased of about 15% ($p = 0.04$), 35% ($p = 0.02$) or 44% ($p = 0.02$) (Figure 1) compared to untreated cells. Similarly, the percent of cholesterol effluxed from U-87 MG, after treatment with BDNF, was about 28% ($p = 0.005$), 49% ($p = 0.005$) or 74% ($p = 0.02$) higher when compared to untreated cells (Figure 1).

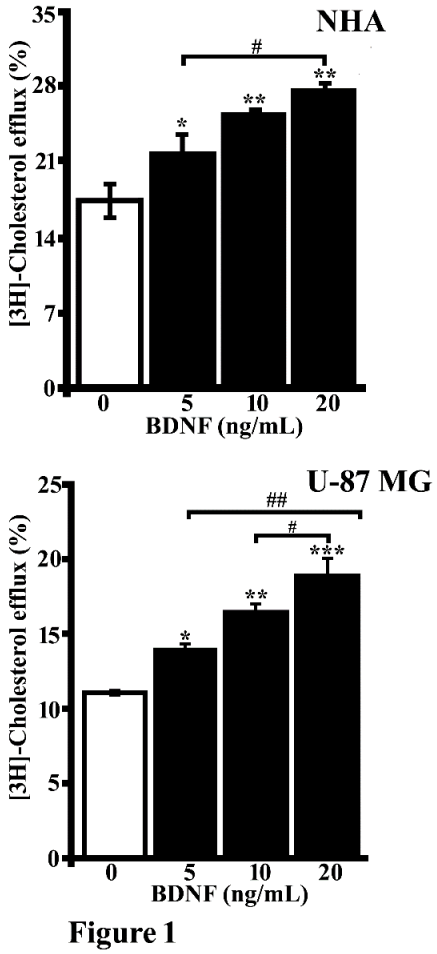

Figure 1

Figure 1. BDNF effect on cholesterol efflux from astrocyte cell models. *Normal human astrocyte (NHA) (top) or U-87 MG (bottom) were cultured in their specific complete medium for 20 hours. After medium removal, cells were labeled by incubation (20 h) with [3H]-Cholesterol (0.026 µCi/well) in AGM medium (NHA) or in DMEM containing 0.5% FBS (U-87 MG), in the presence of BDNF (0, 5, 10 or 20 ng/ml). After medium removal, cells were incubated (5 h) in serum-free medium. Aliquots of supernatants and lysates were then analysed by scintillation counting, and cholesterol effluxed to the medium was calculated as percentage of total radioactivity in the cell lysates and medium. Data were expressed as mean ± SEM. Significant differences from cells cultured in the absence of treatment (open bar; *p < 0.05; **p < 0.01; ***p < 0.001) are indicated. # p < 0.05; ## p < 0.01 (one-way Anova followed by Tukey post-test).*

BDNF modulates ABCA1 and ApoE expression in astrocyte

As known, cholesterol efflux is stimulated by the interaction of ApoE with ABC transporters (Koldamova et al., 2003; Abildayeva et al., 2006). Therefore we supposed that BDNF might promote cholesterol efflux modulating ApoE level and/or ABC transporters expression. In order to investigate whether BDNF affects the expression of ABCA1 gene, NHA or U-87 MG were incubated (0, 1, or 24 h, 37°C) in serum-free medium containing 10 ng/mL BDNF. After treatment, qPCR experiments were performed. BDNF addition significantly increased the transcript level of ABCA1 in NHA cells after 24 h ($p < 0.05$; Figure 2) in agreement with results from cholesterol efflux.

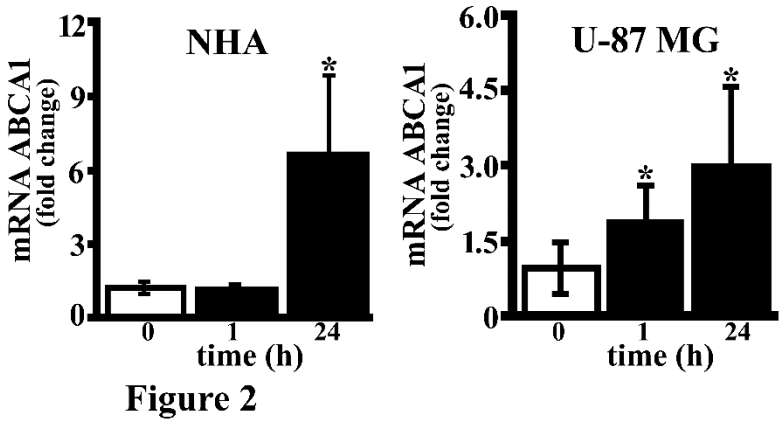

Figure 2

Figure 2. BDNF effect on ABCA1 expression in cellular models of astrocytes. *NHA or U-87 MG were incubated (0, 1, or 24 h) in serum free medium containing 10 ng/mL BDNF. ABCA1 gene expression level was normalized to the reference gene hypoxanthine phosphoribosyltransferase 1 (HPRT1) and calculated by the 2^– ΔΔCt method. The results from independent biological replicates in triplicate are expressed as mean ± SEM. Statistical analysis of the qPCR data was carried out using a two-tailed t test. Significance of difference from time 0 (*, p < 0.05) is shown.*

Also, ABCA1 mRNA levels in U-87 MG increased of about 1.8- and 3 fold ($p < 0.05$) after 1 and 24 hours, respectively. This result supports the hypothesis that BDNF may regulate the expression of this critical transporter involved in cholesterol efflux. We extended the transcript level analysis to ApoE as well, which is mainly synthesized by astrocytes in brain (De Mattos et al., 2001; Vance and Hayashi, 2010). ApoE transcript level in NHA showed a significant increase after 24 h of BDNF treatment ($p < 0.01$; Figure 3 A). The BDNF-dependent increase of ApoE transcript level was confirmed in U-87 MG, both after 1 h and 24 h of treatment with BDNF ($p < 0.01$; Figure 3 A). The effect of BDNF on ApoE secretion by NHA was evaluated by analyzing the amount of protein released in the extracellular medium after incubation of astrocytes (24 h, 37°C) in serum-free medium containing different amounts of BDNF (0, 5, 10, or 20 ng/ml). At the end of incubation, cell culture supernatants were immunoprecipitated by anti-human ApoE and then immunostained, as described in Methods, for measuring protein level. We found that the amount of ApoE in the supernatants collected after incubation with 5, 10 or 20 ng/mL BDNF was about 4 ($p < 0.001$), 5 ($p < 0.001$) or 7 fold ($p < 0.001$) higher than in those collected from untreated cells (Figure 3 B). Further, a significant dose-dependent increase of ApoE level was detected in supernatants from U-87 MG treated with 5, 10 or 20 ng/ml BDNF, as the amount of ApoE was about 1.4 ($p < 0.05$), 1.8 ($p < 0.001$) or 2.7 fold ($p < 0.001$) higher in the supernatants collected from treated cells (Figure 3 B). These results suggest that BDNF promotes ApoE synthesis and secretion by astrocytes.

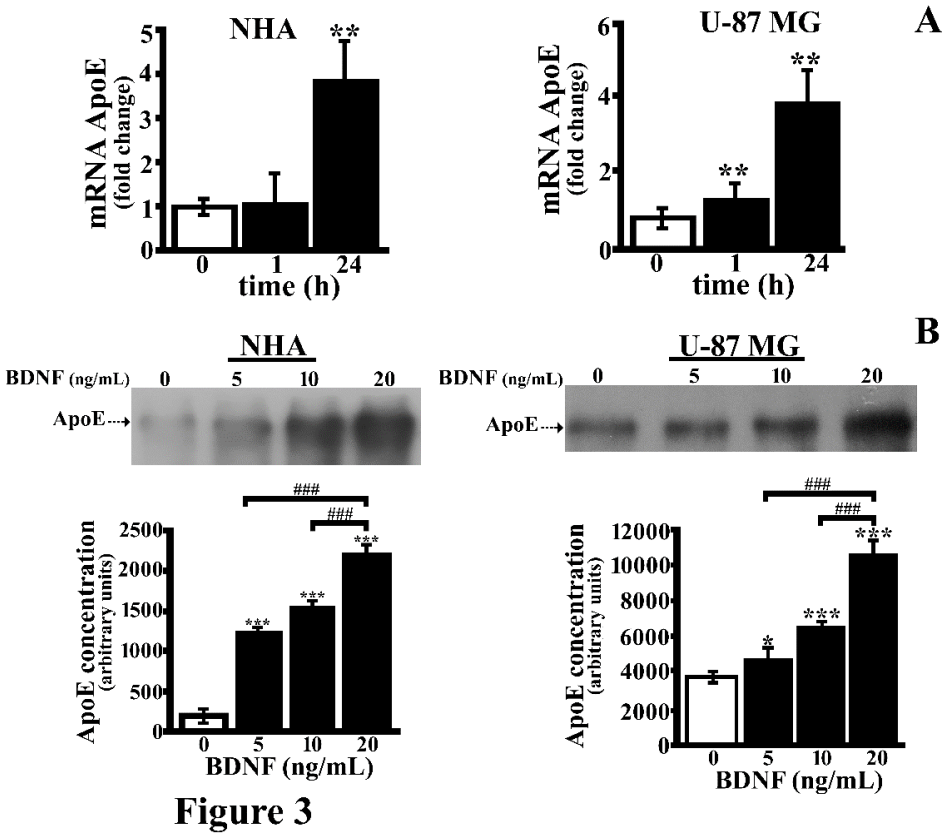

Figure 3

Figure 3. BDNF effect on ApoE expression in cellular models of astrocytes. *Panel A. NHA or U-87 MG were incubated (0, 1, or 24 h) in serum free medium containing 10 ng/mL BDNF. ApoE gene expression level was normalized to the reference gene hypoxanthine phosphoribosyltransferase 1 (HPRT1) and calculated by the 2^−ΔΔCt method. The results from independent biological replicates in triplicate are expressed as mean ± SEM. Statistical analysis of the qPCR data was carried out using a two-tailed t test. Significance of difference from time 0 (**, p < 0.01) is shown. Panel B. NHA or U-87 MG were incubated (24 h) in serum free medium containing different amounts of BDNF (0, 5, 10, or 20 ng/mL). Media samples were immunoprecipitated with anti-human ApoE, and analysed by SDS-PAGE and Western Blotting. Representative Western blotting is shown on the top. Quantitative densitometry of the bands was performed, and band intensities per mg of cell protein is shown (on the bottom). Values are reported as means from three independent experiments± SEM. Significance of difference from cells cultured in the absence of treatment (open bar; *, p < 0.05;***, p< 0.001) is shown. ###, p < 0.001 (one-way Anova followed by Tukey's post test).*

Also, the levels of both BDNF and ApoE were evaluated ex vivo in brain cortex samples of different human subjects (N = 6; one healthy, four AD, and one SCA17) by Western blotting (Figure 4). Interestingly, a positive correlation between the levels of ApoE and BDNF was found (r = 0.962, p = 0.002, Western blotting; r = 0.976). This result from human samples analysed ex vivo, although within the limits of a correlation, shows a possible link between cerebral concentration of BDNF and ApoE, and supports the results obtained from analyses performed with in vitro cell cultures.

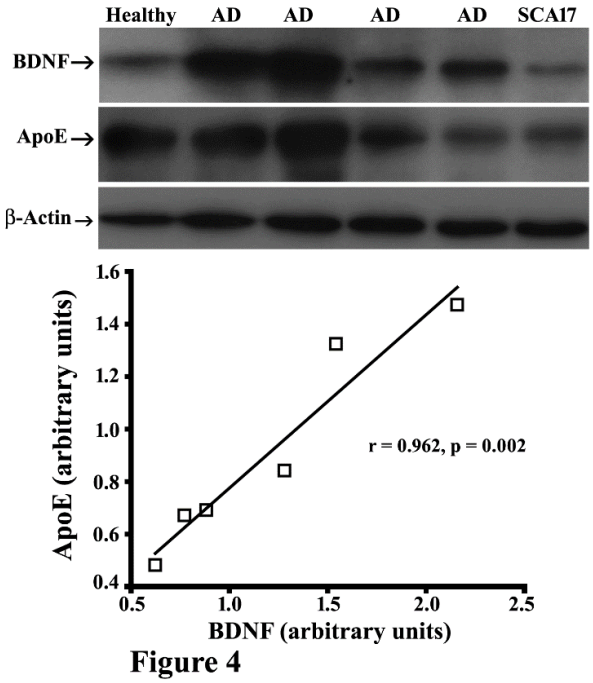

Figure 4

Figure 4. Correlation between BDNF and ApoE in human prefrontal cortex. *Aliquots (30 μg) of homogenates from postmortem brain tissues (prefrontal cortex) from one healthy subject, four AD patients, and one subject affected by SCA17 were processed by 15% SDS-PAGE and Western blotting for titrating BDNF and ApoE. Quantitative densitometry of BDNF, ApoE, and β-actin was carried out. BDNF or ApoE concentrations were calculated relative to β-actin level. Representative Western blots are shown on the top. The statistical program Graph Pad Prism 5.01 performed the linear regression analysis (shown below), and the calculation of Pearson's r (shown below; r = 0.962; p = 0.002).*

BDNF effect on Erk 1/2 pathway in astrocytes

BDNF was previously reported to stimulate the activation of Erk1/2 pathway in mice astrocytes, inducing the expression of the dopamine receptor D5 (Brito et al., 2004), as well as in cortical rat astrocytes modulating GABA Transporter-1 trafficking (Vaz et al., 2011). In order to investigate whether BDNF also provides a rise in the degree of phosphorylation of Erk1/2 in the astrocyte cell models here used, NHA or U-87 MG cells were incubated (30, 60, or 120 min) with BDNF and the activation of the Erk 1/2 pathway, namely the ratio p-Erk/Erk, was evaluated by Western blotting. BDNF treatment of NHA for 30, 60, or 120 min was associated with an increase of both p-Erk1/Erk1 ratio (about 1.4-, 1.5-, or 1.6-fold, respectively; $p < 0.001$; Figure 5 A, B) and pErk2/Erk2 ratio (about 1.3-, 1.5-, or 1.7-fold, respectively; $p < 0.001$; Figure 5 A, B). As shown in Figure 5 C, a slight increase of total Erk1 amount was found only after 30 min of BDNF treatment ($p < 0.05$), while total Erk2 level was not affected by the same treatment.

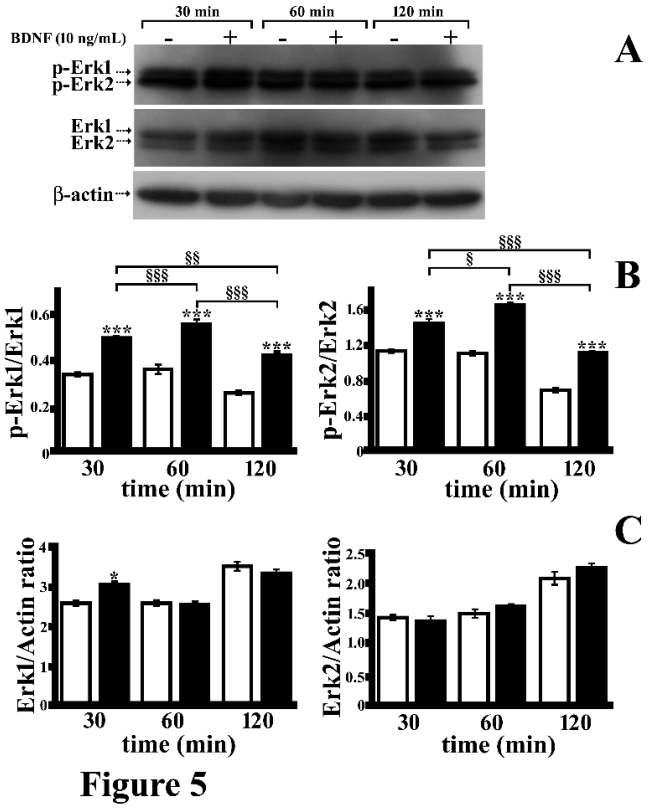

Figure 5

Figure 5. BDNF-induced changes in the Erk1 and Erk2 pathway in NHA. *NHA were incubated (30, 60, or 120 min) in the absence (open bar) or presence of 10 ng/mL BDNF (black bar). Aliquots (30 μg) of cell lysates were then processed by SDS-PAGE and Western Blotting. Representative western blots are shown (Panel A). Quantitative densitometry of Erk 1 and 2, p-Erk 1 and 2 and β-actin was carried out. The degree of activation of Erk 1 and 2 was evaluated by measuring p-Erk/Erk ratio (Panel B). The level of Erk 1 and Erk2 was measured relative to β-actin level (Panel C). Data are reported as means ± SEM. Significance of difference from cells cultured in the absence of treatment (open bar; *p<0.05, ***p<0.001) is shown. §, p < 0.05; §§, p< 0.01; §§§, p < 0.001 (one-way Anova followed by Tukey's post test).*

Similarly, the p-Erk1/Erk1 ratio, in U-87 MG, increased of about 1.4-($p < 0.01$), 2.0- ($p < 0.001$), or 1.5-fold ($p < 0.001$) after 30, 60, or 120 min of BDNF treatment, respectively (Figure 6 A, B). P-Erk2/Erk2 ratio increased of about 2.3-, 1.9-, or 1.2-fold ($p < 0.001$) after 30, 60, or 120 min of BDNF treatment, respectively. As shown in Figure 6 C, total Erk1 amount was not affected by BDNF treatment, while Erk2 amount decreased ($p < 0.001$) after 30 min of incubation with BDNF.

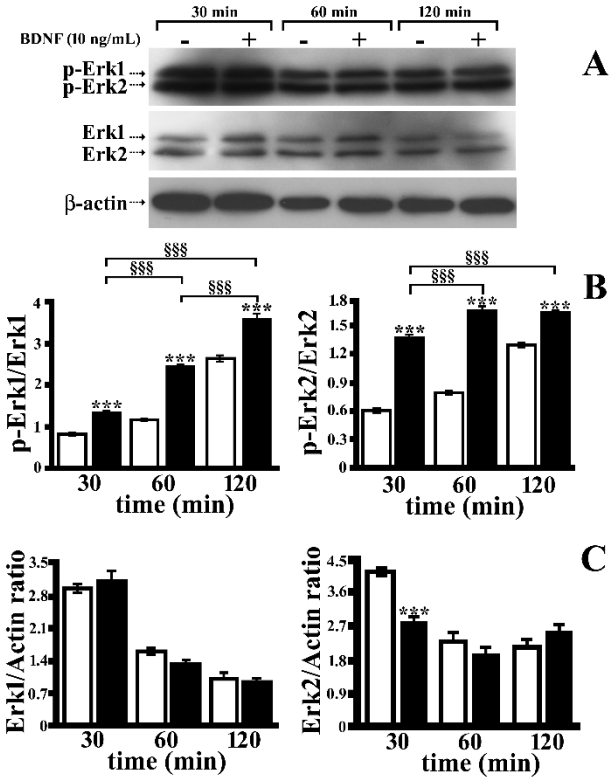

Figure 6

Figure 6. BDNF-induced changes in the Erk1 and Erk2 pathway in U-87 MG cells. *U-87 MG were incubated (30, 60, or 120 min) in the absence (open bar) or presence of 10 ng/mL BDNF (black bar). Aliquots (40 μg) of cell lysates were then processed by 10% SDS-PAGE and Western Blotting. Representative western blots are shown (Panel A). Quantitative densitometry of Erk 1 and 2, p-Erk 1,2 and β-actin was carried out. The degree of activation of Erk 1 and 2 was evaluated by measuring p-Erk/Erk ratio (Panel B). The level of Erk 1 and Erk2 was measured relative to β-actin level (Panel C). Data are reported as means ± SEM. Significance of difference from cells cultured in the absence of treatment (open bar; ***p<0.001) is shown. §§§, p < 0.001 (one-way Anova followed by Tukey's post test).*

BDNF effect on cholesterol metabolism and trafficking genes in neurons

Given the influence of BDNF on the amount of cholesterol released by glial cells, we then evaluated the hypothesis that BDNF might regulate neuronal genes involved in cholesterol metabolism. To this aim, we performed a preliminary analysis of our unpublished microarray data. In particular, the microarray was carried out on RNA extracted from RA-differentiated SH-SY5Y cells that were stimulated with 10 ng/mL BDNF for 24 h as reported in Aliperti and Donizetti (2016). Total RNA extracted from these BDNF-treated cells was analyzed by microarray experiments using not treated cells as a control. The array contained probes for 17,535 randomly chosen protein-coding transcripts, including genes involved in cholesterol metabolism and trafficking. Changes in their transcript level was reported in Supplementary Table 2, where it is worthy of note that HMGCR, the gene encoding for the rate-limiting enzyme of cholesterol synthesis (namely 3-hydroxy-3-methylglutaryl coenzyme A reductase), showed

a fold change above 2. The BDNF-induced upregulation of HMGCR gene was validated by qPCR experiments that confirmed a transcript level increase (2.1 fold change; $p < 0.05$), as reported in Figure 7. This result, in agreement with data from Suzuki et al. (2007), confirms that BDNF might increase endogenous cholesterol synthesis by regulating gene expression of HMGCR.

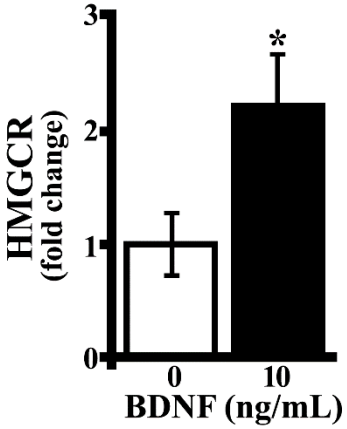

Figure 7

Figure 7. BDNF influence on HMGCR expression in differentiated SH-SY5Y neurons. *Differentiated SH-SY5Y cells were incubated (24 h) in the absence or presence of 10 ng/mL of BDNF. RNA extracted from biological duplicate samples was used for microarray experiments. qPCR validation for HMGCR gene was performed using biological replicates in triplicate as reported in the previous section. Significant differences from untreated cells (open bar) is indicated (*$p < 0.05$).*

BDNF effect on the ApoE-mediated cholesterol incorporation

As above mentioned, adult neurons mainly rely on the import of cholesterol released from astrocytes (Ikonen, 2008). In order to investigate whether BDNF influences cholesterol internalization in neurons, differentiated SH-SY5Y neurons were incubated (3 or 24 h) in serum-free DMEM containing different amounts of BDNF. At the end of incubation, cholesterol uptake was evaluated, by further incubating cells for 3 h with a labeled proteoliposome with [3H]-cholesterol as tracer. The uptake of extracellular cholesterol was significantly reduced after 3 hours incubation with BDNF (about 20%, $p < 0.05$, Figure 8 A). When the treatment with BDNF was carried out for 24 h, the internalization of extracellular cholesterol by neurons was reduced of about 30% or 41% by 5 or 10 ng/ml BDNF respectively ($p < 0.001$; Figure 8 B). The cholesterol uptake by neurons is mediated by the binding of ApoE to specific cell surface receptors (Pfrieger and Ungerer, 2011). Therefore, we investigated whether the ability of neurons to bind ApoE is affected by BDNF, as this binding might reflect changes in the expression of ApoE receptors following incubation with the neurotrophin. Differentiated SH-SY5Y were incubated (3 or 24 h) in serum-free DMEM/F12 containing

different amounts of BDNF (0-50 ng/ml). Cells were then fixed, incubated with 0.7 μM ApoE, and the binding of ApoE to the cells was then evaluated by ELISA. BDNF significantly reduces the ability of cells to interact with ApoE. Indeed, ApoE binding was reduced of about 20 or 40% ($p < 0.05$; Figure 8 C) after 3 hours treatment with 20 or 50 ng/ml BDNF, respectively. Further, after 24 h incubation with 5, 10, 20 or 50 ng/ml BDNF, ApoE binding to differentiated neurons was reduced of about 21, 28, 32 or 36% respectively ($p < 0.05$; Figure 8 D), thus suggesting that BDNF might modulate the exposure of ApoE receptors on cell surface.

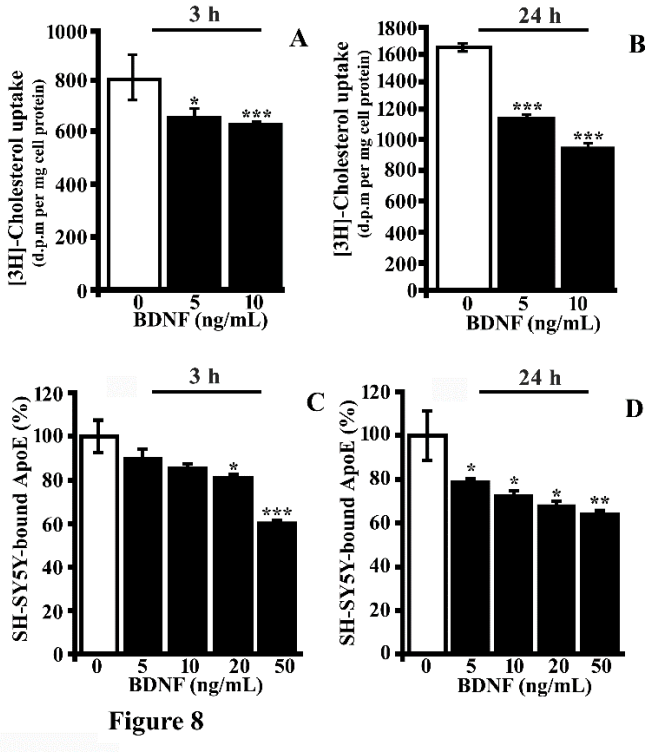

Figure 8

Figure 8. BDNF effect on cholesterol uptake or ApoE binding to neurons. *Panel A-B. Differentiated SH-SY5Y were incubated for 3 (Panel A) or 24 h (Panel B) in serum-free DMEM/F12 containing different amounts of BDNF (0, 5, or 10 ng/mL). At the end of incubation with BDNF, cells were rinsed and the assay of internalization was performed by further incubating cells (3h) with labeled proteoliposome (ApoE final concentration 30 nM; cholesterol final concentration 60 nM), and unlabeled liposome (cholesterol final concentration 300 nM). After incubation, the cells were lysed for measurement of their radioactivity and protein concentration. The amount of cholesterol internalized was measured as dpm per mg of cell protein. Panel C-D. Differentiated SH-SY5Y were incubated for 3 (Panel C) or 24 h (Panel D) with different amounts of BDNF (0-50 ng/mL). Cells were fixed and then incubated with 0.7 μM ApoE. The amount of ApoE bound to cells was measured by incubation with goat anti-ApoE IgG, followed by RAG-HRP and color development at 492 nm. Data are reported as percent of the value obtained by incubation in the absence of BDNF (assumed as 100% of ApoE binding). The samples were analysed in triplicate, and the data are expressed as means ± SEM. Significant differences from untreated cells (open bar) are indicated (*p < 0.05; **p < 0.01; ***p < 0.001).*

Further, in the attempt of unraveling the mechanism underlying BDNF-dependent reduction of cholesterol uptake, we investigated whether the neurotrophin affects LXR-beta expression in

differentiated neurons exposed to cholesterol. In fact LXR is a key regulator of neuronal content of cholesterol, and acts by downregulating lipoprotein receptor cell surface expression (Willy et al., 1995; Mouzat et al., 2016; Courtney and Landreth, 2016). As shown in Figure 9, a dose-dependent increase of LXR-beta expression was observed after 3 ($p < 0.05$) or 24 hours ($p < 0.001$) incubation with BDNF. In particular, LXR-beta level was significantly higher in cells incubated for 3 or 24 hours with 5 (about 20%, $p < 0.05$, or 60%, $p < 0.001$, respectively) or 10 ng/mL BDNF (about 33% or 95%, $p < 0.01$, respectively) compared to untreated neurons. These results strongly support the hypothesis that BDNF reduces neurons uptake of cholesterol by modulating LXR expression.

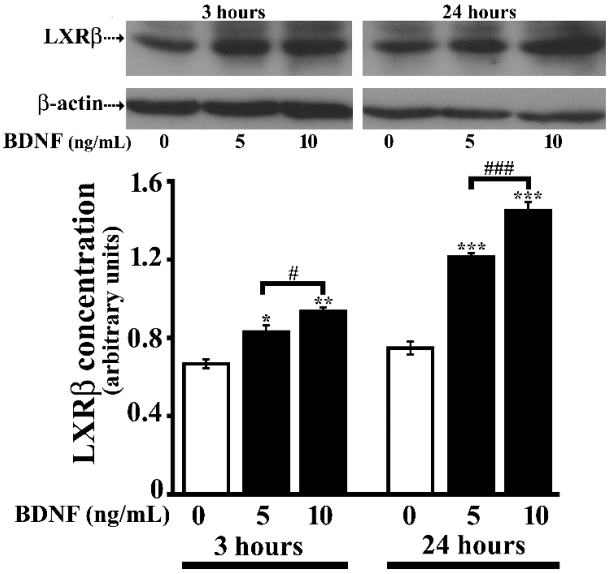

Figure 9

Figure 9. BDNF effect on LXR-beta expression in neuron. *Differentiated SH-SY5Y were incubated (3 or 24 h) in serum free DMEM/F12 containing different amounts of BDNF (0, 5, or 10 ng/ml). At the end of incubation with BDNF cells were rinsed and the assay of internalization was performed by further incubating cells (3h) with labeled proteoliposome (ApoE final concentration 30 nM; cholesterol final concentration 60 nM), and unlabeled liposome (cholesterol final concentration 300 nM). Aliquots (30 μg) of cell lysates were then analysed by 10% SDS-PAGE and Western Blotting for revealing LXR-beta. Representative Western Blots are shown on the top. Quantitative densitometry was carried out, and LXR beta concentrations were calculated relative to β-actin level (on the bottom). The samples were analysed in triplicate, and the data are expressed as means ± SEM. Significant differences from untreated cells (open bar) are indicated (*p < 0.05; **p < 0.01; ***p < 0.001). #, p < 0.05; ###, p < 0.001 (one-way Anova followed by Tukey's post test).*

BDNF effect on cholesterol-induced apoptosis

Numerous lines of evidence showed that high cholesterol concentration and oxysterols, which are formed by auto-oxidation of cholesterol, can induce oxidative stress, inflammation and cell apoptosis (Vejux et al., 2008; Lordan et al., 2009). Since our results demonstrated that BDNF

reduces the uptake of cholesterol by differentiated neurons, we hypothesized that this action might represent a protective mechanism for preventing high cholesterol-induced cell dysfunction. To test this hypothesis, we incubated cells (20 h) with different amounts (0, 5, 10 or 15 μM) of cholesterol, in the absence or presence of 10 ng/mL BDNF. As expected, cholesterol treatment induced apoptosis of differentiated SH-SY5Y at any concentration assayed, as demonstrated by the increase of cleaved caspase 3 amount ($p < 0.001$; Figure 10 A, black bar). Interestingly, the level of cleaved caspase 3 was significantly lower when the cells were incubated with cholesterol in the presence of BDNF compared to cells incubated with cholesterol only ($p < 0.01$; Figure 10 A, grey bar). As shown in Supplementary Figure 2, the amount of native caspase 3 was not affected by the treatment. We further investigated whether cholesterol treatment affect the integrity of PARP, which is a target of caspase-3 (Kaufmann et al., 1993). To this aim, the appearance of the cleaved form (87 kDa) was evaluated, and the extent of PARP degradation was calculated by the ratio between the cleaved and the native form. Cholesterol treatment produced a decrease of native PARP (117 kDa) and the appearance of cleaved form of PARP, at any concentration assayed ($p < 0.001$; Figure 10 B; black bars), thus confirming that cholesterol can promote neuronal apoptosis. The amount of cleaved PARP, calculated respect to the native form, was significantly lower when the treatment with cholesterol was performed in the presence of BDNF ($p < 0.01$; Figure 10 B; grey bar) in line with the previous results of caspase 3 (Figure 10 A). These results demonstrate that BDNF is able to prevent cholesterol-induced apoptosis.

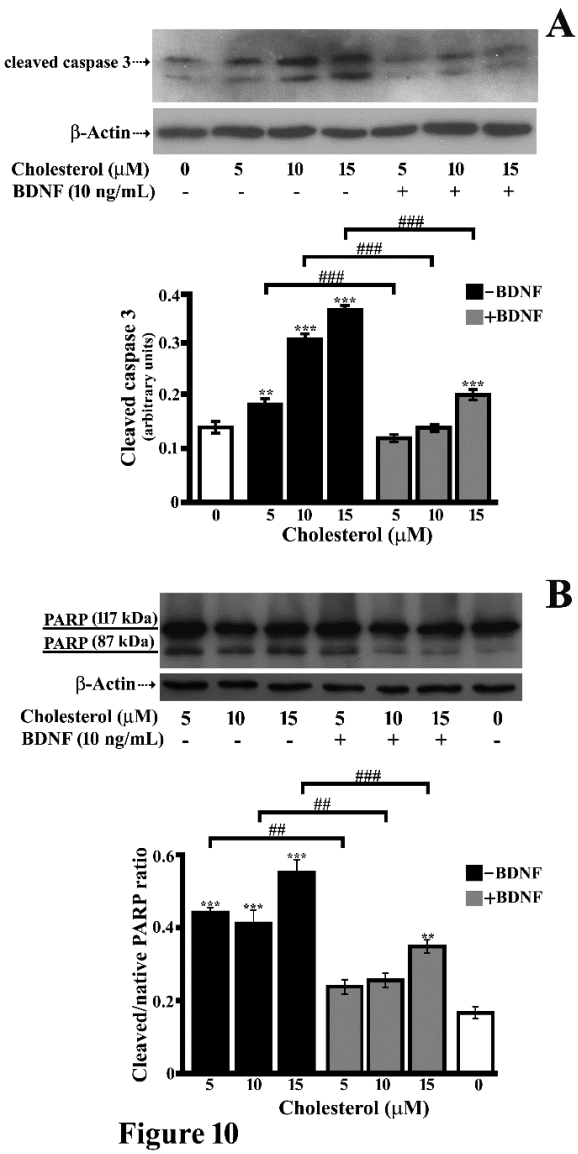

Figure 10

Figure 10. BDNF effect on cholesterol-induced apoptosis. *SH-SY5Y cells were incubated (20 h, 37°C) in serum-free DMEM/F12 containing different amounts of cholesterol (0, 5, 10, or 15 μM) in the absence (black bar) or presence (grey bar) of 10 ng/mL BDNF. At the end of incubation, aliquots of cell lysates were analyzed by 12.5% SDS-PAGE and Western blotting. Representative Western blot is shown on the top in each panel. Quantitative densitometry of cleaved caspase 3, native (117 kDa) and cleaved (87 kDa) PARP and β- actin was carried out and is shown on the bottom of each panel. The extent of PARP degradation was calculated as ratio between the cleaved and the native form. Significant differences from cells not exposed to cholesterol (open bar) are indicated (**p < 0.01; ***p < 0.001). ##, p < 0.01; ###, p < 0.001.*

Cholesterol stimulates BDNF production

It was previously reported that toxic concentrations (12-25 μM) of cholesterol impair BDNF secretion by undifferentiated SH-SY5Y (Huang et al., 2016). Here we investigated whether cholesterol, in a concentration range not affecting cell viability, influences BDNF expression and synthesis by differentiated SH-SY5Y neurons. BDNF concentration in cell lysates was measured, after 20 h of cholesterol treatment, both by Western blotting and ELISA. The results

show that the treatment with 4.5 μM cholesterol stimulates BDNF production (Figure 11 A, $p < 0.001$; Figure 11 B, $p < 0.01$). The level of BDNF mRNA was assessed by qPCR, and no significative change was detected (Figure 11 C). These results show that cholesterol stimulates BDNF synthesis likely affecting post-transcriptional regulation of BDNF expression. Overall these findings suggest that cells might increase BDNF production when challenged with cholesterol as a protective mechanism to limit a harmful intracellular accumulation of this sterol.

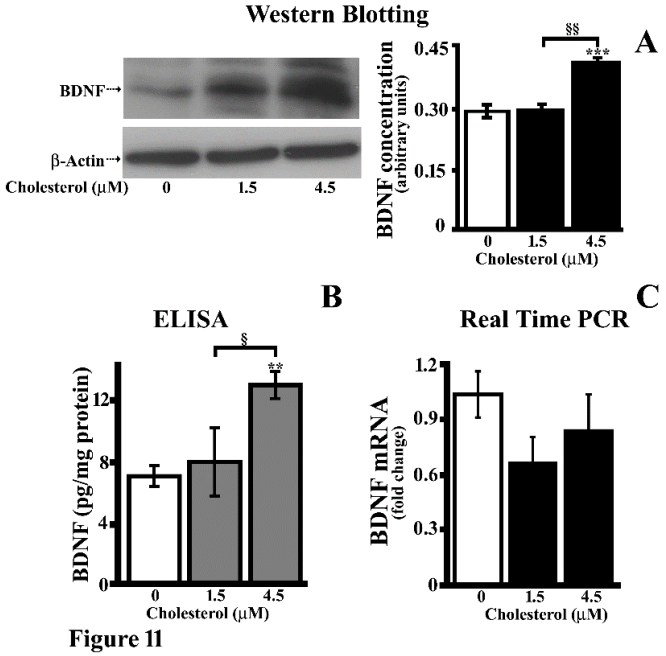

Figure 11

Figure 11. Cholesterol influence on BDNF synthesis. *Differentiated SH-SY5Y cells were incubated (20 h) with different amounts of cholesterol (0, 1.5 or 4.5 μM). At the end of incubation, cells lysates were analyzed by 15% SDS-PAGE and Western Blotting (Panel A) or ELISA (Panel B). Panel A. Representative Western blot of cell lysates is shown on the left. Quantitative densitometry was carried out. BDNF concentrations, calculated relative to β-actin level, are shown on the right. Values are reported as means from three independent experiments± SEM. Panel B. BDNF concentration in cell lysates was measured by sandwich ELISA. Data are reported as pg of BDNF per mg of cell proteins. Panel C. BDNF gene expression level was normalized to the reference gene hypoxanthine phosphoribosyltransferase 1 (HPRT1) and calculated by the 2^ – ΔΔCt method. The results from independent biological replicates in triplicate are expressed as mean ± SEM. Statistical analysis of the qPCR data was carried out using a two-tailed t test. Significance of difference from cells cultured in the absence of treatment (open bar; **, $p < 0.01$; ***, $p < 0.001$) is shown. §, $p < 0.05$; §§, $p < 0.01$ (one-way Anova followed by Tukey's post test).*

Discussion

The decrease in BDNF as well as dysregulation of cholesterol balance is increasingly being correlated to brain dysfunction and neurodegenerative diseases such as AD (Holsinger et al., 2000; Siegel and Chauhan, 2000; Peng et al., 2005; Vance, 2012). Thus, a better understanding

of further physiological roles played by BDNF in cholesterol and lipid homeostasis is important to unravel the mechanisms underlying neurodegeneration and to elucidate the link between cholesterol metabolism and brain physio-pathology. In this paper, we particularly addressed the role of BDNF on cholesterol homeostasis, focusing on both the modulation of ApoE expression by astrocytes and cholesterol trafficking between astrocytes and neurons. Astrocytes are able to respond to BDNF through expressing both full length (TrkB-FL) and truncated (TrkB-T) tropomyosin receptor kinase B (TrkB) receptors (Ohira et al., 2005; Aroeira et al., 2015). Astrocytes seem to express predominantly the TrkB-T receptors, which are able to mediate BDNF-evoked Ca2+ signaling in glia cells and the activation of PLC (Rose et al., 2003). We found that the truncated isoform is predominantly expressed over the TrkB-FL receptor in the cell models, normal human astrocytes (NHA) and glioblastoma-astrocytoma cell line U-87 MG, used in this study. The here presented results show that BDNF treatment stimulates cholesterol efflux from astrocytes as well as an increased expression of ABCA1 transporters in these cells. Cholesterol efflux is known to be promoted by ApoE, which interacts with ABC transporters and also acts as cholesterol acceptor (Koldamova et al., 2003; Abildayeva et al., 2006; Huang and Mahley, 2014). The cholesterol transporter ABCA1, in turn, modulates the level of ApoE protein and its lipidation state, which are crucial for the apolipoprotein capacity to regulate cholesterol metabolism (Tokuda et al., 2000; de Lange, 2004). Interestingly, this work provides evidence, for the first time, that BDNF enhances ApoE expression in astrocytes, besides ABCA1. On the basis of our results it seems reasonable that the increase in cholesterol efflux, observed after BDNF treatment, can be related on the increased expression of ABCA1 and ApoE. The BDNF-induced increase in ApoE is a relevant issue and might represent a further beneficial effect displayed by this neurotrophin on brain physiology. In fact, besides to cholesterol/lipid homeostasis, ApoE is far known to modulate CNS multiple mechanistic pathways that collectively affect cognition, including synaptic function, glucose metabolism, neurogenesis, tau phosphorylation, neuroinflammation, amyloid beta metabolism and aggregation (Huang and Mahley, 2014). Moreover, ApoE is also required for maintenance of the neural stem or progenitor cell pool in the adult dentate gyrus region of the hippocampus (Yang et al., 2011). Neurotrophin engagement of Trk receptors leads to increased downstream activities of Erk1 and Erk2 (Skaper, 2008), thus regulating neuronal differentiation, including neurite development, and survival (Bonni et al., 1999; Gupta et al., 2013). Also the BDNF-dependent activation of Erk1/2 signaling pathway in cultured astrocytes was previously reported to induce the expression of dopamine receptor D5 (Brito et al., 2004) or GABA Transporter-1 (Vaz et al., 2011). Accordingly with these previous reports, we found that BDNF

also upregulates the Erk1/2 signaling pathway in our astrocyte models. The Erk pathway plays a crucial role in cell proliferation and differentiation (Segal and Greenberg, 1996), and its involvement in astroglial regulation of ApoE by BDNF is intriguing. The implication of Erk1/2 pathway in the enhancement of ApoE expression and secretion by astrocytes (Yin et al., 2012) and neuronal cells (Harris et al., 2004) has been previously reported. Further, Erk1/2 signaling regulates ABCA1 expression in different cell types as well (Chang et al., 2013; Mulay et al., 2013). Although further experiments are required for clarifying the underlying mechanicistic pathway, it can be hypothesized that the BDNF-induced Erk activation participates in the modulation of ApoE and ABCA1 expression in our astrocytes model. Cholesterol homeostasis in the brain involves not only the production and efflux of cholesterol from cells but also its cellular uptake in neurons via lipoprotein receptors. Given the influence of BDNF on cholesterol efflux, we wondered whether this neurotrophic factor, by virtue of its growth promoting activities, could also influence cholesterol synthesis and/or uptake in neurons. It was previously published that BDNF increased, in cultured cortical and hippocampal neurons, the mRNA for HMGCoA reductase (HMGCR), the first committed enzyme in cholesterol biosynthesis (Suzuki et al., 2007). Accordingly, the results presented herein indicate that the neurotrophin stimulates the transcription of HMGCR into differentiated SH-SY5Y neurons. We also found that BDNF significantly reduces cholesterol internalization in differentiated neurons and the interaction of ApoE with the same cells. The family of receptors implicated in cholesterol incorporation includes low density lipoprotein (LDL) receptor (LDLR), the very low-density lipoprotein receptor (VLDLR), apoE receptor 2 (apoER2), and LDLR-related protein 1 (LRP1) (Lane- Donovan et al., 2014), that are expressed ubiquitously in the brain. Activation of LXRs downregulate lipoprotein receptor cell surface expression, thus reducing cholesterol uptake (Courtney and Landreth, 2016). The key role of LXRs as major regulators of neuronal content of cholesterol prompted us to investigate whether BDNF effect on neuronal cholesterol uptake might be related to LXR beta modulation, and interestingly we demonstrate that the neurotrophin enhances the expression of LXR beta. The BDNF-induced decrease of cholesterol uptake might therefore depend on the reduced expression of lipoprotein receptors on cell, through the enhanced expression of LXR. We believe that BDNF might exert a critical neuroprotective role by limiting cholesterol accumulation into neurons. In fact cholesterol may be toxic to its host cell, and when accumulated, causes cell apoptosis and death (Liu et al., 2010; Spagnuolo et al., 2014 a; Huang et al., 2016; Kim et al., 2017). Excess brain cholesterol has been also associated with increased formation and deposition of amyloid beta peptide from amyloid precursor protein (Shobab et al., 2005). A number of studies have shown that

cholesterol content affects transport, proteolytic cleavage, aggregation, and toxicity of amyloid beta (Cossec et al., 2010), and this represents an additional mechanism responsible for cholesterol-induced apoptosis. In addition, some oxysterols, including 7-ketocholesterol and 7-betahydroxycholesterol, which are formed by auto-oxidation of cholesterol, can activate inflammation, induce oxidative stress, and trigger cell death (Jang and Lee, 2011; Vejux et al., 2008; Vejux and Lizard, 2009; Lordan et al., 2009). Here we provide evidence that BDNF protects neurons from apoptosis, as reduced levels of both cleaved caspase 3 and PARP were detected in the presence of the neurotrophin. Our hypothesis is that BDNF exerts a neuroprotective role, as it participates in cholesterol homeostasis by regulating the amount internalized by neurons. The BDNF dependent reduction of cholesterol excess uptake, and possibly of the resulting oxidized products, might prevent apoptosis. Given the critical role played by BDNF in cholesterol homeostasis, we next evaluated whether cholesterol itself may affect BDNF synthesis by differentiated SH-SY5Y neurons. The data demonstrate that cholesterol, at levels not affecting neuron survival, does not affect BDNF mRNA level but significantly induces its protein level. This led us to the hypothesis that cholesterol likely influences the translation of BDNF mRNA. This can be presumably due to the fact that alterations of rafts cholesterol levels are known to lead to activation of multiple pathways (George and Wu, 2012), including BDNF level regulation. Hence the production of the neurotrophic factor could be influenced by the alteration of lipid composition of the brain and might represent a physiological/pathological response to cholesterol changes in brain. The induction of BDNF might work to preserve brain functioning from cholesterol homeostasis alteration. Interestingly cholesterol can induce ApoE production in neurons as well (Xu et al., 2006) and very recently it was reported that the three ApoE isoforms differentially regulate expression and secretion of BDNF from human astrocytes (Sen et al., 2017). Intriguingly both BDNF and ApoE have been related to AD development. In fact the ApoE 4 allele is the greatest genetic risk factor for sporadic AD (Liu et al., 2013). In addition, considerable evidence suggests that a reduction in BDNF is associated with AD (Siegel et al., 2000; Holsinger et al., 2000; Peng et al., 2005). Given the common role of ApoE and BDNF in synaptogenesis, neuroprotection, and synaptic plasticity, our results highlight a link between ApoE and BDNF in maintaining cholesterol homeostasis. According to our findings in vitro, the analysis ex vivo of both BDNF and ApoE levels in human post-mortem brain tissues showed that a positive correlation between the two proteins exists. Despite the limit of a correlation, these data in samples ex vivo confirm a link between cerebral concentration of BDNF and ApoE and supports the results obtained from analyses performed with in vitro culture. Overall, our data

point to a novel role of BDNF in cholesterol homeostasis in brain. Taken together, they show that BDNF regulates ApoE expression and secretion and, therefore, provide additional mechanistic insight as to how BDNF may offer neuroprotection through ApoE and modulation of cholesterol content in glial and neuronal cells (Figure 12).

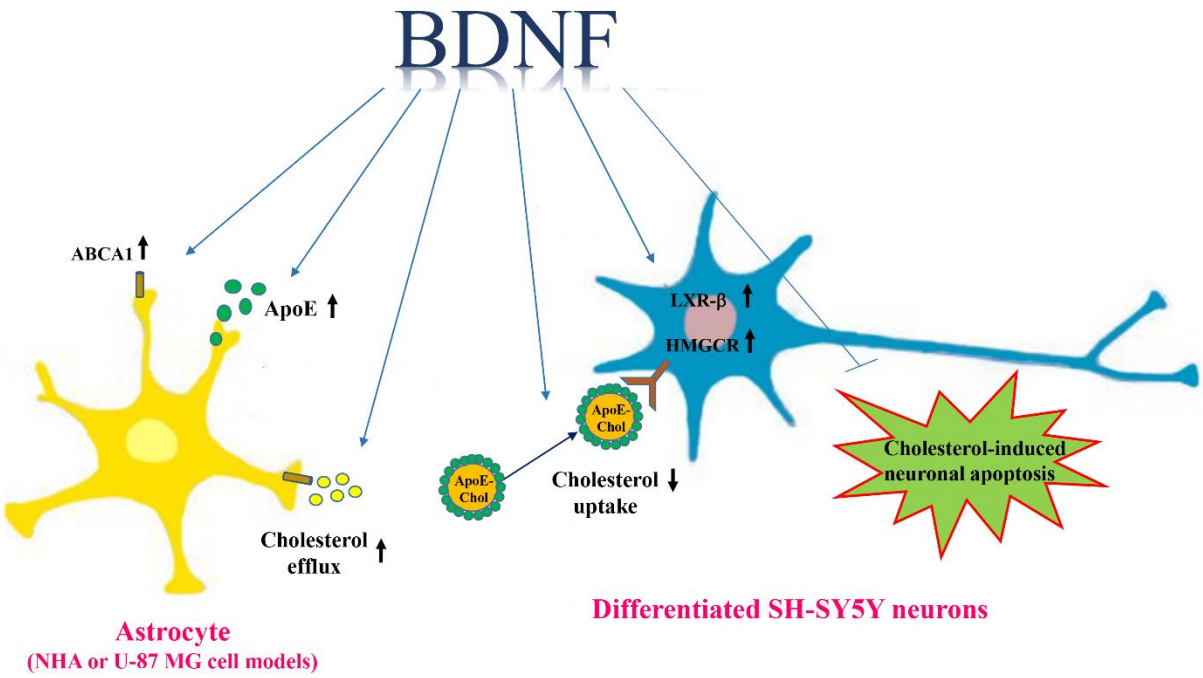

Figure 12. BDNF modulates cholesterol metabolism. *BDNF stimulates cholesterol (chol) efflux, ATP binding cassette A1 (ABCA1) transporter and Apolipoprotein E (ApoE) expression in astrocytes. Also, BDNF downregulates the uptake of cholesterol and prevents cholesterol-induced apoptosis in differentiated SH-SY5Y neurons.*

By providing insight into a previously unknown role of the neurotrophin, this study may contribute to a better understanding of the mechanisms by which neurotrophic factors regulate lipid metabolism, thus representing a framework for future studies.

Supplementary data

Supplementary Table 1. Primers used for qPCR analysis

Gene symbol	Primer Sequence
HPRT1	F_ 5'- CAGACTTTGCTTTCCTTGGT -3' R_ 5'- TGGCTTATATCCAACACTTC -3'
ABCA1	F_ 5'- TGTAATGCCAACAACCCCTG -3' R_ 5'- AAAGAAGCCTCCGAGCATCT -3'
APOE	F_ 5'- ACCCAGGAACTGAGGGC -3' R_ 5'- CTCCTTGGACAGCCGTG -3'
$APOE_{NHA}$	F_ 5'- CACTGGGTCGCTTTTGGG -3' R_ 5'- CCAGTTCCGATTTGTAGGCC-3'
HMGCR	F_ 5'- AGTGACACTGACCATCTGCA -3' R_ 5'- TGTCACTGCTCAAAACATCCTC -3'
BDNF	F_ 5'- ACACAAAAGAAGGCTGCAGG -3' R_ 5'- TGCTATCCATGGTAAGGGCC -3'

Supplementary Table 2.

Selected list of genes involved in cholesterol metabolism and trafficking from the Microarray analysis.

Gene symbol	Regulation	FC
HMGCR	up	2,1
BIN1	up	1,6
SREBP-2	-	-
PPAR	-	-
LXR	-	-
MPD	-	-
SORL1	-	-
PICALM	-	-
IDOL	-	-

FC: fold change, linear scale;
- : no change detected.

Supplementary figure 1

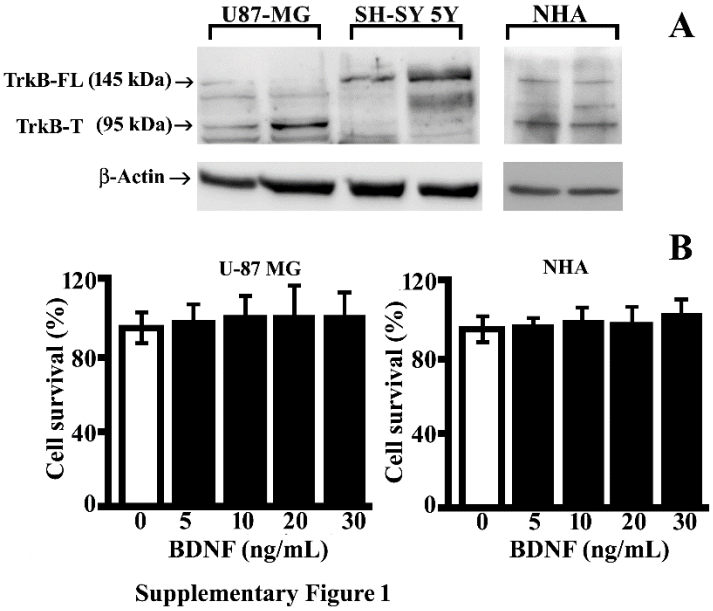

Supplementary Figure 1

TrkB expression and cell viability assay. *Panel A. Aliquots of lysates from U-87 MG or NHA or from differentiated SH-SY5Y (incubated for 20 hours in serum free medium) were analysed by 10% SDS-PAGE and Western Blotting. TrkB was detected by rabbit anti-human TrkB IgG and Goat anti-rabbit-horseradish peroxidase conjugated IgG. β-Actin was revealed by mouse anti- -Actin and Goat anti-mouse-horseradish peroxidase conjugated IgG. Representative Western blotting of two different samples of astrocytes and neurons is shown. Panel B. U-87 MG (on the left) or NHA (on the right) were incubated into 96 well-plates (20 h; 15,000 or 4,000 cells/well, respectively) in serum-free medium containing different amounts of BDNF (0-30 ng/mL). Cell survival was evaluated by MTT assay, and it was expressed as percentage of viability of the control (cells cultured without BDNF addition; open bar). Data are reported as mean ± SEM.*

Supplementary Figure 2

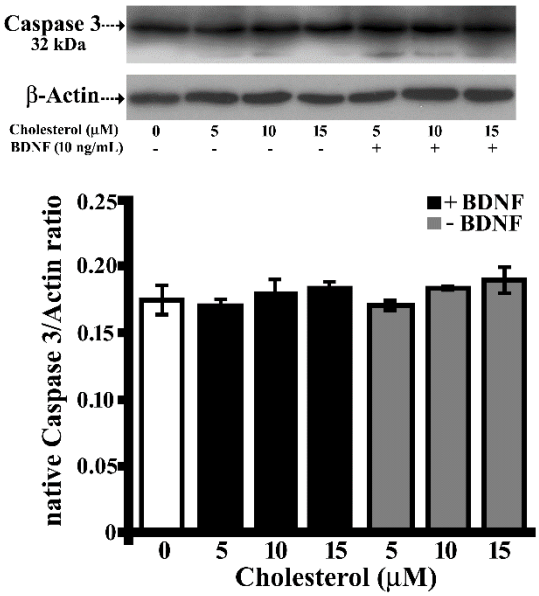

Supplementary Figure 2

BDNF effect on native caspase 3 level in SH-SY5Y. *SH-SY5Y cells (150,000 cells/well; 12-well plate) were incubated (20 h, 37°C) in serum-free DMEM/F12 containing different amounts of cholesterol (0, 5, 10, or 15 μM) in the absence (black bar) or presence (grey bar) of 10 ng/mL BDNF. At the end of incubation, aliquots of cell lysates were analyzed by 12.5% SDS-PAGE and Western blotting. Immunocomplexes were detected by rabbit anti-Caspase 3 (Immunological Science, AB-83625). After caspase3 detection, the membrane was stripped for reprobing with anti-β-actin. Representative Western blot is shown on the top. Quantitative densitometry of native caspase 3 and β-actin was carried out and the ratio is shown on the bottom.*

References

Abildayeva K, Jansen PJ, Hirsch-Reinshagen V, Bloks VW, Bakker AH, Ramaekers FC, de Vente J, Groen AK, Wellington CL, Kuipers F, Mulder M. (2006). 24(S)-hydroxycholesterol participates in a liver X receptor-controlled pathway in astrocytes that regulates apolipoprotein E-mediated cholesterol efflux. J Biol Chem 281:12799-12808. doi: 10.1074/jbc.M601019200.

Aliperti V, Donizetti A. (2016). Long Non-coding RNA in Neurons: New Players in Early Response to BDNF Stimulation. Front Mol Neurosci 9:15. doi: 10.3389/fnmol.2016.00015.

Aroeira RI, Sebastião AM, Valente CA. (2015). BDNF, via truncated TrkB receptor, modulates GlyT1 and GlyT2 in astrocytes. Glia 63:2181-2197. doi: 10.1002/glia.22884.

Bonni A, Brunet A, West AE, Datta SR, Takasu MA, Greenberg ME. (1999). Cell survival promoted by the Ras-MAPK signaling pathway by transcription-dependent and -independent mechanisms. Science 286:1358-1362.

Bradford MM. (1976). A rapid and sensitive method for the quantitation of microgram quantities of protein utilizing the principle of protein-dye binding. Anal Biochem 72:248-254.

Brito V, Beyer C, Küppers E. (2004). BDNF-dependent stimulation of dopamine D5 receptor expression in developing striatal astrocytes involves PI3-kinase signaling. Glia 46:284-295. doi: 10.1002/glia.10356

Cartocci V, Servadio M, Trezza V, Pallottini V. (2017). Can Cholesterol Metabolism Modulation Affect Brain Function and Behavior? J Cell Physiol 232:281-286. doi: 10.1002/jcp.25488

Chang YC, Sheu WH, Chien YS, Tseng PC, Lee WJ, Chiang AN. (2013). Hyperglycemia accelerates ATP-binding cassette transporter A1 degradation via an ERK-dependent pathway in macrophages. J Cell Biochem 114:1364-1373. doi: 10.1002/jcb.24478.

Cossec JC, Marquer C, Panchal M, Lazar AN, Duyckaerts C, Potier MC. (2010). Cholesterol changes in Alzheimer's disease: methods of analysis and impact on the formation of enlarged endosomes. Biochim Biophys Acta 1801:839-845. doi: 10.1016/j.bbalip.2010.03.010.

Courtney R, Landreth GE. (2016). LXR Regulation of Brain Cholesterol: From Development to Disease. Trends Endocrinol Metab 27:404-414. doi: 10.1016/j.tem.2016.03.018.

de Lange EC. (2004). Potential role of ABC transporters as a detoxification system at the blood-CSF barrier. Adv Drug Deliv Rev 56:1793-1809. doi: 10.1016/j.addr.2004.07.009

DeMattos RB, Brendza RP, Heuser JE, Kierson M, Cirrito JR, Fryer J, Sullivan PM, Fagan AM, Han X, Holtzman DM. (2001). Purification and characterization of astrocyte-secreted apolipoprotein E and Jcontaining lipoproteins from wild-type and human apoE transgenic mice. Neurochem Int 39:415-425.

Foley P. (2010). Lipids in Alzheimer's disease: A century-old story. Biochim Biophys Acta 1801:750-753. doi: 10.1016/j.bbalip.2010.05.004.

George KS, Wu S. (2012). Lipid Raft: A Floating Island Of Death or Survival. Toxicol Appl Pharmacol 259:311-319. doi: 10.1016/j.taap.2012.01.007.

Guirland C, Suzuki S, Kojima M, Lu B, Zheng JQ. (2004). Lipid rafts mediate chemotropic guidance of nerve growth cones. Neuron. 42:51-62.

Gupta VK, You Y, Gupta VB, Klistorner A, Graham SL. (2013). TrkB Receptor Signalling: Implications in Neurodegenerative, Psychiatric and Proliferative Disorders. Int J Mol Sci 14:10122-142. doi: 10.3390/ijms140510122.

Harris FM, Tesseur I, Brecht WJ, Xu Q, Mullendorff M, Chang S, Wyss-Coray T, Mahley RW, Huang Y. (2004). Astroglial regulation of apolipoprotein E expression in neuronal cells. Implications for Alzheimer's disease. J Biol Chem 279:3862-3868. doi: 10.1074/jbc.M309475200

Herz J. (2009). Apolipoprotein E Receptors in the Nervous System. Curr Opin Lipidol 20:190-196. doi: 10.1097/MOL.0b013e32832d3a10.

Holsinger RM, Schnarr J, Henry P, Castelo VT, Fahnestock M. (2000). Quantitation of BDNF mRNA in human parietal cortex by competitive reverse transcription-polymerase chain reaction: decreased levels in Alzheimer's disease. Brain Res Mol Brain Res 76:347-354.

Huang EJ, Reichardt LF. (2001). Neurotrophins: roles in neuronal development and function. Annu Rev Neurosci 24:677-736. doi: 10.1146/annurev.neuro.24.1.677

Huang YN, Lin CI, Liao H, Liu CY, Chen YH, Chiu WC, Lin SH. (2016). Cholesterol overload induces apoptosis in SH-SY5Y human neuroblastoma cells through the up regulation of flotillin-2 in the lipid raft and the activation of BDNF/Trkb signaling. Neuroscience 328:201-209. doi: 10.1016/j.neuroscience.2016.04.043.

Huang Y, Mahley RW. (2014). Apolipoprotein E: structure and function in lipid metabolism, neurobiology, and Alzheimer's diseases. Neurobiol Dis 72:3-12. doi: 10.1016/j.nbd.2014.08.025.

Ikonen E. (2008). Cellular cholesterol trafficking and compartmentalization. Nat Rev Mol Cell Biol 9:125-138. doi: 10.1038/nrm2336.

Jang ER, Lee CS. (2011). 7-Ketocholesterol induces apoptosis in differentiated PC12 cells via reactive oxygen species-dependent activation of NF-kB and Akt pathways. Neurochem Int 58:52-59. doi: 10.1016/j.neuint.2010.10.012.

Kaufmann SH, Desnoyers S, Ottaviano Y,Davidson NE, Poirier GG. (1993). Specific proteolytic cleavage of poly (ADP-ribose) polymerase: an early marker of chemotherapy-induced apoptosis. Cancer Res 53:3976-3985.

Kim A, Nam YJ, Lee CS. (2017). Taxifolin reduces the cholesterol oxidation product-induced neuronal apoptosis by suppressing the Akt and NF-κB activation-mediated cell death. Brain Res Bull 34:63-71. doi: 10.1016/j.brainresbull.2017.07.008.

Koldamova RP, Lefterov IM, Ikonomovic MD, Skoko J, Lefterov PI, Isanski BA, DeKosky ST, Lazo JS. (2003). 22R-hydroxycholesterol and 9-cis-retinoic acid induce ATP-binding cassette transporter

A1 expression and cholesterol efflux in brain cells and decrease amyloid β secretion. J Biol Chem 278:13244-13256. doi: 10.1074/jbc.M300044200

Kotti TJ, Ramirez DM, Pfeiffer BE, Huber KM, Russell DW. (2006). Brain cholesterol turnover required for geranylgeraniol production and learning in mice. Proc Natl Acad Sci U S A 103:3869-3874. doi: 10.1073/pnas.0600316103

Lane-Donovan C, Philips GT, Herz J. (2014). More than cholesterol transporters: lipoprotein receptors in CNS function and neurodegeneration. Neuron 83:771-787. doi: 10.1016/j.neuron.2014.08.005.

Liu CC, Liu CC, Kanekiyo T, Xu H, Bu G. (2013). Apolipoprotein E and Alzheimer disease: risk, mechanisms and therapy. Nat Rev Neurol 9:106-118. doi: 10.1038/nrneurol.2012.263.

Liu JP, Tang Y, Zhou S, Toh BH, McLean C, Li H. (2010). Cholesterol involvement in the pathogenesis of neurodegenerative diseases. Mol Cell Neurosci 43:33-42. doi: 10.1016/j.mcn.2009.07.013.

Lordan S, Mackrill JJ, O'Brien NM. (2009). Oxysterols and mechanisms of apoptotic signaling: implications in the pathology of degenerative diseases. J Nutr Biochem 20: 321-336. doi: 10.1016/j.jnutbio.2009.01.001.

Maresca B, Spagnuolo MS, Cigliano L. (2015). Haptoglobin modulates beta-amyloid uptake by U-87 MG astrocyte cell line. J Mol Neurosci 56:35-47. doi: 10.1007/s12031-014-0465-6.

Mauch DH, Nägler K, Schumacher S, Göritz C, Müller EC, Otto A, Pfrieger FW. (2001). CNS synaptogenesis promoted by glia-derived cholesterol. Science 294:1354-1357. doi: 10.1126/science.294.5545.1354

Mouzat K, Raoul C, Polge A, Kantar J, Camu W, Lumbroso S. (2016). Liver X receptors: from cholesterol regulation to neuroprotection-a new barrier against neurodegeneration in amyotrophic lateral sclerosis? Cell Mol Life Sci. 73:3801-3808. doi: 10.1007/s00018-016-2330-y.

Mulay V, Wood P, Manetsch M, Darabi M, Cairns R, Hoque M, Chan KC, Reverter M, Alvarez-Guaita A, Rye KA, Rentero C, Heeren J, Enrich C, Grewal T. (2013). Inhibition of mitogen-activated protein kinase Erk1/2 promotes protein degradation of ATP binding cassette transporters A1 and G1 in CHO and HuH7 cells. PLoS One 8:e62667. doi: 10.1371/journal.pone.0062667.

Nordin-Andersson M, Walum E, Kjellstrand P, Forsby A. 2003. Acrylamide-induced effects on general and neurospecific cellular functions during exposure and recovery. Cell Biol Toxicol 19:43-51.

Ohira K. (2005). A truncated tropo-myosine-related kinase B receptor, T1, regulates glial cell morphology via Rho GDP dissociation inhibitor 1. J Neurosci 25:1343-1353. doi: 10.1523/JNEUROSCI.4436-04.2005

Ohira K, Funatsu N, Homma KJ, Sahara Y, Hayashi M, Kaneko T, Nakamura S. (2007). Truncated TrkB-T1 regulates the morphology of neocortical layer I astrocytes in adult rat brain slices. Eur J Neurosci 25:406-416. doi: 10.1111/j.1460-9568.2007.05282.x

Påhlman S, Ruusala AI, Abrahamsson L, Mattsson ME, Esscher T. (1984). Retinoic acid-induced differentiation of cultured human neuroblastoma cells: a comparison with phorbolester-induced differentiation. Cell Differ 14:135-144.

Paratcha G, Ibáñez CF. (2002). Lipid rafts and the control of neurotrophic factor signaling in the nervous system: variations on a theme. Curr Opin Neurobiol 12:542-549.

Peng S, Wuu J, Mufson EJ, Fahnestock M. (2005). Precursor form of brain-derived neurotrophic factor and mature brain-derived neurotrophic factor are decreased in the pre-clinical stages of Alzheimer's disease. J Neurochem 93:1412-1421. doi: 10.1111/j.1471-4159.2005.03135.x

Pfrieger FW, Ungerer N. (2011). Cholesterol metabolism in neurons and astrocytes. Prog Lipid Res 50:357-371. doi: 10.1016/j.plipres.2011.06.002.

Poo MM. (2001). Neurotrophins as synaptic modulators. Nat Rev Neurosci 2:24-32. doi: 10.1038/35049004

Posse De Chaves EI, Vance DE, Campenot RB, Kiss RS, Vance JE. (2000). Uptake of lipoproteins for axonal growth of sympathetic neurons. J Biol Chem 275:19883-19890.

Reichardt LF. (2006). Neurotrophin-regulated signalling pathways. Philos Trans R Soc Lond B Biol Sci 361:1545-1564. doi: 10.1098/rstb.2006.1894

Rose CR, Blum R, Pichler B, Lepier A, Kafitz KW, Konnerth A. (2003). Truncated TrkB-T1 mediates neurotrophin-evoked calcium signalling in glia cells. Nature 426:74-78.

Segal RA, Greenberg ME. (1996). Intracellular signaling pathways activated by neurotrophic factors. Annu Rev Neurosci 19:463-489. doi: 10.1146/annurev.ne.19.030196.002335

Sen A, Nelson TJ, Alkon DL. (2017). ApoE isoforms differentially regulates cleavage and secretion of BDNF. Mol Brain. doi: 10.1186/s13041-017-0301-3.

Shobab LA, Hsiung GY, Feldman HH. (2005). Cholesterol in Alzheimer's disease. Lancet Neurol 4:841-852.doi:

Siegel GJ, Chauhan NB. (2000). Neurotrophic factors in Alzheimer's and Parkinson's disease brain. Brain Res Brain Res Rev 33:199-227. doi: 10.1016/S1474-4422(05)70248-9

Simons K, Toomre D. (2000). Lipid rafts and signal transduction. Nat Rev Mol Cell Biol 1:31-39. doi: 10.1038/35036052

Skaper SD. 2008. The biology of neurotrophins, signalling pathways, and functional peptide mimetics of neurotrophins and their receptors. CNS Neurol Disord Drug Targets 7:46-62.

Solomon A, Kåreholt I, Ngandu T, Winblad B, Nissinen A, Tuomilehto J, Soininen H, Kivipelto M. (2007). Serum cholesterol changes after midlife and late-life cognition: twenty-one-year follow-up study. Neurology 68:751-756. doi: 10.1212/01.wnl.0000256368.57375.b7

Spagnuolo MS, Maresca B, Mollica MP, Cavaliere G, Cefaliello C, Trinchese G, Esposito MG, Scudiero R, Crispino M, Abrescia P, Cigliano L. (2014) (a). Haptoglobin increases with age in rat hippocampus and modulates Apolipoprotein E mediated cholesterol trafficking in neuroblastoma cell lines. Front Cell Neurosci 8:212. doi: 10.3389/fncel.2014.00212

Spagnuolo MS, Maresca B, La Marca V, Carrizzo A, Veronesi C, Cupidi C, Piccoli T, Maletta RG, Bruni AC, Abrescia P, Cigliano L. (2014) (b). Haptoglobin interacts with apolipoprotein E and betaamyloid and influences their crosstalk. ACS Chem Neurosci 5:837-847. doi: 10.1021/cn500099f.

Spagnuolo MS, Mollica MP, Maresca B, Cavaliere G, Cefaliello C, Trinchese G, Scudiero R, Crispino M, Cigliano L. (2015). High Fat Diet and Inflammation - Modulation of Haptoglobin Level in Rat Brain. Front Cell Neurosci 9:479. doi: 10.3389/fncel.2015.00479.

Suzuki S, Kiyosue K, Hazama S, Ogura A, Kashihara M, Hara T, Koshimizu H, Kojima M. (2007). Brain-derived neurotrophic factor regulates cholesterol metabolism for synapse development. J Neurosci 27:6417-6427. doi: 10.1523/JNEUROSCI.0690-07.2007

Suzuki S, Numakawa T, Shimazu K, Koshimizu H, Hara T, Hatanaka H, Mei L, Lu B, Kojima M. (2004). BDNF-induced recruitment of TrkB receptor into neuronal lipid rafts: roles in synaptic modulation. J Cell Biol 167:1205-1215. doi: 10.1083/jcb.200404106

Tokuda T, Calero M, Matsubara E, Vidal R, Kumar A, Permanne B, Zlokovic B, Smith JD, Ladu MJ, Rostagno A, Frangione B, Ghiso J. (2000). Lipidation of apolipoprotein E influences its isoform-specific interaction with Alzheimer's amyloid beta peptides. Biochem J 348:359-365.

Valiante S, Falanga A, Cigliano L, Iachetta G, Busiello RA, La Marca V, Galdiero M, Lombardi A, Galdiero S. (2015). Peptide gH625 enters into neuron and astrocyte cell lines and crosses the blood-brain barrier in rats. Int J Nanomedicine 10:1885-1898. doi: 10.2147/IJN.S77734

Vance JE, Hayashi H. (2010). Formation and function of apolipoprotein E containing lipoproteins in the nervous system. BBA Molecular Cell Biol Lipids 1801:806-818. doi: 10.1016/j.bbalip.2010.02.007.

Vance JE. (2012). Dysregulation of cholesterol balance in the brain: contribution to neurodegenerative diseases. Dis Model Mech 5:746-755. doi: 10.1242/dmm.010124

Vaz SH, Jørgensen TN, Cristóvão-Ferreira S, Duflot S, Ribeiro JA, Gether U, Sebastião AM. (2011). Brain-derived neurotrophic factor (BDNF) enhances GABA transport by modulating the trafficking of GABA transporter-1 (GAT-1) from the plasma membrane of rat cortical astrocytes. J Biol Chem 286:40464-40476. doi: 10.1074/jbc.M111.232009.

Vejux A, Malvitte L, Lizard G. (2008). Side effects of oxysterols: cytotoxicity, oxidation, inflammation, and phospholipidosis. Braz J Med Biol Res 41:545-556.

Vejux A, Lizard G. (2009). Cytotoxic effects of oxysterols associated with human diseases: Induction of cell death (apoptosis and/or oncosis), oxidative and inflammatory activities, and phospholipidosis. Mol Asp Med 30:153-170. doi: 10.1016/j.mam.2009.02.006.

Vitali C, Wellington CL, Calabresi L. (2014). HDL and cholesterol handling in the brain. Cardiovasc Res 103:405-413. doi: 10.1093/cvr/cvu148.

Willy PJ, Umesono K, Ong ES, Evans RM, Heyman RA, Mangelsdorf DJ. (1995). LXR, a nuclear receptor that defines a distinct retinoid response pathway. Genes Dev 9:1033-1045.

Xu Q, Bernardo A, Walker D, Kanegawa T, Mahley RW, Huang Y. (2006). Profile and regulation of apolipoprotein E (ApoE) expression in the CNS in mice with targeting of green fluorescent protein gene to the ApoE locus. J Neurosci 26:4985-4994. doi: 10.1523/JNEUROSCI.5476-05.2006

Yang CP, Gilley JA, Zhang G, Kernie SG. (2011). ApoE is required for maintenance of the dentate gyrus neural progenitor pool. Development 138:4351-4362. doi: 10.1242/dev.065540.

Yin C, Zhou S, Sun X. (2012). Mechanical injured neurons stimulate astrocytes to express apolipoprotein E through ERK pathway. Neurosci Lett 515:77-81. doi: 10.1016/j.neulet.2012.03.023.

Chapter 3

Brain Nrf2 pathway, autophagy, and synaptic function proteins are modulated by a short-term fructose feeding in young and adult rats

*Maria Stefania Spagnuolo, Paolo Bergamo, Raffaella Crescenzo, **Lucia Iannotta**, Lucia Treppiccione, Susanna Iossa & Luisa Cigliano*

Nutritional Neuroscience, 2018, doi: 10.1080/1028415X.2018.1501532

Introduction

A significant increase of food and daily energy intake has been described in the last forty years, (McCrory et al., 2016) and the increasing worldwide prevalence of overweight and obesity has been linked to the shift toward a Western diet pattern (Carlson et al., 2012). In this context, the consumption of sugar-added foods was reported to be associated with increased risk for obesity, metabolic disorders, and cognitive decline (Rippe and Angelopoulos, 2016). In the last decade a strong rise of the fructose content in the human diet has occurred, as corn syrup is widely used as a sweetener for beverages, snacks, bakeries and processed food in general. Fructose has been suggested as a potential contributor to the worldwide rise in overweight and body weight gain, (Malik et al., 2010) and accordingly the association of high fructose intake with the onset of dyslipidemia, insulin resistance, related metabolic diseases (Crescenzo et al., 2013; Aragno, 2017), and impairment of brain structure and function (Hsu et al., 2015; Mastrocola et al., 2016; Cigliano et al., 2018) was evidenced in clinical or animal studies. Long-term feeding (more than 4 weeks) with fructose was reported to induce an impairment of insulin signalling in the hippocampus, (Yin et al., 2014) reduction of neurogenesis, (Van der Borght et al., 2011) widespread reactive gliosis and neuroinflammation, altered mitochondrial activity as well as oxidative stress (Mastrocola et al, 2016; Li et al., 2015). Even short time of fructose feeding was recently shown to have detrimental effects on brain physiology. In fact, we recently reported that a two weeks fructose diet induces inflammation, oxidative stress, impairment of insulin signaling as well as a significant decrease in mitochondrial function in the hippocampus of young and adult rats (Cigliano et al., 2018). Interestingly, one week of fructose ingestion was also shown to have a negative impact on brain plasticity (Jiménez-Maldonado et al., 2018). Young people are known to make a widespread consumption of added sugars, especially fructose-sweetened beverages, (Ford et al., 2008) and therefore investigations on young models could contribute to clarify the early risks to which brain is exposed as a result of diets rich in fructose. Since most of the studies aiming at the comprehension of the effect of fructose in brain have been performed in hippocampus, the present work is focused in frontal cortex, to highlight the effects of a two-weeks fructose diet on redox homeostasis, autophagy and synaptic markers in rats of different age, young (30 days old) and adult rats (90 days). We focused on this specific region, since it includes areas critically implicated in the regulation of higher-order cognitive functions such as working memory, attention or behavioral flexibility, (Robbins, 2000) and, unlike most other brain areas, maturation in the frontal cortex continues until late adolescence, thus being the last brain region to achieve full maturity in humans (Giedd et al., 1999; Gogtay et al., 2004) and rodents (O'Donnell, 2011; Manitt et al.,2013). Accordingly, it has been

demonstrated that high-fat diets or high-fat high-sugar diets induce severe frontal-dependent cognitive deficits when the dietary exposure begins during adolescence as compared to adulthood (Morin et al., 2017; Reichelt, 2016; Reichelt et al., 2015). In order to study the effect of fructose on redox balance we focused on Nuclear factor (erythroid derived 2)-like 2 (Nrf2)-activated defences. Nrf2 is the key transcriptional activator of genes responsible for the maintenance of redox homeostasis through the synthesis/recycling of reduced glutathione (GSH), (Johnson and Johnson, 2015) a fundamental brain antioxidant. Fructose effect on the expression of PPAR-alpha and PPAR-gamma, transcription factors exerting anti-inflammatory and antioxidant effects in central nervous system, (Deplanque, 2004; Rinwa et al., 2010) was further assessed. Moreover, as perturbation of redox homeostasis is known to induce autophagic pathway activation, (Mizushima and Komatsu, 2011) which in turn can cause an impairment of synaptic function, (Chen et al, 2013; Zhang et al., 2017) we further evaluated specific autophagy and brain synaptic proteins in the frontal cortex. Finally, as further marker of brain function, we chose to analyze the activity of Acetylcholinesterase (AChE), that plays a key role not only for cholinergic signaling, (Pope and Brimijoin, 2018) since it hydrolyzes and thus terminates the synaptic action of acetylcholine, but also in neurotransmitter recycling, proteolysis, neurogenesis, morphogenesis and neural differentiation (Janeczek et al., 2018).

Methods

Materials

Bovine serum albumin fraction V (BSA), acetylthiocholine iodide (ATCI), 5,5-dithiobis-2-nitrobenzoate (DTNB), salts and buffers were purchased from Sigma-Aldrich (St. Louis, MO, USA). The dye reagent for protein titration, and the polyvinylidene difluoride (PVDF) membrane were from Bio-Rad (Bio-Rad, Hercules, CA). Fuji Super RX 100 films were from Laboratorio Elettronico Di Precisione (Naples, Italy).

Animals and treatments

Male Sprague–Dawley rats (Charles River, Italy), of 30 (young) or 90 (adult) days of age were caged singly in a temperature-controlled room (23±1°C) with a 12-h light/dark cycle (06.30–18.30). Young (N = 12) and adult (N = 12) rats were divided in two groups and were fed a fructose-rich (Young, N = 6; Adult, N = 6) or control diet (Young, N = 6; Adult, N = 6) for 2 weeks (for composition see Table 1).

TABLE 1

Composition of experimental diets

	CONTROL DIET	FRUCTOSE DIET
Component (g/100 g)		
Standard chow*	50.5	50.5
Sunflower oil	1.5	1.5
Casein	9.2	9.2
Alphacel	9.8	9.8
Starch	20.4	---
Fructose	---	20.4
Water	6.4	6.4
AIN-76 mineral mix	1.6	1.6
AIN-76 vitamin mix	0.4	0.4
Choline	0.1	0.1
Methionine	0.1	0.1
Gross energy density, kJ/g	17.2	17.2
Metabolisable energy density, kJ/g **	11.1	11.1
Protein, % metabolisable energy	29.0	29.0
Lipids, % metabolisable energy	10.6	10.6
Carbohydrates, % metabolisable energy	60.4	60.4
Of which: Fructose	-----	30.0
Starch	52.8	22.8
Sugars	7.6	7.6

** Mucedola 4RF21; Italy. **estimated by computation using values (kJ/g) for energy content as follows: protein 16.736, lipid 37.656, and carbohydrate 16.736.*

Rats were pair-fed for the whole experimental period, by giving them the same amount of diet, both as weight and as caloric content, and each rat consumed the full portion of the diet. This

cohort of rats was the same as that used in Cigliano et al., 2018 where hippocampus was analyzed. During the treatment, body weight, food and water intake were monitored daily. At the end of the experimental period, the rats were euthanized by decapitation and blood was collected for subsequent analyses. The brains were quickly removed, transferred to a metal plate, on ice, and carefully washed with PBS to wipe off surface blood. Frontal cortex dissection was performed according to published protocols (Spijker, 2011; Chiu et al., 2007). In detail, brain was cut, longitudinally, into right and left hemisphere and, from the medial view of the hemisphere, a first cut was performed to remove olfactory bulb. Then frontal cortex was dissected from a slice about 2.5–4.5 mm anterior to bregma, taking into account published stereotaxic atlas resources. (Paxinos and Watson, 1997; Swanson, 2004; Papp et al., 2014.) Samples were snap frozen in liquid nitrogen immediately and stored at –80°C for subsequent analyses.

Protein extraction

Proteins were extracted from frontal cortex by homogenizing frozen tissues (–80°C) in ten volumes (w/v) of cold RIPA buffer (150 mM NaCl, 50 mM Tris–HCl, 0.5% NP-40, 0.5% sodium deoxycholate, 0.1% SDS, pH 8) containing Tissue Protease Inhibitor Cocktail (Sigma-Aldrich, 1:500, v/v) and Tissue Phosphatase inhibitor cocktail (Sigma-Aldrich, 1:100, v/v) (Spagnuolo et al., 2015). The levels of specific markers of synaptic plasticity (brain derived neurotrophic factor, BDNF; synaptophysin, synapsin I; synaptotagmin I), PPAR alpha and PPAR gamma, autophagic pathway (Beclin 1; P62-sequestosome-1, P62; Microtubule associated protein light chain, LC3), and Tropomyosin receptor kinase B (TrkB) receptor were evaluated by Western blotting. Cytosolic and nuclear protein extracts from brain cortex were prepared accordingly to a published protocol, (Zvonic Et al., 2004) and used for investigating diet-induced modification of the brain redox status. Glutathione/Oxidized Glutathione (GSH/GSSG) ratio, Glucose 6-phosphate dehydrogenase (G6PD) and Glutathione reductase (GSR) activities were measured into cytosolic extracts, while Nrf2 amount was evaluated by Western blotting into nuclear extracts.

Brain redox status and phase 2 enzymes activity

GSH and GSSG concentrations were quantified using the DTNB-GSSG reductase recycling assay accordingly to a published protocol (Rahman et al., 2007). Total GSH (GSH +GSSG), GSH and GSSG concentrations, upon normalization to the protein content, were expressed as nmol/mg min and the GSH/GSSG ratio was used to indicate brain RedOx modification. GSR

and G6PD activities were spectrophotometrically assayed in cytoplasmic extracts, (Monaco et al., 2018) and, upon normalization to the protein content, they were expressed as nmol of NADPH/mg min or as IU/mg min, respectively.

AChE activity assay

Fontal cortex aliquots (about 20 mg) were homogenized in 0.3 mL of TBS (100 mM Tris–HCl, pH 8.1) and upon centrifugation (4 minutes, 2000g, 4°C), AChE assay was performed essentially according to a published protocol, (Ellman et al., 1961) using ATCI as a substrate. The rate of production of thiocholine was determined by the reaction of the thiol with DTNB to produce the yellow anion of 5-thio-2-nitro-benzoic acid. Briefly, six aliquots (20 µL containing 20 µg of proteins) from extracts were plated into 96 well plate. Wells containing TBS were used as blank. Aliquots (100 µL) containing 2 mM ATCI in TBS was added to one triplicate series (assay), while 100 µL of TBS was added to the second series (control). Finally, 100 µL of TBS containing 2.4 mM DTNB was added to both series and the absorbance was measured at 405 nm after 10 minutes of incubation at room temperature. AChE activity was corrected by subtracting the spontaneous hydrolysis of the substrate (blank) or the DTNB reaction with protein thiols (control) and enzyme activity was expressed as nmol/min mg protein.

Western blotting

Aliquots (50 µg) of cortex homogenates were fractionated by electrophoresis on 12.5% (to quantify PPAR-alpha, PPAR-gamma, P62, LC3, beclin, BDNF, synaptophysin, synaptotagmin I), or 10% (to quantify synapsin I or TRkB) polyacrylamide gel, under denaturing and reducing conditions (Spagnuolo et al., 2018). After electrophoresis, proteins were blotted onto PVDF membrane, the membrane was rinsed in T-TBS (130 mM NaCl, 20 mM Tris–HCl, 0.05% Tween 20, pH 7.4), and blocking was carried out with T-TBS containing 5% non-fat milk (60 minutes, 37°C). BDNF was revealed by incubation (overnight, 4°C) with anti-human BDNF IgG (Santa Cruz Biotechnology, CA, USA; 1:500 dilution in T-TBS containing 0.25% non-fat milk), followed by goat anti-rabbit Horseradish Peroxidase-conjugated IgG (GAR-HRP; Sigma-Aldrich; 1:4000 dilution in TTBS containing 0.25% non-fat milk; 1 hour, 37°C). PPAR-alpha was detected by incubation (overnight, 4°C) with anti- PPAR-alpha IgG (Thermo Fisher, IL, USA; 1:1000 dilution in T-TBS containing 3% BSA) followed by GAR-HRP IgG (Sigma-Aldrich; 1: 20 000 dilution in T-TBS containing 1% non-fat milk; 1 hour, 37°C). PPAR-gamma was detected by incubation (overnight, 4°C) with anti-PPAR-gamma IgG (Santa Cruz

Biotechnology; 1:300 dilution in T-TBS containing 3% BSA) followed by GAR-HRP IgG (Sigma-Aldrich; 1:4000 dilution in T-TBS containing 1% non-fat milk; 1 hour, 37°C). LC3 was revealed by incubation (overnight, 4°C) with anti- LC3A/B (D3U4C) XP IgG (Cell Signaling, MA, USA; 1:2000 dilution in T-TBS containing 3% BSA) followed by GAR-HRP IgG (Sigma-Aldrich; 1:5000 dilution in T-TBS containing 1% non-fat milk; 1 hour, 37°C). Beclin was revealed by incubation (overnight, 4°C) with anti-Beclin-1 (D40C5) IgG (Cell Signaling; 1:2000 dilution in T-TBS containing 3% BSA) followed by GAR-HRP IgG (Sigma-Aldrich; 1:7000 dilution in T-TBS containing 1% non-fat milk; 1 hour, 37°C) and ChemiDoc detection. P62 was revealed by incubation (overnight, 4°C) with anti- Phospho-SQSTM1/P62 (Thr269/Ser272) IgG (Cell Signaling; 1:1500 dilution in T-TBS containing 3% non-fat milk) followed by GAR-HRP IgG (Sigma-Aldrich; 1:25 000 dilution in T-TBS containing 3% non-fat milk; 1 hour, 37°C) and ChemiDoc detection. Synaptophysin was revealed by incubation (overnight, 4°C) with anti-Synaptophysin IgG (Merk Millipore, Milan, Italy; 1:200 000 dilution in T-TBS containing 3% BSA) followed by GAR-HRP IgG (Sigma-Aldrich; 1:20 000 dilution in T-TBS containing 1% non-fat milk; 1 hour, 37°C). Synapsin I was revealed by incubation (overnight, 4° C) with anti-Synapsin I IgG (Genetex, distributed by Prodotti Gianni, Milan Italy; 1:500 dilution in TTBS containing 3% BSA) followed by GAR-HRP IgG (Sigma-Aldrich; 1:5000 dilution in T-TBS containing 3% non-fat milk; 1 hour, 37°C) and ChemiDoc detection. Synaptotagmin I was revealed by incubation (overnight, 4°C) with anti-Synaptotagmin I IgG (Cell Signaling; 1:1000 dilution in T-TBS containing 3% non-fat milk) followed by GAR-HRP IgG (Immunoreagents, distributed by Microtech, Naples, Italy; 1:500 000 dilution in T-TBS containing 3% non-fat milk; 1 hour, 37°C). TrkB was revealed by incubation (overnight, 4°C) with rabbit anti-TrkB (Santa Cruz Biotechnology; 1:2000 dilution in T-TBS containing 3% non-fat milk) followed by GAR-HRP IgG (Immunoreagents; 1: 140 000 dilution in T-TBS containing 3% non-fat milk; 1 hour, 37°C). Nrf2 and GSR levels, in nuclear and cytoplasmic extracts (respectively) were revealed accordingly to a published study (Monaco et al., 2018). For loading control, the membranes were stripped (Spagnuolo et al., 2014) and then incubated (overnight, 4°C) with mouse anti-β-actin IgG (Sigma-Aldrich; 1000 dilution in T-TBS containing 0.25% non-fat milk) followed by goat anti-mouse Horseradish Peroxidase-conjugated IgG (GAM-HRP; Sigma-Aldrich; 1:10 000 dilution in 0.25% non-fat milk; 1 hour, 37°C). All the above immunocomplexes were detected by the ECL detection system. The Excellent Chemiluminescent detection Kit (ElabScience, Microtech, Naples, Italy) was used for detection of TrkB and synaptotagmin; the chemiluminescent HRP substrate (Immobilon Western, Merk Millipore) was used for detection of the other antigens. Quantitative

densitometry of the bands was carried out by analyzing chemidoc images or digital images of X-ray films exposed to immunostained membranes, and the quantification of the signal was performed by Un-Scan-It gel software (Silk Scientific, UT, USA). For each marker, all procedures, from transfer to PVDF membrane to detection, were carried out in the same way. For each parameter and for each pair of blotting the same method (X-ray or chemidoc), antibody dilutions and time of exposure were used in order to compare differences in signal intensity. A representative blotting was shown for each parameter.

Statistical analysis

Data were expressed as mean values±SEM. The program GraphPad Prism 6 (GraphPad Software, San Diego, CA) was used to perform two-way ANOVA, followed by the Tukey post-hoc test. $P<0.05$ was considered significant.

Results

Animal data

As reported in Figure 1, during the two weeks of dietary treatment, no significant variation was evident in body weight and food intake between control and fructose-fed rats. Further, the whole time course of changes in body weight and food intake during the experimental period shows the wellbeing state of the animals and the efficacy of the pair feeding protocol.

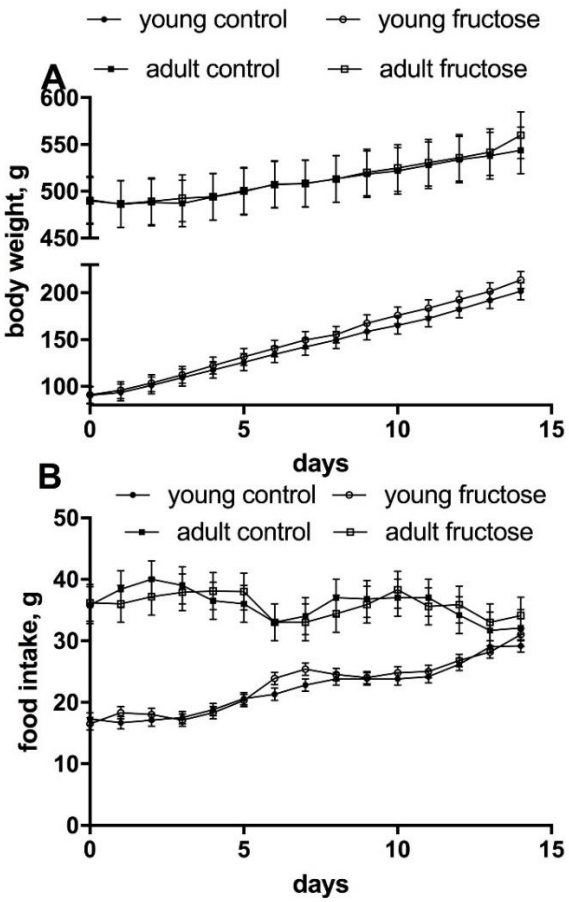

Figure 1. Animal data. *Young (30 days old) and adult (90 days old) rats were fed a fructose-rich or a control diet for 2 weeks. During the treatment, body weight (panel A) and food intake (panel B) were monitored daily. Data are reported as means±SEM of six rats/group.*

Analysis of Nrf2 pathway in the cortex of fructose-fed rats

We previously showed that 2 weeks of fructose feeding induces an increase in lipid and protein markers of oxidative stress in rat brain (Cigliano et al., 2018). As Nrf2 plays a critical role in brain redox homeostasis, (Johnson and Johnson, 2015) we investigated whether short-term fructose feeding affects Nrf2 pathway in the rat frontal cortex. To this aim, the amount of GSH, the major intracellular antioxidant, and GSSG, the activities of the phase-2 enzymes GSR and G6PD, modulated by the Nrf2 pathway and responsible for the maintenance of GSH homeostasis, as well as the amount of Nrf2 were quantified. GSSG content was affected by diet but not age (source of variation from two-way ANOVA: age, not significant; treatment, $P<0.01$; interaction, not significant). Conversely neither diet-nor age-related changes of GSH amount were observed. The diet associated GSSG increase resulted into a marked decrease of the GSH/GSSG ratio (age, not significant; treatment, $P<0.01$; interaction, not significant Figure 2A), and the extent of this diet-dependent decrease was similar (about 1.5 fold) in the two groups of age. Diet-dependent changes in the activities of G6PD and GSR were observed

(Figure 2B and C, respectively), while no age effect was revealed (for both parameters: age, not significant; treatment, P<0.01; interaction, not significant). In particular, the diet-dependent decrease of G6PD activity (about 1.4 fold) and GSR activity (about 1.2 fold) did not differ between young and adult fructose-fed animals.

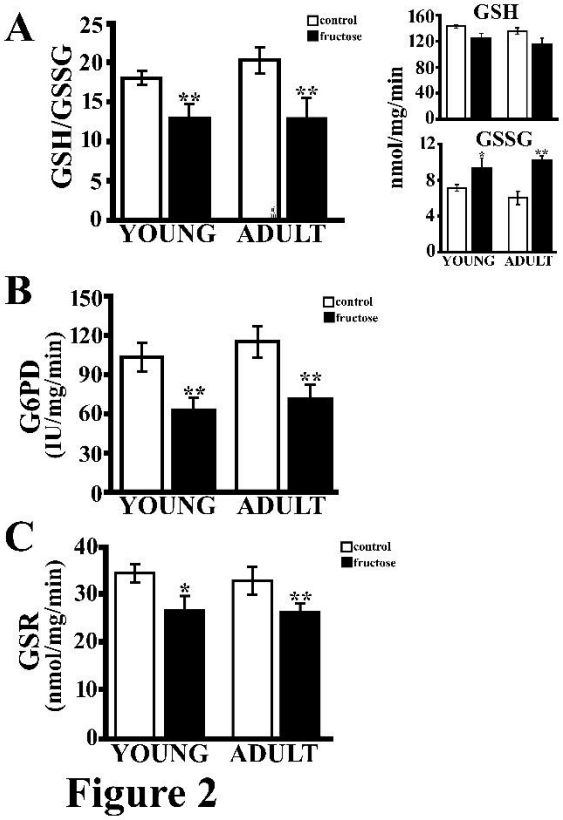

Figure 2

Figure 2. Analysis of Nrf2-activated defences in rat cerebral cortex. *Panel A. The ratio between reduced (GSH) and oxidized (GSSG) glutathione (panel A), G6PD (panel B) and GSR (panel C) activities were quantified in protein extracts from cortex of young and adult rats fed a control or fructoserich diet for 2 weeks. Data are reported as means±SEM of six rats/group. Diet effect: *P<0.05, **P<0.01 compared to control rats. Source of variation from two-way ANOVA followed by Tukey post-test: age, not significant; treatment, P<0.01; interaction, not significant.*

In addition, a diet-dependent decrease of GSR (Figure 3A) and Nrf2 protein content (Figure 3B) in brain cytoplasmic and nuclear extracts, respectively, was observed (age, not significant; treatment, P<0.01; interaction, not significant). Taken together, these results strongly suggest that two weeks fructose feeding negatively influences Nrf2 pathway, impairing the brain antioxidant defence system.

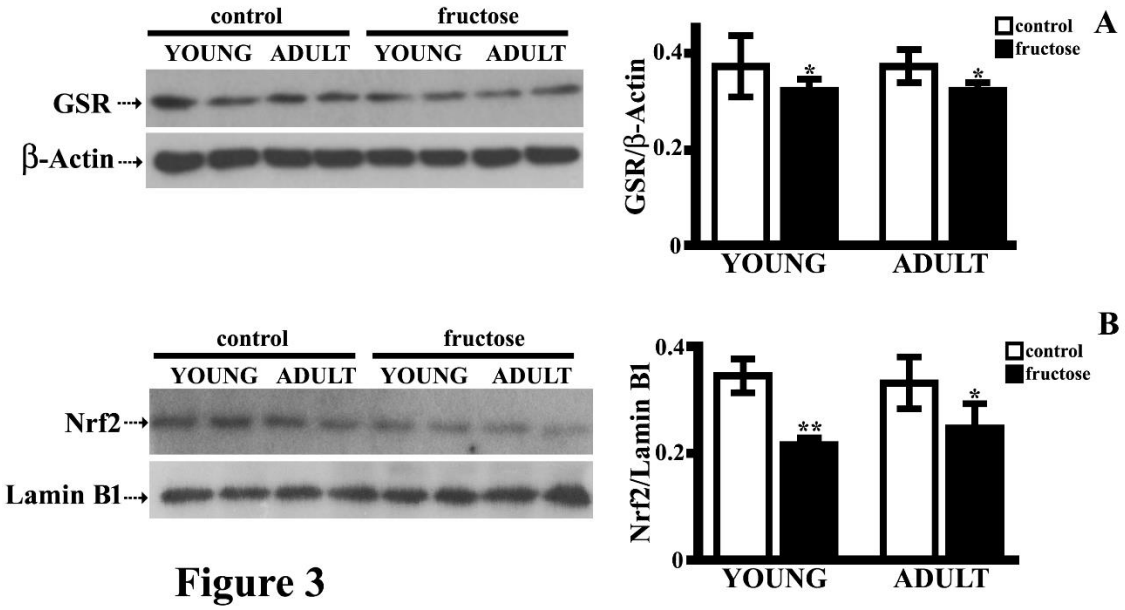

Figure 3

Figure 3. GSR and Nrf2 levels in rat cerebral cortex. *Representative immunoblot of GSR (panel A) and Nrf2 (panel B) expression in cytoplasmic and nuclear protein extracts, respectively, from cortex of young and adult rats fed a control or fructose-rich diet for 2 weeks. Quantitative densitometry was carried out, band intensities were calculated, and GSR or Nrf2 concentrations were expressed relative to β-actin level or Lamin B1, respectively. Data are reported as means±SEM of six rats/group. Diet effect: *P<0.05, **P<0.01, compared to control rats. Source of variation from two-way ANOVA followed by Tukey post-test: age, not significant; treatment, P<0.01; interaction, not significant.*

Analysis of PPARs in cortex

The expression of PPAR-alpha and PPAR-gamma, which are transcription factors exerting neuroprotective and anti-inflammatory effects in central nervous system (Deplanque, 2004: Rinwa et al., 2010) was also investigated. As shown in Figure 4, significant diet-related changes of PPAR-alpha and PPAR-gamma were found. PPAR-alpha amount was affected by diet but not by age (age, not significant; treatment, P<0.01; interaction, not significant; Figure 4A), in fact it was lower in fructose fed than in control rats, both in young (about 1.6 fold) and adult animals (1.9 fold), with no significant difference in the extent of the diet-dependent decrease between the two groups of age (Figure S1A). Conversely, PPAR-gamma amount was affected by both diet and age (age, P<0.001; treatment, P<0.01; interaction, not significant; Figure 4B). In particular, a similar diet-dependent decrease of PPARgamma level (about 1.9 fold) was observed in both group of treated rats (Figure S1B), and an age-related increase was found in both control and fructose-fed adult rats (Figure 4B).

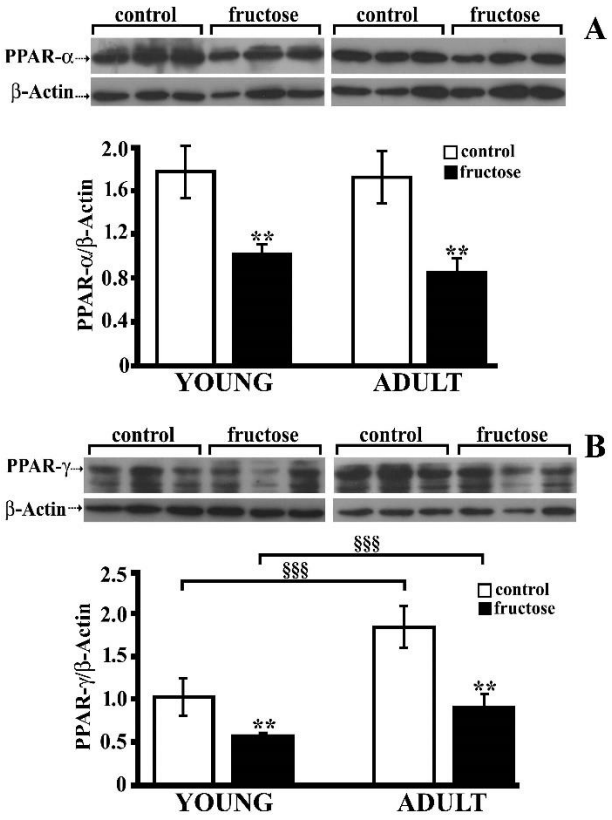

Figure 4

Figure 4. PPAR-alpha and gamma levels in rat cerebral cortex. *PPAR-alpha (panel A) and PPAR-gamma (panel B) levels were assessed by western blot on protein extracts from cortex of young (left) or adult rats (right) fed a control or fructose-rich diet for 2 weeks. Representative western blots are shown (top). Quantitative densitometry was carried out, band intensities were calculated, and PPARs concentrations were expressed relative to β-actin level (bottom). Data are reported as means±SEM of six rats/group. Diet effect: **P<0.01 compared to control rats. Age effect: §§§P<0.001 compared to young rats. Panel A: source of variation from two-way ANOVA followed by Tukey post-test: age, not significant; treatment, P<0.01; interaction, not significant). Panel B. Source of variation from two-way ANOVA followed by Tukey post-test: age, P<0.001; treatment, P<0.01; interaction, not significant.*

Fructose diet induces activation of autophagy pathway

As excessive autophagy prompts rapid cell death, (Levine and Yuan, 2005) we investigated whether fructose feeding is associated with the activation of autophagy, and we observed significant changes of specific markers of this pathway. As shown in Figure 5A, significant age- and diet-related increases of beclin amount were observed (age, P<0.01; treatment, P<0.01; interaction, not significant). In particular, a similar age-related increase (about 1.3 fold) was observed in control and treated animals. Further, the diet-dependent increase of beclin level was similar (about 1.4 fold) in both young and adult animals (Figure S2A). Conversely, the amount of LC3 II was affected by diet but not by age (age, not significant; treatment, P<0.01; interaction, not significant; Figure 5B), and its increase was similar in both young (2.42±0.40) and adult (2.02 ±0.20) fructose-fed rats (Figure S2B).

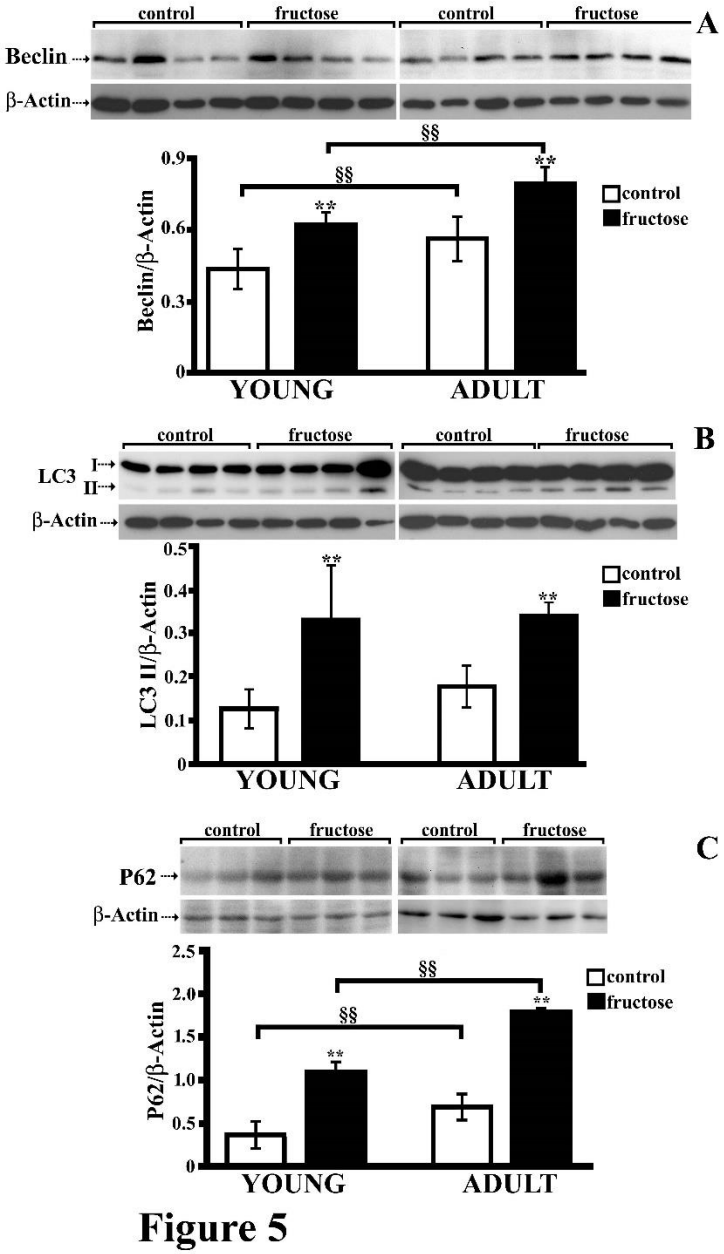

Figure 5

Figure 5. Autophagic markers level in rat cerebral cortex. *Beclin (panel A), LC3 II (panel B), and P62 (panel C) levels were assessed by western blot on protein extracts from cortex of young (left) or adult rats (right) fed a control or fructose-rich diet for 2 weeks. Representative western blots are shown (top). Quantitative densitometry was carried out, band intensities were calculated, and concentrations were expressed relative to β-actin level (bottom). Data are reported as means±SEM of six rats/group. Diet effect: **P<0.01 compared to control rats. Age effect: §§ P<0.01 compared to young rats. Panel A. Source of variation from two-way ANOVA followed by Tukey post-test: age, P<0.01; treatment, P<0.01; interaction, not significant. Panel B. Source of variation from two-way ANOVA followed by Tukey post-test: age, not significant; treatment, P<0.01; interaction, not significant. Panel C. Source of variation from two-way ANOVA followed by Tukey post-test: age, P<0.01; treatment, P<0.01; interaction, not significant.*

Finally, a significant diet- and age-dependent increase of P62 level was observed (age, P<0.01; treatment, P<0.01; interaction, not significant; Figure 5C). In particular, the diet-dependent increase of P62 level did not differ between young and adult animals (Figure S2C). The increase

of these markers suggests that fructose diet induces the activation of autophagy, likely as a protective mechanism for maintaining cell metabolism and homeostasis.

Effect of fructose diet on the expression of BDNF and synaptic proteins

The level of BDNF, a reliable marker of brain function, that plays a critical role in learning and memory by maintaining synaptic plasticity, (Leal et al., 2015) was titrated in frontal cortex homogenates, and an interaction between age and diet effect was observed (age, P<0.001; treatment, P<0.01; interaction, P<0.01; Figure 6A).

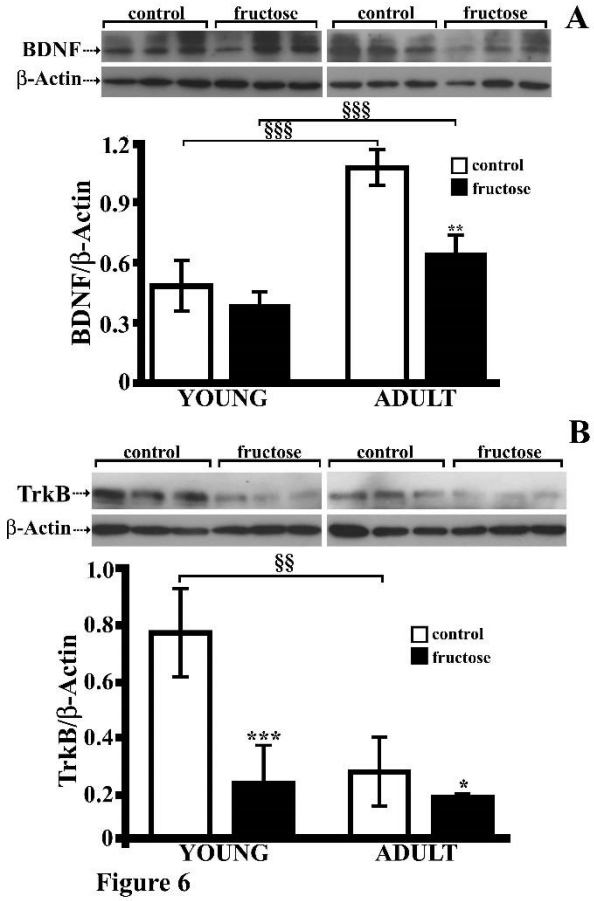

Figure 6

Figure 6. BDNF and TrkB amount in rat cerebral cortex. *BDNF (panel A) and TrkB (panel B) levels were assessed by western blot on protein extracts from cortex of young (left) or adult rats (right) fed a control or fructose-rich diet for 2 weeks. Representative western blots are shown (top). Quantitative densitometry was carried out, band intensities were calculated, and concentrations were expressed relative to β-actin level (bottom). Data are reported as means±SEM of six rats/group. Diet effect: *P<0.05, **P<0.01, ***P<0.001 compared to control rats. Age effect: §§ P<0.01, §§§ P<0.001 compared to young rats. Panel A. Source of variation from two-way ANOVA followed by Tukey post-test: age, P<0.001; treatment, P<0.01; interaction, P<0.01. Panel B Source of variation from two-way ANOVA followed by Tukey post-test: age, P<0.01; treatment, P<0.001; interaction, P<0.05.*

In particular, the age-related increase of BDNF level was observed both in control (about 2 fold) and treated rats (about 1.4 fold) (Figure 6A), while a diet-related decrease of BDNF

amount (about 1.6 fold) was observed only in the adult group of fructose-fed rats (Figure S3 A). Since BDNF effect on neuron development, survival, and differentiation occurs by the binding to TrkB, we also investigated whether the receptor level is modulated by the fructose-rich diet. Interestingly, also for TrkB an interaction between age and diet effect was observed (age, $P<0.01$; treatment, $P<0.001$; interaction, $P<0.05$; Figure 6B), as a significant age-dependent decrease of receptor level was observed only in control rats (about 2.5 fold; $P<0.01$), in agreement with previously published data (Croll et al., 1998; Silhol et al., 2007). Notably, the extent of diet-dependent decrease of TrkB amount was significantly higher ($P<0.05$; Figure S3B) in young (about 2.7 fold) than in adult rats (about 1.6 fold). In order to clarify the impact of the fructose diet on synaptic function as well, the levels of synaptophysin, synapsin I and synaptotagmin I were evaluated. As shown in Figure 7A, an interaction between age and diet effect on synaptophysin amount was found (age, $P<0.01$; treatment, $P<0.001$; interaction, $P<0.05$).

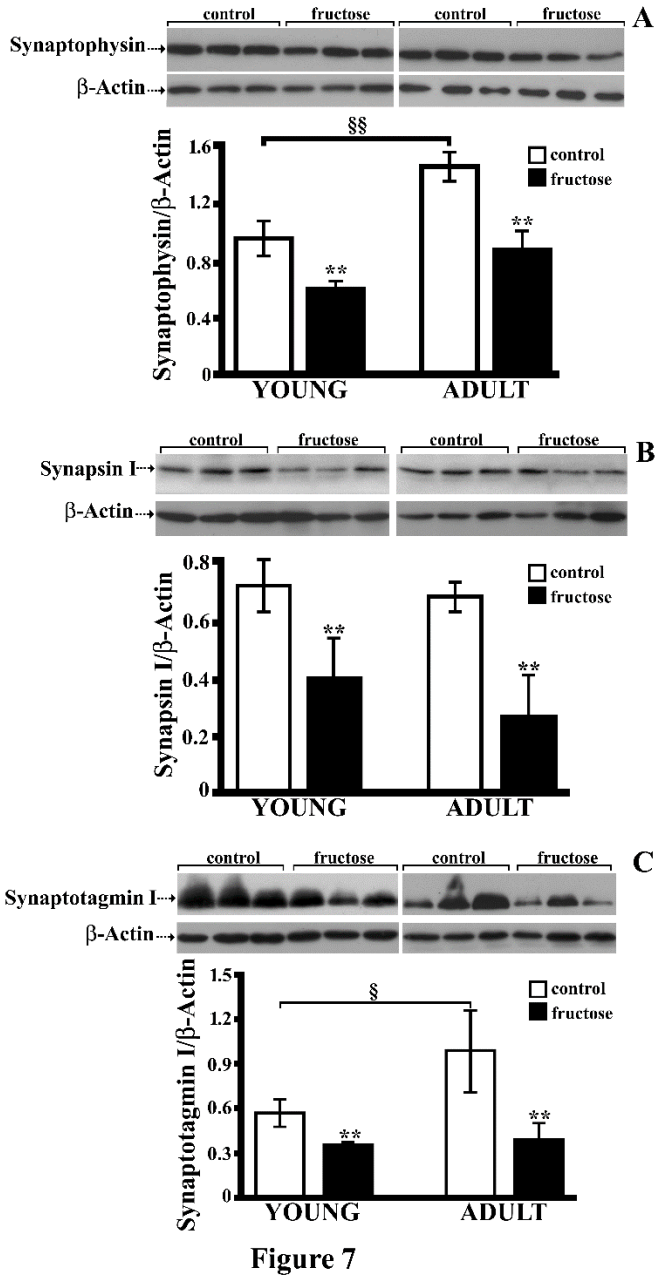

Figure 7

Figure 7. Synaptic plasticity markers levels in rat cerebral cortex. *Synaptophysin (panel A), synapsin I (panel B), and synaptotagmin I (panel C) levels were assessed by western blot on protein extracts from cortex of young (left) or adult rats (right) fed a control or fructose-rich diet for 2 weeks. Representative western blots are shown (top). Quantitative densitometry was carried out, band intensities were calculated, and concentrations were expressed relative to β-actin level (bottom). Data are reported as means±SEM of six rats/group. Diet effect: **P<0.01 compared to control rats. Age effect: § P<0.05, §§ P<0.01 compared to young rats. Panel A. Source of variation from two-way ANOVA followed by Tukey post-test: age, P<0.01; treatment, P<0.01; interaction, P<0.05. Panel B. Source of variation from two-way ANOVA followed by Tukey post-test: age, not significant; treatment, P<0.001; interaction, not significant. Panel C. Source of variation from two-way ANOVA followed by Tukey post-test: age, P<0.05; treatment, P<0.001; interaction, P<0.05*

Indeed, an age-dependent increase of the protein level (about 1.6 fold; P<0.01) was observed only in control animals. Further synaptophysin amount was lower in fructose-fed rats compared

to control animals, both in young (about 1.5 fold) and adult (about 1.7 fold) group, and the extent of this dietdependent decrease did not differ between young and adult animals (Figure S4A). In addition, a diet associated decrease of synapsin I level (Figure 7B) was observed in young (about 1.7 fold) and adult (about 2 fold) animals (age, not significant; treatment, $P<0.001$; interaction, not significant), and this change was not different between the two groups of age (Figure S4B). An interaction between age and diet effect on synaptotagmin I amount was detected (age, $P<0.05$; treatment, $P<0.001$; interaction, $P<0.05$; Figure 7C), as a significant age-related increase of synaptotagmin I (about 1.7 fold) was observed only in control rats. Protein level was significantly lower in fructose-fed rats compared to control animals, both in young (about 1.5 fold) and adult (about 2.5 fold) group. The considerable decrease ($P<0.05$) of synaptotagmin level in adult more than in young treated rats (Figure S4C) suggests an age-dependent difference in the ability to counteract the deleterious effect of fructose on the level of this specific synaptic protein.

Effect of fructose diet on AChE activity

The effect of the short-term fructose diet on the activity of AChE, one of the most ubiquitous enzymes present in central cholinergic pathways, was then evaluated in frontal cortex samples. As shown in Figure 8, an interaction between age and diet effect was observed, as fructose feeding resulted in a significant increase of AChE activity only in frontal cortex of young animals (about 1.7 fold; $P<0.05$). Further, an age-dependent decrease of enzyme activity was observed only in fructose-fed animals (age, $P<0.05$; treatment, not significant; interaction, $P<0.01$).

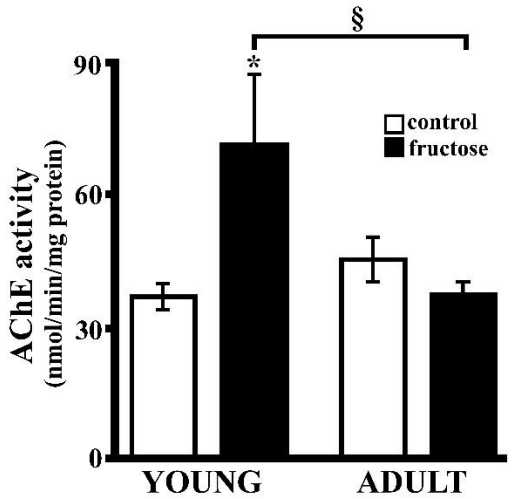

Figure 8

Figure 8. AChE activity in rat cerebral cortex. *AChE activity was measured in protein extracts from cortex of young or adult rats fed a control or fructose-rich diet for 2 weeks, using acetylthiocholine*

*iodide as a substrate. The rate of production of thiocholine was determined by the reaction of the thiol with 5,5-dithiobis-2-nitrobenzoate to produce the yellow anion of 5-thio-2-nitro-benzoic acid. Enzyme activity is expressed as nmol/min/mg protein. Data are reported as means±SEM of six rats/group. Diet effect: *P<0.05 compared to control rats. Age effect: § P<0.05 compared to young rats; source of variation from two-way ANOVA followed by Tukey post-test: age P<0.05; treatment, not significant; interaction, P<0.01.*

Discussion

A clear impact of fructose on metabolism has been shown in the last years, but further insight into the molecular roots of the specific effects of this sugar on brain is required. To date no information about the early effects of a short-term fructose intake on Nrf2 and autophagy pathways, as well as on critical synaptic markers is available, hence we focus on these issues, by comparing the effect of a two weeks fructose-rich diet in young and adults rats. Nrf2 plays a critical role in brain redox homeostasis, as modulating the expression of the phase-2 enzymes GSR and G6PD that are implicated in the production/ recycling of GSH, the main intracellular antioxidant (Johnson and Johnson, 2015). We report here, for the first time, that two weeks of fructose-rich diet led, in both groups of age, to the decline of Nrf2-dependent antioxidant enzymes involved in GSH homeostasis. In fact, the cortex of fructose-fed rats exhibited significantly lower amount of Nrf2, lower activity of GSR and G6PD enzymes, as well as a decrease in the GSH/GSSG ratio compared with control rats. The overall imbalance of redox homeostasis is corroborated by the lower levels of PPAR-alpha and PPAR-gamma, in both young and adult rats after short-term fructose-rich diet. Notably, PPAR-alpha and PPARgamma other than possessing neuroprotective, anti-inflammatory and anti-oxidant properties (Deplanque, 2004; Rinwa et al., 2010) are also known to modulate synaptic plasticity, (Moreno et al., 2004) and enhance cognitive performance (Hajjar et al., 2012). Hence, we could speculate that the impairment of Nrf2 pathway together with the decrease of PPARs in brain of fructose-fed rats might be involved in the induction of brain oxidative stress and synaptic dysfunction in fructose-fed rats. Although fructose-enriched diets were previously reported to reduce the expression of PPAR alpha and gamma in liver, (Nagai et al., 2002; Roglans et al., 2007) this is the first time that a similar effect is reported in brain. Fructose-dependent suppression of PPAR-alpha activity was reported to induce endoplasmic reticulum stress, (Su et al., 2014) which is a main cause of autophagy activation, (Spijker, 2011; Qin et al., 2010) a crucial mechanism for maintaining cell homeostasis (Mizushima and Komatsu, 2011, Qin et al., 2010). Indeed autophagy is actually activated as a protective mechanism in response to different stress, such as oxidative or endoplasmic reticulum stress (Qin et al., 2010, Keller et al., 2004). Notably, we

here show that a short-term fructose-rich diet is associated with the activation of autophagy in brain of young and adult rats, as increased levels of beclin 1, LC3 II and P62 were detected in frontal cortex of young and adult rats. This result is in agreement with previous reports on the autophagic activation induced by fructose feeding in mice cardiac tissue (Mellor et al., 2011) and skeletal muscle, (De Stefanis et al., 2017) as well as in rat pancreatic β cells (Maiztegui et al., 2017). In this context, it should be pointed out that excessive autophagy damages proteins and organelles, and may prompt rapid cell death. (Levine and Yuan, 2005) In particular, disordered autophagy could disrupt the flow of pre-synaptic terminals and cause axonal dystrophy, (Sanchez-Varo et al., 2012) also altering synaptic plasticity (Chen et al., 2013; Zhang et al., 2017). In line with these reports, we found lower amounts of the synaptic markers synaptophysin, synapsin I and synaptotagmin in the frontal cortex of fructose-fed rats, showing higher amounts of autophagic markers compared to the control ones. Both synaptophysin and synapsin I are involved in synaptic growth, as they play key roles in synapse formation, maturation and maintenance. (58, 59) Further, synaptophysin, synapsin I and synaptotagmin I participate in the regulation of synaptic vesicle exocytosis (Cesca et al., 2010; Bacaj et al., 2013). Synaptotagmin, in particular, was proposed as a marker of synaptic activity, (Mundigl et al., 1995) as acting as calcium sensor for fast synchronous evoked neurotransmitter release. (Bacaj et al., 2013) The effect of fructose feeding was here assessed on a further critical marker of brain function that is BDNF. This neurotrophin plays a key role in the modulation of adult neurogenesis, (Scharfman et al, 2005) synaptic plasticity, (Leal et al., 2015) and stabilization of postsynaptic density (Yoshii et al., 2007). A diet-dependent regulation of BDNF level was previously reported (Molteni et al., 2002; Wu et al., 2004). In particular, a seven days high-fat/high fructose diet was associated with both BDNF and synaptic reduction in rat hippocampus. (Calvo-Ochoa et al., 2014) Our investigation revealed a significant reduction of BDNF levels in adult, but not in young animals, in line with recent data showing that a long-term (12 weeks) high fructose diet decreased BDNF expression in adult rats (Liu et al., 2018). Interestingly significant lower amount of the neurotrophin receptor TrkB was found in both young and adult fructose-fed rats. Although the level of BDNF was not affected by fructose diet in young rats, the finding of a significant decrease of TrkB suggests that an impairment of neurotrophin signalling might occur also in this group. Although further research is required, our data led us to hypothesize that the decrease of synaptic proteins together with the effect on BDNF/TrkB, in the two groups of fructose-fed rats, might reflect an alteration of brain plasticity, in line with data demonstrating that BDNF decrease is responsible for impaired synaptic plasticity and cognitive performance (Lindqvist et al., 2006; Stranahan et al., 2008).

Interestingly, the short-term fructose-rich diet showed an age-dependent effect on the activity of AChE, which plays a critical role in central cholinergic synapses (Pope and Brimijoin, 2018). In particular, the cholinergic innervation of the cerebral cortex is intimately involved in the cognitive processes related to memory and attention, and the inhibition of AChE was reported to improve cognitive performance (Pope and Brimijoin, 2018). Interestingly, the activity of this enzyme was previously found increased following a hypercholesterolemia-induced cognitive impairment in mice, (Moreira et al., 2014) and also used to evaluate the antioxidant effects of several food nutrients in aluminum-induced neurotoxicity (Jangra et al., 2015; Hosny et al., 2018). The increase of AChE activity was associated with impaired learning and memory functions in stressed rats, (Nawaz et al., 2018) but at the best of our knowledge, the effects of dietary fructose on AChE activity has been never investigated. The finding of a significantly higher AChE activity only in young treated rats, suggests a more detrimental effect of fructose feeding in the frontal cortex of young animals. A putative mechanism for the fructose effects on AChE remains to be fully elucidated; however, we can speculate on the possibility that alterations in lipid and protein induced by oxidative stress modulate the enzymatic activity of AChE through a yet unidentified mechanism. It should be mentioned that synaptotagmin I was suggested to play a critical role in modulating acetylcholine release at the neuromuscular junction, (Searl and Silinsky, 2006) but whether the observed decrease of synaptotagmin level in fructose-fed rats can be involved in the AChE mediated modulation of brain cholinergic system in the central nervous system as well remains to be clarified. One limitation of this study is the lack of behavioural analyses on the effects of our experimental diet, so we cannot assess causal links between brain alterations and cognitive impairments in fructose-fed rats. Also, future in vitro cause–effect experiments on brain cells might further clarify the mechanism by which fructose impairs brain functioning. Our results indicate that the perturbation of redox homeostasis and autophagy are implicated in the deleterious consequences of a fructose-rich diet, and probably they both contribute to the observed decrease of synaptic markers in fructose-fed rats. An interesting issue that remains to be investigated is whether changes in redox status and autophagy are maintained after cessation of the fructose-rich diet. Notably, our findings in frontal cortex give further support to the data found in hippocampus from other research groups that even a short-term fructose diet can induce brain alterations. Overall, this investigation is among the first studies to suggest that even young animals may severely suffer from the deleterious effects of fructose on brain health as the adults, and provide additional experimental data suggesting the need of targeted nutritional strategies to reduce the amount of this sugar in foods.

Supplementary data

Figure S1.

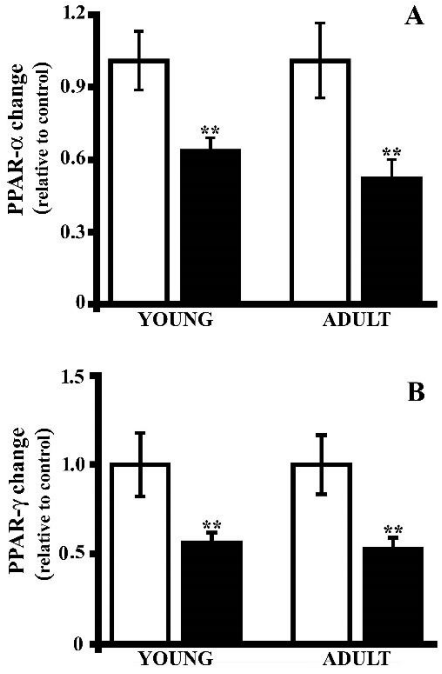

Figure S1

PPAR-alpha and gamma levels in rat cerebral cortex. *PPAR-alpha (panel A) and PPAR-gamma (panel B) levels were assessed by western blot on protein extracts from cortex of young or adult rats fed a control or fructose-rich diet for 2 weeks. Quantitative densitometry was carried out, band intensities were calculated, and PPARs concentrations were expressed relative to β-actin level. Data are reported as means ± SEM of six rats/group. Diet dependent protein decrease calculated relative to control animals: **p < 0.01*

Figure S2.

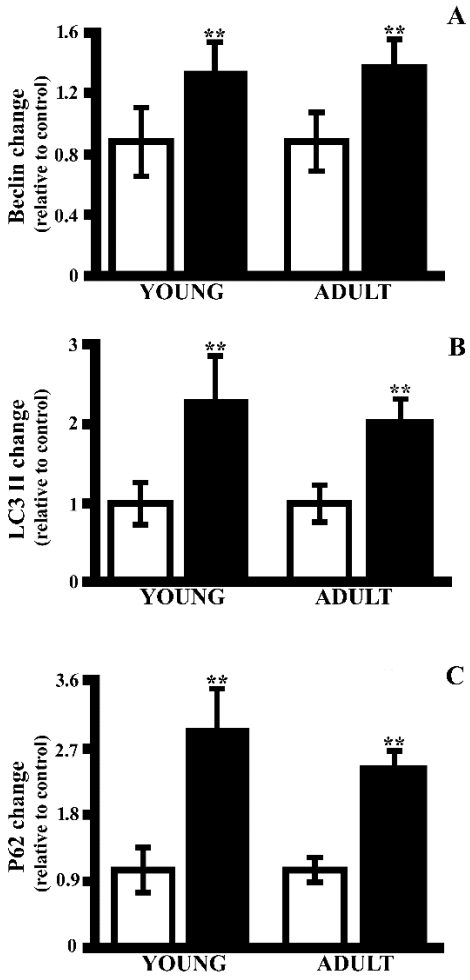

Figure S2

*Autophagic markers level in rat cerebral cortex. Beclin (panel A), LC3 II (panel B), and P62 (panel C) levels were assessed by western blot on protein extracts from cortex of young or adult rats fed a control or fructose-rich diet for 2 weeks. Quantitative densitometry was carried out, band intensities were calculated, and concentrations were expressed relative to β-actin level. Data are reported as means ± SEM of six rats/group. Diet dependent protein increase calculated relative to control animals: **p < 0.01.*

Figure S3.

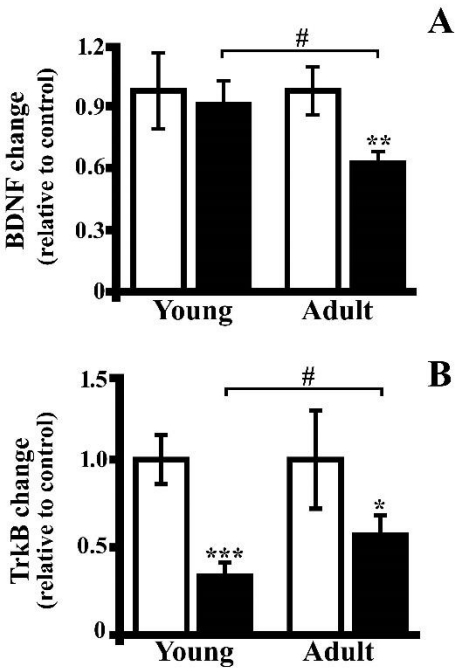

Figure S3

BDNF and TrkB amount in rat cerebral cortex. *BDNF (panel A) and TrkB (panel B) levels were assessed by western blot on protein extracts from cortex of young or adult rats fed a control or fructose-rich diet for 2 weeks. Quantitative densitometry was carried out, band intensities were calculated, and concentrations were expressed relative to β-actin level. Data are reported as means ± SEM of six rats/group. Diet dependent protein decrease calculated relative to control animals: *p < 0.05, **p < 0.01, ***p < 0.001. # p < 0.05 compared to young treated rats.*

Figure S4.

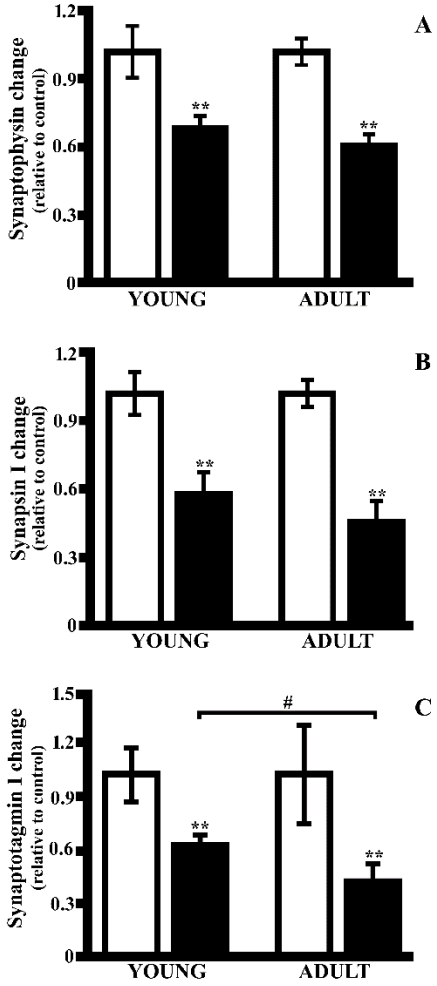

Figure S4

Synaptic plasticity markers levels in rat cerebral cortex. *Synaptophysin (panel A), synapsin I (panel B), and synaptotagmin I (panel C) levels were assessed by western blot on protein extracts from cortex of young or adult rats fed a control or fructose-rich diet for 2 weeks. Quantitative densitometry was carried out, band intensities were calculated, and concentrations were expressed relative to β-actin level. Data are reported as means ± SEM of six rats/group. Diet dependent protein decrease calculated relative to control animals: **p < 0.01 # p < 0.05 compared to young treated rats.*

References

Aragno M, Mastrocola R. (2017). Dietary Sugars and Endogenous Formation of Advanced Glycation Endproducts: Emerging Mechanisms of Disease. Nutrients. 9(4). pii: E385. doi: 10.3390/nu9040385.

Bacaj T, Wu D, Yang X, Morishita W, Zhou P, Xu W, Malenka RC, Südhof TC. (2013). Synaptotagmin-1 and synaptotagmin-7 trigger synchronous and asynchronous phases of neurotransmitter release. Neuron;80:947–59. doi: 10.1016/j.neuron.2013.10.026.

Calvo-Ochoa E, Hernandez-Ortega K, Ferrera P, Morimoto S, Arias C. (2014). Short-term high-fat-and-fructose feeding produces insulin signaling alterations accompanied by neurite and synaptic reduction and astroglial activation in the rat hippocampus. J Cereb Blood Flow Metab.34:1001-8. doi: 10.1038/jcbfm.2014.48.

Carlson JA, Crespo NC, Sallis JF, Patterson RE, Elder JP. (2012). Dietary related and physical activity-related predictors of obesity in children: a 2-year prospective study. Child Obes;8(2):110–5. doi: 10.1089/chi.2011.0071.

Cesca F, Baldelli P, Valtorta F, Benfenati F. (2010). The synapsins: key actors of synapse function and plasticity. Prog Neurobiol;91:313–48. doi:10.1016/j.pneurobio.2010.04.006.

Chen L, Miao Y, Chen L, Jin P, Zha Y, Chai Y, et al. (2013). The role of elevated autophagy on the synaptic plasticity impairment caused by CdSe/ZnS quantum dots. Biomaterials;34:10172–81. doi: 10.1016/j.biomaterials.2013.09.048.

Chiu K, Lau WM, Lau HT, So KF, Chang RC. (2007). Micro-dissection of rat brain for RNA or protein extraction from specific brain region. J Vis Exp.;7:269. doi: 10.3791/269.

Cigliano L, Spagnuolo MS, Crescenzo R, Cancelliere R, Iannotta L, Mazzoli A, Liverini G, Iossa S. (2018). Short-Term fructose feeding induces inflammation and oxidative stress in the hippocampus of young and adult rats. Mol Neurobiol.;55:2869–83. doi: 10.1007/s12035-017-0518-2.

Crescenzo R, Bianco F, Coppola P, Mazzoli A, Cigliano L, Liverini G, Iossa S. (2013). Increased skeletal muscle mitochondrial efficiency in rats with fructose-induced alteration in glucose tolerance. Br J Nutr.;110(11):1996–2003. doi: 10.1017/S0007114513001566.

Croll SD, Ip NY, Lindsay RM, Wiegand SJ. (1998). Expression of BDNF and trkB as a function of age and cognitive performance. Brain Res.;812(1–2):200–8.

De Stefanis D, Mastrocola R, Nigro D, Costelli P, Aragno M. (2017). Effects of chronic sugar consumption on lipid accumulation and autophagy in the skeletal muscle. Eur J Nutr;56:363–73. doi: 10.1007/s00394-015-1086-8

Deplanque D. (2004). Cell protection through PPAR nuclear receptor activation. Therapie;59:25–29.

Ellman GL, Courtney KD, Andres V Jr, Feather-Stone RM. (1961). A new and rapid colorimetric determination of acetylcholinesterase activity. Biochem Pharmacol.;7:88–95.

Ford CN, Slining MM, Popkin BM. (2013). Trends in dietary intake among US 2- to 6-year-old children, 1989-2008. J Acad Nutr Diet.;113:35–42. doi: 10.1016/j.jand.2012.08.022.

Giedd JN, Blumenthal J, Jeffries NO, Castellanos FX, Liu H, Zijdenbos A, Paus T, Evans AC, Rapoport JL. (1999). Brain development during childhood and adolescence: a longitudinal MRI study. Nat Neurosci.;2:861–3. doi: 10.1038/13158.

Gogtay N, Giedd JN, Lusk L, Hayashi KM, Greenstein D, Vaituzis AC, Nugent TF 3rd, Herman DH, Clasen LS, Toga AW, Rapoport JL, Thompson PM. (2004). Dynamic mapping of human cortical development during childhood through early adulthood. Proc Natl Acad Sci USA.;101: 8174–79. doi: 10.1073/pnas.0402680101.

Hajjar T, Meng GY, Rajion MA, Vidyadaran S, Othman F, Farjam AS, Li TA, Ebrahimi M. (2012). Omega 3 polyunsaturated fatty acid improves spatial learning and hippocampal peroxisome proliferator activated receptors (PPARα and PPARγ) gene expression in rats. BMC Neurosci.;13:109. doi: 10.1186/1471-2202-13-109.

Hosny EN, Sawie HG, Elhadidy ME, Khadrawy YA. (2018). Evaluation of antioxidant and anti-inflammatory efficacy of caffeine in rat model of neurotoxicity. Nutr Neurosci.;7:1–8. doi:10.1080/1028415X.2018.1446812. doi: 10.1080/1028415X.2018.1446812.

Hsu TM, Konanur VR, Taing L, Usui R, Kayser BD, Goran MI, Kanoski SE. (2015). Effects of sucrose and high fructose corn syrup consumption on spatial memory function and hippocampal neuroinflammation in adolescent rats. Hippocampus;25:227–39. doi: 10.1002/hipo.22368.

Janeczek M, Gefen T, Samimi M, Kim G, Weintraub S, Bigio E, Rogalski E, Mesulam MM, Geula C1. (2018). Variations in acetylcholinesterase activity within human cortical pyramidal neurons across Age and cognitive trajectories. Cereb Cortex.;28(4):1329–37.

Jangra A, Kasbe P, Pandey SN, Dwivedi S, Gurjar SS, Kwatra M, Mishra M, Venu AK, Sulakhiya K, Gogoi R, Sarma N, Bezbaruah BK, Lahkar M. (2015). Hesperidin and silibinin ameliorate aluminuminduced neurotoxicity: modulation of antioxidants and inflammatory cytokines level in mice hippocampus. Biol Trace Elem Res;168:462–71. doi: 10.1093/cercor/bhx047.

Janz R, Südhof TC, Hammer RE, Unni V, Siegelbaum SA, Bolshakov VY. (1999). Essential roles in synaptic plasticity for synaptogyrin I and synaptophysin I. Neuron;24:687–700.

Jiménez-Maldonado A, Ying Z, Byun HR, Gomez-Pinilla F. (2018). Short-term fructose ingestion affects the brain independently from establishment of metabolic syndrome. Biochim Biophys Acta.;1864(1):24–33. doi: 10.1016/j.bbadis.2017.10.012.

Johnson DA, Johnson JA. (2015). Nrf2 – a therapeutic target for the treatment of neurodegenerative diseases. Free Radic Biol Med.;88(Pt B):253–67. doi: 10.1016/j.freeradbiomed.2015.07.147

Keller JN, Dimayuga E, Chen Q, Thorpe J, Gee J, Ding Q. (2004). Autophagy, proteasomes, lipofuscin, and oxidative stress in the aging brain. Int J Biochem Cell Biol;36:2376–91.

Leal G, Afonso PM, Salazara IL, Duarte CB. (2015). Regulation of hippocampal synaptic plasticity by BDNF. Brain Res.;1621: 82–101. doi: 10.1016/j.biocel.2004.05.003.

Levine B, Yuan J. (2005). Autophagy in cell death: an innocent convict? J Clin Invest.;115:2679–88. doi: 10.1172/JCI26390

Li JM, Ge CX, Xu MX, Wang W, Yu R, Fan CY, Kong LD. (2015). Betaine recovers hypothalamic neural injury by inhibiting astrogliosis and inflammation in fructose-fed rats. Mol Nutr Food Res.;59:189–202. doi: 10.1002/mnfr.201400307.

Lindqvist A1, Mohapel P, Bouter B, Frielingsdorf H, Pizzo D, Brundin P, Erlanson-Albertsson C. (2006). High-fat diet impairs hippocampal neurogenesis in male rats. Eur J Neurol;13:1385–88. doi: 10.1111/j.1468-1331.2006.01500.x.

Liu WC, Wu CW, Tain YL, Fu MH, Hung CY, Chen IC, Chen LW, Wu KLH. (2018). Oral pioglitazone ameliorates fructose-induced peripheral insulin resistance and hippocampal gliosis but not restores inhibited hippocampal adult neurogenesis. Biochim Biophys Acta;1864(1):274–85. doi: 10.1016/j.bbadis.2017.10.017.

Maiztegui B, Boggio V, Román CL, Flores LE, Zotto HD, Ropolo A, Grasso D, Vaccaro MI, Gagliardino JJ. (2017). VMP1-related autophagy induced by a fructoserich diet in β-cells: its prevention by incretins. Clin Sci;131: 673–87. doi: 10.1042/CS20170010.

Malik VS, Popkin BM, Bray GA, Després JP, Hu FB. (2010). Sugarsweetened beverages, obesity, type 2 diabetes mellitus, and cardiovascular disease risk. Circulation;121:1356–64. doi: 10.1161/CIRCULATIONAHA.109.876185.

Manitt C, Eng C, Pokinko M, Ryan RT, Torres-Berrío A, Lopez JP, Yogendran SV, Daubaras MJ, Grant A, Schmidt ER, Tronche F, Krimpenfort P, Cooper HM, Pasterkamp RJ, Kolb B, Turecki G, Wong TP, Nestler EJ, Giros B, Flores C. (2013). Dcc orchestrates the development of the prefrontal cortex during adolescence and is altered in psychiatric patients. Transl Psychiatry.;3:e338. doi: 10.1038/tp.2013.105.

Mastrocola R, Nigro D, Cento AS, Chiazza F, Collino M, Aragno M. (2016). High-fructose intake as risk factor for neurodegeneration: Key role for carboxy methyllysine accumulation in mice hippocampal neurons. Neurobiol Dis.;89:65–75. doi: 10.1016/j.nbd.2016.02.005.

McCrory MA, Shaw AC, Lee JA. (2016). Energy and nutrient timing for weight control. Endocrinol Metab Clin N Am. 45(3):689–718. doi: 10.1016/j.ecl.2016.04.017.

Mellor KM, Bell JR, Young MJ, Ritchie RH, Delbridge LM. (2011). Myocardial autophagy activation and suppressed survival signalling is associated with insulin resistance in fructose-fed mice. J Mol Cell Cardiol.;50:1035–43. doi: 10.1016/j.yjmcc.2011.03.002.

Mizushima N, Komatsu M. (2011). Autophagy: renovation of cells and tissues. Cell;147:728–41. doi: 10.1016/j.cell.2011.10.026.

Molteni R, Barnard RJ, Ying Z, Roberts CK, Gómez-Pinilla F. (2002). A high-fat, refined sugar diet reduces hippocampal brain-derived neurotrophic factor, neuronal plasticity, and learning. Neuroscience;112:803–14.

Monaco A, Ferrandino I, Boscaino F, Cocca E, Cigliano L, Maurano F, Luongo D, Spagnuolo MS, Rossi M, Bergamo P. (2018). Conjugated linoleic acid prevents age-dependent neurodegeneration in

a mouse model of neuropsychiatric lupus via the activation of an adaptive response. J Lipid Res.;59:48–5. doi: 10.1194/jlr.M079400.

Moreira EL, de Oliveira J, Engel DF, Walz R, de Bem AF, Farina M, Prediger RD. (2014). Hypercholesterolemia induces short-term spatial memory impairments in mice: up-regulation of acetylcholinesterase activity as an early and causal event? JNeural Transm;121(4):415–26. doi: 10.1007/s00702-013-1107-9.

Moreno S, Farioli-Vecchioli S, Cerù MP. (2004). Immunolocalization of peroxisome proliferator-activated receptors and retinoid X receptors in the adult rat CNS. Neuroscience;123:131–45.

Morin JP, Rodríguez-Durán LF, Guzmán-Ramos K, Perez-Cruz C, Ferreira G, Diaz-Cintra S, Pacheco-López G. (2017). Palatable hyper-caloric foods impact on neuronal plasticity. Front Behav Neurosci.;11:19. doi: 10.3389/fnbeh.2017.00019

Mundigl O, Verderio C, Krazewski K, De Camilli P, Matteoli M. (1995). A radioimmunoassay to monitor synaptic activity in hippocampal neurons in vitro. Eur J Cell Biol;66: 246–56.

Nagai Y, Nishio Y, Nakamura T, Maegawa H, Kikkawa R, Kashiwagi A. (2002). Amelioration of high fructose-induced metabolic derangements by activation of PPARalpha. Am J Physiol Endocrinol Metab.;282:E1180–90. doi: 10.1152/ajpendo.00471.2001

Nawaz A,Batool Z, Shazad S,Rafiq S, Afzal A,Haider S. (2018). Physical enrichment enhances memory function by regulating stress hormone and brain acetylcholinesterase activity in rats exposed to restraint stress. Life Sci.;207:42–49. doi:10.1016/ j.lfs.2018.05.049. doi: 10.1016/j.lfs.2018.05.049.

O'Donnell P. (2011). Adolescent onset of cortical disinhibition in schizophrenia: insights from animal models. Schizophr Bull.;37: 484–92. doi: 10.1093/schbul/sbr028.

Papp EA, Leergaarda TB, Calabrese E, Johnson GA, Bjaalie JG. (2014). Waxholm space atlas of the Sprague Dawley rat brain. NeuroImage 2014;97:374–86. doi: 10.1016/j.neuroimage.2014.04.001.

Paxinos G, Watson C. (1997). The Rat brain in stereotaxic coordinates. 3th ed. San Diego: Academic Press.

Pope CN, Brimijoin S. (2018). Cholinesterases and the fine line between poison and remedy. Biochem Pharmacol.; 153:205–16. doi: 10.1016/j.bcp.2018.01.044.

Qin L, Wang Z, Tao L, Wang Y. (2010). ER stress negatively regulates AKT/TSC/mTOR pathway to enhance autophagy. Autophagy;6(2):239–47.

Rahman I, Kode A, Biswas SK. (2007). Assay for quantitative determination of glutathione and glutathione disulfide levels using enzymatic recycling method. Nat Protoc.;1:3159–65. doi: 10.1038/nprot.2006.378

Reichelt AC, Killcross S, Hambly LD, Morris MJ, Westbrook RF. (2015). Impact of adolescent sucrose access on cognitive control, recognition memory, and parvalbumin immunoreactivity. Learn Mem.;22:215–24. doi: 10.1101/lm.038000.114.

Reichelt AC. (2016). Adolescent maturational transitions in the prefrontal cortex and dopamine signaling as a risk factor for the development of obesity and high Fat/high sugar diet induced cognitive deficits. Front Behav Neurosci.;10:189. doi:10.3389/fnbeh.2016.00189

Rinwa P, Kaur B, Jaggi AS, Singh N. (2010). Involvement of PPARgamma in curcumin-mediated beneficial effects in experimental dementia. Naunyn-Schmied Arch Pharmacol.;381:529–39. doi: 10.1007/s00210-010-0511-z.

Rippe JM, Angelopoulos TJ. (2016). Relationship between added sugars consumption and chronic disease risk factors: current understanding. Nutrients;8:697. doi: 10.3390/nu8110697

Robbins TW. (2000). From arousal to cognition: the integrative position of the prefrontal cortex. Prog Brain Res.;126:469–83. doi: 10.1016/S0079-6123(00)26030-5

Roglans N, Vilà L, Farré M, Alegret M, Sánchez RM, Vázquez-Carrera M, Laguna JC. (2007). Impairment of hepatic stat-3 activation and reduction of PPARalpha activity in fructose-fed rats. Hepatology;45:778–88. doi: 10.1002/hep.21499

Sanchez-Varo R, Trujillo-Estrada L, Sanchez-Mejias E, Torres M, Baglietto-Vargas D, Moreno-Gonzalez I, De Castro V, Jimenez S, Ruano D, Vizuete M, Davila JC, Garcia-Verdugo JM, Jimenez AJ, Vitorica J, Gutierrez A. (2012). Abnormal accumulation of autophagic vesicles correlates with axonal and synaptic pathology in young Alzheimer's mice hippocampus. Acta Neuropathol;123:53e70. doi: 10.1007/s00401-011-0896-x.

Scharfman H, Goodman J, Macleod A, Phani S, Antonelli C, Croll S. (2005). Increased neurogenesis and the ectopic granule cells after intrahippocampal BDNF infusion in adult rats. Exp Neurol;192:348–56. doi: 10.1016/j.expneurol.2004.11.016

Searl TJ, Silinsky EM. (2006). Modulation of calcium-dependent and-independent acetylcholine release from motor nerve endings. J Mol Neurosci;30(1–2):215–8. doi: 10.1385/JMN:30:1:215

Silhol M, Arancibia S, Maurice T, Tapia-Arancibia L. (2007). Spatial memory training modifies the expression of brain-derived neurotrophic factor tyrosine kinase receptors in young and aged rats. Neuroscience;146:962–73. doi: 10.1016/j.neuroscience.2007.02.013

Spagnuolo MS, Donizetti A, Iannotta L, Aliperti V, Cupidi C, Bruni AC, Cigliano L. (2018). Brain-derived neurotrophic factor modulates cholesterol homeostasis and Apolipoprotein E synthesis in human cell models of astrocytes and neurons. J Cell Physiol.;233(9):6925–43. doi: 10.1002/jcp.26480

Spagnuolo MS, Maresca B, Mollica MP, Cavaliere G, Cefaliello C, Trinchese G, Esposito MG, Scudiero R, Crispino M2, Abrescia P, Cigliano L2. (2014). Haptoglobin increases with age in rat hippocampus and modulates Apolipoprotein E mediated cholesterol trafficking in neuroblastoma cell lines. Front Cell Neurosci.;8:212. eCollection 2014. doi: 10.3389/fncel.2014.00212.

Spagnuolo MS, Mollica MP, Maresca B, Cavaliere G, Cefaliello C, Trinchese G, Scudiero R, Crispino M, Cigliano L. (2015). High Fat diet and inflammation – modulation of haptoglobin level in rat brain. Front Cell Neurosci.;9:479. doi: 10.3389/fncel.2015.00479.

Spijker S. Dissection of rodent brain regions. In: Li KW. (2011) (ed.) Neuroproteomics. New York: Springer Science+ Business Media LLC;. p. 13–26.

Stranahan AM, Norman ED, Lee K, Cutler RG, Telljohann RS, Egan JM, Mattson MP. (2008). Diet-induced insulin resistance impairs hippocampal synaptic plasticity and cognition in middle-aged rats. Hippocampus;18:1085–88. doi: 10.1002/hipo.20470

Su Q, Baker C, Christian P, Naples M, Tong X, Zhang K, Santha M, Adeli K. (2014). Hepatic mitochondrial and ER stress induced by defective PPARα signaling in the pathogenesis of hepatic steatosis. Am J Physiol Endocrinol Metab;306:E1264–73. doi: 10.1152/ajpendo.00438.2013.

Swanson L. (2004). Brain maps: structure of the rat brain. 3rd ed. Amsterdam: Elsevier;.

van der Borght K, Köhnke R, Göransson N, Deierborg T, Brundin P, Erlanson-Albertsson C, Lindqvist A. (2011). Reduced neurogenesis in the rat hippocampus following high fructose consumption. Regul Pept.;167:26–30. doi: 10.1016/j.regpep.2010.11.002.

Wu A, Ying Z, Gomez-Pinilla F. (2004). The interplay between oxidative stress and brain-derived neurotrophic factor modulates the outcome of a saturated fat diet on synaptic plasticity and cognition. Eur J Neurosci;19:1699–707. doi: 10.1111/j.1460-9568.2004.03246.x

Yin Q, Ma Y, Hong Y, Hou X, Chen J, Shen C, Sun M, Shang Y, Dong S, Zeng Z, Pei JJ, Liu X. (2014). Lycopene attenuates insulin signaling deficits, oxidative stress, neuroinflammation, and cognitive impairment in fructose-drinking insulin resistant rats. Neuropharmacol.;86:389–96. doi: 10.1016/j.neuropharm.2014.07.020.

Yoshii A, Constantine-Paton M. (2007). BDNF induces transport of PSD-95 to dendrites through PI3K-AKT signaling after NMDA receptor activation. Nat Neurosci;10:702–711. doi: 10.1038/nn1903

Zhang H, Shang Y, Xiao X, Yu M, Zhang T. (2017). Prenatal stressinduced impairments of cognitive flexibility and bidirectional synaptic plasticity are possibly associated with autophagy in adolescent male-offspring. Exp Neurol.;298(Pt A):68–78. doi: 10.1016/j.expneurol.2017.09.001.

Zvonic S, Hogan JC, Arbour-Reily P, Mynatt RL, Stephens JM. (2004). Effects of cardiotrophin on adipocytes. J Biol Chem.;279: 47572–9. doi: 10.1074/jbc.M403998200

Chapter 4

Concluding remarks

Concluding remarks

Alterations of cholesterol homeostasis have been suggested to play a role in the onset and development of neurodegenerative diseases such as AD (Arenas et al., 2017). Also, a reduction of BDNF levels was observed in AD patients and was correlated with the pathology severity (Bisht et al., 2018). This PhD work elucidates, for the first time, a critical role for BDNF, in modulating cholesterol homeostasis and inducing ApoE synthesis in both glial cell lines and primary astrocytes (Spagnuolo et al., 2018; a). ApoE represent the strongest genetic risk factor for AD, which in particular depends on the presence of ε4 allele that worsen the ability of this protein to modulate cholesterol and β-amyloid homeostasis in brain (Rebeck GW, 2017; Shi and Holtzman, 2018). In view of further clarifying the role of BDNF, it would be interesting in future to evaluate whether BDNF affects ApoE expression and release by glial cells in different way for the three isoforms of the apolipoprotein (ApoE2, ApoE3 and ApoE4). This analysis might be useful to better understand the mechanisms underling the onset of AD and the strong link between ApoE and AD. Recent data provided evidence for the link between disturbances in autophagy and changes in cholesterol homeostasis. Specifically, high intracellular cholesterol enhances beta amyloid-induced autophagosome formation, but impairs lysosomal fusion ability by altering RAB7A and SNAP receptors (SNAREs) content and distribution, which results in decreased beta amyloid lysosomal clearance, a critical step to avoid beta amyloid-induced neuronal death (Barbero-Camps et al, 2018). Interestingly, BDNF was previously shown to promote neuronal survival by suppressing autophagy induced by fasting (Nikoletopoulou et al., 2017). Deciphering the potential role of BDNF in autophagy induced by neuronal cholesterol alteration will be a forthcoming challenge for our group.

Recent studies also demonstrated that BDNF release in brain is mediated by receptor σ1 (σ1R) which is localized at mitochondria-associated ER membranes (MAMs), intracellular lipid rafts that include multiple lipid synthesizing enzymes such as cholesterol biosynthesis enzymes (Fujimoto et al., 2012; Dalwadi et al., 2017). It has been shown that an alteration of σ1R activity lead to the onset of neurodegenerative disease such as AD, Parkinson's disease (PD), Huntington's disease (HD) and amyotrophic lateral sclerosis (ALS) (Maurice et al., 2018; Weng et al., 2017). Since it has been demonstrated that cholesterol binds σ1R (Palmer et al., 2007) but the regulation of this receptor is not yet completely known, a future objective could be the study of cholesterol influence on σ1R activity and, consequently, on BDNF release from neuronal cells.

Besides cholesterol, some foods and dietary components are able to modulate BDNF expression and activity (Pase et al., 2015). Since in the last decade fructose content in diet increased and an high consumption of this sugar has been related to the onset of obesity, metabolic diseases (Dupas et al. 2016; Aguilera- Mendez et al., 2018; Shi et al., 2018), cognitive decline and reduced synaptic plasticity (Chou et al., 2016; Cisternas et al., 2015), we investigated the effect of a short-term fructose rich diet in young and adult rats. Our results showed that even two weeks of treatment with fructose may induce alteration in brain redox homeostasis, autophagy and synaptic function markers including BDNF (Spagnuolo et al., 2018; b). Our data are supported by the recent finding that a maternal excess of fructose intake may induce hippocampal dysfunction in offspring by modification of BDNF promoter (Yamazaki et al., 2018) and that cognitive defects induced by a high-fat-high-fructose diet can be reverted by inducing BDNF signalling pathways in the CNS (Mi et al. 2017). These results suggest the need of educating people, in particular youngs, to a healthy lifestyle, in particular to reduce sugar amount and the use of industrial foods, in order to prevent brain functions alterations and in the long run neurodegenerative diseases.

References

Aguilera-Mendez A, Hernández-Equihua MG, Rueda-Rocha AC, Guajardo-López C, Nieto-Aguilar R, Serrato-Ochoa D, Ruíz Herrera LF, Guzmán-Nateras JA. (2018). Protective effect of supplementation with biotin against high-fructose-induced metabolic syndrome in rats. Nutr Res., 57:86-96. doi: 10.1016/j.nutres.2018.06.007.

Arenas F, Garcia-Ruiz C, Fernandez-Checa JC. (2017). Intracellular Cholesterol Trafficking and Impact in Neurodegeneration. Front Mol Neurosci. 10:382. doi:10.3389/fnmol.2017.00382.

Barbero-Camps E, Roca-Agujetas V, Bartolessis I, de Dios C, Fernández-Checa JC, Marí M, Morales A, Hartmann T, Colell A. (2018). Cholesterol impairs autophagy-mediated clearance of amyloid beta while promoting its secretion. Autophagy.;14(7):1129-1154. doi: 10.1080/15548627.2018.1438807.

Bisht K, Sharma K, Tremblay MÈ. (2018). Chronic stress as a risk factor for Alzheimer's disease: Roles of microglia-mediated synaptic remodeling, inflammation, and oxidative stress. Neurobiol Stress. 9:9-21. doi: 10.1016/j.ynstr.2018.05.003. eCollection 2018 Nov

Chou LM, Lin CI, Chen YH, Liao H, Lin SH. (2016). A diet containing grape powder ameliorates the cognitive decline in aged rats with a long-term high-fructose-high-fat dietary pattern. J Nutr Biochem, 34:52-60. doi: 10.1016/j.jnutbio.2016.04.006.

Cisternas P, Salazar P, Serrano FG, Montecinos-Oliva C, Arredondo SB, Varela-Nallar L, Barja S, Vio CP, Gomez-Pinilla F, Inestrosa NC. (2015). Fructose consumption reduces hippocampal synaptic plasticity underlying cognitive performance. Biochim Biophys Acta, 1852(11):2379-90. doi: 10.1016/j.bbadis.2015.08.016.

Dalwadi DA, Kim S, Schetz JA. (2017). Activation of the sigma-1 receptor by haloperidol metabolites facilitates brain-derived neurotrophic factor secretion from human astroglia. Neurochem Int.;105:21-31. doi: 10.1016/j.neuint.2017.02.003.

Dupas J, Goanvec C, Feray A, Guernec A, Alain C, Guerrero F, Mansourati J. (2016). Progressive Induction of Type 2 Diabetes: Effects of a Reality-Like Fructose Enriched Diet in Young Wistar Rats. PLoS One., 11(1):e0146821. doi: 10.1371/journal.pone.0146821.

Fujimoto M, Hayashi T, Urfer R, Mita S, Su TP. (2012). Sigma-1 receptor chaperones regulate the secretion of brain-derived neurotrophic factor. Synapse.;66(7):630-9. doi: 10.1002/syn.21549. Epub 2012 Mar 16.

Maurice T, Strehaiano M, Duhr F, Chevallier N. (2018). Amyloid toxicity is enhanced after pharmacological or genetic invalidation of the σ1 receptor. Behav Brain Res.;339:1-10. doi: 10.1016/j.bbr.2017.11.010.

Mi Y, Qi G, Fan R, Qiao Q, Sun Y, Gao Y, Liu X. (2017). EGCG ameliorates high-fat- and high-fructose-induced cognitive defects by regulating the IRS/AKT and ERK/CREB/BDNF signaling pathways in the CNS. FASEB J., 31(11):4998-5011. doi: 10.1096/fj.201700400RR.

Nikoletopoulou V, Sidiropoulou K, Kallergi E, Dalezios Y, Tavernarakis N. (2017). Modulation of Autophagy by BDNF Underlies Synaptic Plasticity. Cell Metab.;26(1):230-242.e5. doi: 10.1016/j.cmet.2017.06.005.

Palmer CP, Mahen R, Schnell E, Djamgoz MB, Aydar E. (2007). Sigma-1 receptors bind cholesterol and remodel lipid rafts in breast cancer cell lines. Cancer Res. ;67(23):11166-75.

Pase CS, Teixeira AM, Roversi K, Dias VT, Calabrese F, Molteni R, Franchi S, Panerai AE, Riva MA, Burger ME. (2015). Olive oil-enriched diet reduces brain oxidative damages and ameliorates neurotrophic factor gene expression in different life stages of rats. J Nutr Biochem., 26(11):1200-7. doi: 10.1016/j.jnutbio.2015.05.013.

Rebeck GW. (2017). The role of APOE on lipid homeostasis and inflammation in normal brains. .J Lipid Res.;58(8):1493-1499. doi: 10.1194/jlr.R075408.

Shi Y and Holtzman DM. (2018). Interplay between innate immunity and Alzheimer disease: APOE and TREM2 in the spotlight. Nat Rev Immunol. doi: 10.1038/s41577-018-0051-1. [Epub ahead of print]

Shi YS, Li CB, Li XY, Wu J, Li Y, Fu X, Zhang Y, Hu WZ. (2018). Fisetin Attenuates Metabolic Dysfunction in Mice Challenged with a High-Fructose Diet. J Agric Food Chem., 66(31):8291-8298. doi: 10.1021/acs.jafc.8b02140.

Spagnuolo MS, Donizetti A, Iannotta L, Aliperti V, Cupidi C, Bruni AC, Cigliano L. (2018) (a). Brain-derived neurotrophic factor modulates cholesterol homeostasis and Apolipoprotein E synthesis in human cell models of astrocytes and neurons. J Cell Physiol., 233(9):6925-6943. doi: 10.1002/jcp.26480.

Spagnuolo MS, Bergamo P, Crescenzo R, Iannotta L, Treppiccione L, Iossa S, Cigliano L. (2018) (b). Brain Nrf2 pathway, autophagy, and synaptic function proteins are modulated by a short-term fructose feeding in young and adult rats. Nutr Neurosci., 1-12. doi: 10.1080/1028415X.2018.1501532. [Epub ahead of print]

Weng TY, Tsai SA, Su TP. (2017). Roles of sigma-1 receptors on mitochondrial functions relevant to neurodegenerative diseases. J Biomed Sci.;24 (1):74. doi: 10.1186/s12929-017-0380-6.

Saito K, Suzuki K, Hashimoto S, Ohashi K. (2018). Excess maternal fructose consumption impairs hippocampal function in offspring via epigenetic modification of BDNF promoter. FASEB J. 32(5):2549-2562. doi: 10.1096/fj.201700783RR.

Appendix

Publications

1. Cigliano L, Spagnuolo MS, Crescenzo R, Cancelliere R, **Iannotta L**, Mazzoli A, Liverini G, Iossa S. (2018). Short-Term Fructose Feeding Induces Inflammation and Oxidative Stress in the Hippocampus of Young and Adult Rats. Mol Neurobiol. 55(4):2869-2883. doi: 10.1007/s12035-017-0518-2. Epub 2017 Apr 28.
2. Spagnuolo MS, Bergamo P, Crescenzo R, **Iannotta L**, Treppiccione L, Iossa S, Cigliano L. (2018). Brain Nrf2 pathway, autophagy, and synaptic function proteins are modulated by a short-term fructose feeding in young and adult rats. Nutr Neurosci. 24:1-12. doi:10.1080/1028415X.2018.1501532. [Epub ahead of print]
3. Spagnuolo MS, Donizetti A, **Iannotta L**, Aliperti V, Cupidi C, Bruni AC, Cigliano L. (2018). Brain-derived neurotrophic factor modulates cholesterol homeostasis and Apolipoprotein E synthesis in human cell models of astrocytes and neurons. J Cell Physiol. 233(9):6925-6943. doi: 10.1002/jcp.26480. Epub 2018 Mar 25.

List of communication

1. M.S. Spagnuolo, **L. Iannotta**, R.Crescenzo, C. Gatto, S.Iossa, Luisa Cigliano. Imbalance of redox homeostasis, autophagy activation, and modulation of synaptic markers in frontal cortex of young and adult rats are involved in the early response to a short term fructose feeding: an intriguing menage a trois. 69th National Congress Italian Physiological Society (SIF) Firenze: 148 (2018).
2. **L. Iannotta**, M.S. Spagnuolo, R. Nunziante, J. Di Ceglie, L. Cigliano. Brain-derived neurotrophic factor reduces apoptosis in differentiated neurons by limiting cholesterol uptake. 68th National Congress Italian Physiological Society (SIF) Pavia: 20, 146 (2017).
3. M.S. Spagnuolo, **L. Iannotta**, M.Nazzaro, M Canè, R.Crescenzo, S.Iossa, L. Cigliano. Short term fructose-rich diet affects markers of neuronal survival and differentiation in young and adult rats. 68th National Congress Italian Physiological Society (SIF) Pavia: 22, 180 (2017).
4. Cigliano L, **Iannotta L**, Farina V, Spagnuolo MS. The extracellular chaperone Haptoglobin binds Complement Receptor 1 (CR1) and influences its activation in microglia. 13th International Conference on Alzheimer's and Parkinson's Diseases and Related Neurological Disorders (ADPD), Wien: 175 (2017).
5. M.S. Spagnuolo, **L. Iannotta**, A. Gentile, F. Cozzolino, L. Cigliano. BDNF modulates Apolipoprotein E mediated cholesterol trafficking between astrocytes and neurons. 67th National Congress Italian Physiological Society, (SIF) Catania 20, 144 (2016).